A STUDY OF THE EFFECT OF A BOUNDARY LAYER PROFILE ON THE DYNAMIC RESPONSE AND ACOUSTIC RADIATION OF FLAT PANELS

A Dissertation

Presented to

the Faculty of the School of Engineering and Applied Science

University of Virginia

In Partial Fulfillment

of the Requirements for the Degree

Doctor of Philosophy in Applied Mechanics

by

John Scott Mixson

June 1973

(NASA-TM-X-69568) A STUDY OF THE EFFECT OF A BOUNDARY LAYER PROFILE ON THE DYNAMIC RESPONSE AND ACOUSTIC RADIATION OF FLAT PANELS Ph.D. Thesis - Virginia Univ. (NASA) 132 p HC $8.75 CSCL 20D
N73-30232
Unclas
G3/12 12189
133

Reproduced by
NATIONAL TECHNICAL
INFORMATION SERVICE
US Department of Commerce
Springfield, VA. 22151

SEP 1973
RECEIVED
NASA STI FACILITY
INPUT BRANCH

A Study of the Effect of a Boundary Layer Profile on the Dynamic Response and Acoustic Radiation of Flat Panels

John S. Mixson

ABSTRACT

A thin, flat, elastic plate of length L and infinite width lies in the x-y plane. The rest of the x-y plane is occupied by a rigid baffle that separates the upper z space from the lower. A harmonic force drives the plate from below, and a compressible air stream with a viscous boundary layer flows parallel to the upper surface along the length L. Linear partial differential equations governing the forced response of the coupled plate-aerodynamic system are derived along with appropriate boundary conditions. Solution of these equations involves modal series solution of the plate equation, Fourier transform of the aerodynamic equation in the direction parallel to the plate, and Frobenius - series or Runge-Kutta numerical solution of the resulting o.d.e. with variable coefficients (due to the boundary layer) in the direction normal to the plate. The aerodynamic solution depends on the dimensionless ratios Mach number, Prandtl number, temperature boundary condition, boundary layer thickness and acoustic coincidence number. The plate response solution depends in addition on the parameters

plate frequency ratio, density coupling number, plate eigenvalue spectrum, and the force distribution. Numerical results for Mach number, M, of 0.5 are presented to illustrate the method of solution and the effects of boundary layer thickness on the fluid pressures along the plate and on the plate response. Calculations for limiting cases are presented showing that the method produces appropriate results for $M = 0$, and for $M = 0.5$ but zero boundary layer thickness. The surface pressure distributions show that peak pressure shifts forward and decreases slightly as the boundary layer thickness increases. Variations of boundary layer thickness caused large percentage changes of the "virtual mass" and aerodynamic damping associated by analogy with the fluid effects on the plate dynamic response. Calculations of basic solution parameters for a linear velocity profile and for a Blasius profile showed that the same system response could be obtained from each profile provided that an appropriate value of boundary layer thickness was chosen for each profile.

JSM 22 April 1973

APPROVAL SHEET

This dissertation is submitted in partial fulfillment of the requirements for the degree of Doctor of Philosophy in Applied Mechanics

John S Mixson
Author

Approved:

Faculty Adviser

Dean, School of Engineering and Applied Science

June 1973

Acknowledgements

The author's gratitude is hereby expressed to all those whose efforts contributed to the successful completion of this work. A special word of thanks is offered to those without whose contributions this work would not have been possible, specifically to my wife Cynthia who provided much needed encouragement to carry on and a peaceful home atmosphere congenial to study; to the National Aeronautics and Space Administration who provided manpower and financial resources for the work; to Christine Brown who tended with imagination and perseverance to the details of coaxing the appropriate numbers from the digital computer; and to my University of Virginia Advisory Committee, headed by Dr. F. W. Barton, whose consultations kept the work moving on the right track.

CONTENTS

Tables

Figures

SYMBOLS

a^2 $= \delta^2[(1+M\hat{c})^2-\hat{c}^2]/\lambda^2$

a_n , coefficients of eigenfunction expansion, and coefficients in Frobenius series solution for $\overset{o}{p}_n$

B_{mn} , Aerodynamic coupling coefficients in plate equation,$= B^r_{mn} + iB^c_{mn}$

b $= \sqrt{-a^2}$

$C_p(\hat{x})$, pressure coefficient, $= e^{-iwt}p(x,z,t)/(\rho_0(0)cfL)$, $= \frac{a_1}{\lambda}\int_{-\infty}^{\infty} \overset{o}{p}_1(\hat{k},\hat{z})e^{i\hat{k}\hat{x}}\,d\hat{k}$

C_p^r, C_p^c , real and imaginary parts of C_p

c , sound speed, $= \sqrt{\gamma RTo}$

$\bar{c}$, dimensionless sound speed, $= c(z)/c_\infty$

c_∞ , sound speed at $z = \infty$

C_v , specific heat at constant volume

$\hat{c}$, wave length parameter, $= kc/\omega$; $= \hat{k}\lambda$

D , plate stiffness parameter

$D(\ )$, total derivative, $= \frac{\partial}{\partial t} + \bar{u}^* \cdot \nabla$

$d(\ )$, total derivative, $= \frac{\partial}{\partial t} + \bar{U} \cdot \nabla$

f , frequency, cps, $= \omega/2\pi$

$\bar{f}_b$, body forces in Navier-Stoke equation

i , complex quantity $\sqrt{-1}$

$\underline{i},\underline{j},\underline{k}$, unit vectors in x,y,z directions

i,j , indices in matrix and cartesian tensor notation

K , thermal conductivity

k , Fourier transform parameter, x transform

$\hat{k}$, dimensionless transform parameter, $\hat{k} = kL$

L , plate length in x direction

M , Mach number, U_∞ / c_∞

m,n , indices

$p(x,y,z,t)$, perturbation (acoustic) pressure

p_0 , pressure in basic flow

p^* , total pressure, $= p_o + p$

$\bar{p}(x,z)$, reduced dimensional pressure

$\hat{p}(\hat{x},\hat{z})$, dimensionless pressure, $\bar{p} = \rho_o(0)\omega^2 L^2 \hat{p}$

$\overset{o}{p}(\hat{k},\hat{z})$, Fourier transform of $\hat{p}$

$\overset{o}{p}_n(\hat{k},\hat{z})$, component of series expansion of $\overset{o}{p}$

Q_m , generalized force in m-th mode

$q(x,y,t)$, applied force (dimensional)

$\bar{q}(x)$, applied force of one dimension

$\hat{q}(\hat{x})$, dimensionless force, $\hat{q} = \bar{q}L^3/D$

R , universal gas constant, $= 1 - \gamma$

$R(\hat{x})$, modulus of $C_p(\hat{x})$

T , temperature due to perturbation (acoustic) motion

T_0 , temperature in basic flow

T^* , total temperature, $= T_o + T$

$\bar{T}_{ij}$, elements of transfer matrix for arbitrary $\overset{o}{z}$

T_{ij} , elements of transfer matrix for $\overset{o}{z} = 1$

t , time

$\bar{U}$, velocity of basic flow (vector), $= U\underline{i} + V\underline{j} + W\underline{k}$

$\bar{U}$, dimensionless velocity in x direction, $= U(z)/U_\infty$

U,V,W , components of $\bar{U}$ in x,y,z directions

$\bar{u}$, velocity of perturbation motion, $= u\underline{i} + v\underline{j} + w\underline{k}$

u,v,w , components of $\bar{u}$ in x,y,z directions

$\bar{u}^*$, total velocity, $= \bar{U} + \bar{u}$

$w(x,y,t)$, w_p , plate displacement

$\bar{w}(x)$, reduced dimension plate displacement

$\hat{w}(\hat{x})$, dimensionless plate displacement, $= \bar{w}(x)/L$

$\hat{w}_m(\hat{x})$, eigenfunctions of plate operator

x,y,z , cartesian coordinate axes

$\hat{x},\hat{y},\hat{z}$, dimensionless coordinates, = x/L, y/L, z/L

$\overset{\circ}{z}$, coordinate non-dimensionalized by boundary layer thickness, = $\hat{z}/\delta$

$Z_m(\hat{k})$, Fourier transform of m-th eigenfunction

$Z_m^*(\hat{k})$, Complex conjugate of $Z_m(\hat{k})$

γ , ratio of specific heats, = C_p/C_v

δ , dimensionless boundary layer thickness, = (Geometric thickness)/L

$\hat{\delta}$, = δ/λ

λ , wave length parameter, = $c/L\omega$

λ_m , eigenvalues of plate operator

μ , viscosity in basic fluid equations

μ , mass ratio in non-dimensional coupled equations, $= \frac{\rho_0(0)L}{\rho_p}$

ρ_p , area density of plate material

ρ , density change of perturbation motion in fluid

ρ_0 , density in basic flow

ρ^* , total density

$\Phi(x)$, phase of pressure coefficient $C_p(\hat{x})$

Ω , dimensionless frequency parameter, $= \omega L^2\sqrt{\rho_p/D}$

ω , circular frequency

$(\frac{\delta p_r}{\lambda}), (\frac{\delta p_c}{\lambda})$, real and imaginary parts of pressure coefficient

$\nabla = \frac{\partial}{\partial x}\underline{i} + \frac{\partial}{\partial y}\underline{j} + \frac{\partial}{\partial z}\underline{k}$

$\nabla^2 = \frac{\partial^2}{\partial x^2} + \frac{\partial^2}{\partial y^2} + \frac{\partial^2}{\partial z^2}$

$\nabla^4 = \nabla^2(\nabla^2)$

A prime denotes differentiation with respect to a coordinate argument.

Chapter I

Introduction

The practical problem

Turbulent boundary layers are often formed on the surfaces of aircraft in flight. The response of the aircraft skin structure to the fluctuating pressures associated with the turbulence can lead to structural fatigue failure due to fluctuating stress response,[1] and can lead to unwanted transmission of noise from the boundary layer to the interior of the aircraft.[2,3] The ability to predict the structural responses is required in order to design structures that will withstand fatigue and that will minimize the transmission of noise.

Panel-Aerodynamic Coupling

The response of aircraft structural panels is affected in an important way by its coupling to the passing air stream, in addition to the fact that the turbulence in the air stream is driving the panel motions. When the panel responds to the turbulence, its motion generates additional pressures in the air stream; these pressures act on the panel to alter its motion. The panel motion is thus coupled to the pressure in the air stream in such a way that calculation of the panel motion requires solution for the air pressures as an integral part of the calculation. The importance of this

coupling has long been recognized as the key factor leading to the instability known as panel flutter.[4,5] In addition, some work has suggested that the coupling with a supersonic air stream can introduce damping that is large in comparison with damping from structural sources.[4,6] It has also been found that coupling of panel motion with a heavy fluid, such as water, can cause large reductions of the plate resonant frequencies, compared to the in-vacuo natural frequencies.[7,8]

Previous Panel Response Research

The mathematical difficulties involved in solving the equations describing the motion of a flexible plate coupled to a compressible, flowing air stream and driven by a statistically random pressure field have led to the use of approximations of various kinds. First, the aerodynamic pressure field is separated into two parts that do not interact.[9] One part is the random pressure field associated with the boundary layer turbulence, which is taken to be given from experimental measurements. The other part is the additional pressures caused by the motion of the panel. The effects of interaction of these two pressure fields apparently cannot be calculated within the current state of the art. For some simple types of structures, such as uniform spherical and cylindrical shells and infinite flat plates the panel motion-pressure interaction problem is simplified because the fluid

pressures don't change or couple the in-vacuo normal modes of the structure,[10] or because the panel motion can be represented by a simple traveling wave.[11,12,13] In some studies the panel pressures were not included at all, and attention was thus focused on the statistical[14] or plate model[15] aspects of the problem. In other studies the effects of panel motion pressures were included as an equivalent damping or radiation resistance factor, and numerical values obtained from experiment.[16,17] Aerodynamic piston theory has been used to analyze the coupled response for air stream Mach numbers greater than one.[1,6] This theory simplifies the coupling of plate motion to aerodynamic pressure because it relates the pressure at a point on the plate to the motion at only a few points, rather than to the motion at all other points of the plate, as is done in the more exact aerodynamic theories.[9,18] For plates vibrating in water, the "virtual mass" feature of the coupling has been included but the damping feature not included.[19] Additional research on various aspects of this plate response problem is described in the papers referenced by Lin,[1] Dowell,[9] Strawderman,[14] Maestrello[16] and Leibowitz.[19] All the work described in the above papers contains the assumption that the gradients of velocity and temperature associated with the boundary layer do not influence the coupled dynamic response of the

plate-fluid system.

Boundary Layer Effects

Recent research has shown that the thickness of the boundary layer over a panel can have an important effect on the flutter properties of the panel.[20,21] The experimental results[20] show that the dynamic pressure at flutter in the presence of a particular boundary layer was twice the dynamic pressure value obtained (by extrapolation) for zero boundary layer thickness. Calculated results[21] also show the large influence of boundary layer thickness on flutter dynamic pressure. Because of the close connection between panel response and panel flutter,[6,22] these flutter results imply that the characteristics of panel response will depend on the thickness of the adjacent boundary layer. Such effects might also be expected on intuitive grounds. For example, in the case of an extremely thick boundary layer the fluid velocities existing at large distances from the panel could be expected to have only small effects on the panel motion, as compared to a thin boundary layer in which the large velocities exist within a fraction of an inch of the panel surface. Considerations such as these suggest that it would be worthwhile to develop methods for calculating the response of panels that are coupled to a passing air stream through a boundary layer containing gradients of

velocity and temperature. Development of such methods is the purpose of the work described in this paper.

The procedures developed by Dowell[9,21] for calculating flutter of panels take into account the effects of velocity and temperature gradients and are sufficiently general to allow calculation of response as well. Dowell's method of solution uses a combination of plate modal series expansion, Fourier transforms in the direction parallel to the plate and finite differences across the boundary layer to reduce the governing partial differential equations to ordinary differential equations in time which are then solved numerically on a digital computer. This procedure is very general and can incorporate a great variety of phenomena such as plate nonlinearity, aerodynamic velocity and temperature gradients, and transient input forces. When calculating results for particular practical configurations this method is probably the best type to use. Such great generality however, tends to increase the computation effort required to obtain each data point, and consequently increases the difficulty of carrying out trend studies to explore the effects of boundary layer thickness, for example, and increases the difficulty of obtaining the statistics of the panel response from the statistics of the forcing pressures of the boundary layer. An approach alternative to the time domain solution of

Dowell is the frequency domain solution. This procedure makes use of either a harmonic time dependence or a Fourier transform in time instead of the numerical integration in time. The frequency domain solution appears to offer the advantages of (1) requiring less difficulty in carrying out trend studies, (2) allowing more straightforward development of relations between input and output statistics, and (3) allowing easier incorporation of simplifications such as asymptotic solutions of integrals. The frequency domain solution is used in the work described in this paper.

The Present Research

The purpose of the work reported herein, then, is to develop methods for calculating the response of panels coupled to a passing air stream through a boundary layer using a frequency domain solution. In order to focus attention on the effects of the boundary layer, other aspects of the problem are simplified. The structural panel considered is uniform, flat, isotropic, elastic, initially un-stressed, and responds in the linear, small-deflection, amplitude range. The panel has infinite width and finite length. The flow is parallel to the panel length. The applied force is harmonic, rather than random. The fluid is considered to be compressible and Newtonian; its motion is taken in two parts: (1) a large magnitude shear-flow motion parallel

to the panel surface, and (2) an acoustic motion of infinitesimal magnitude and arbitrary direction. The large motion is taken to be steady, laminar, and unidirectional. Viscosity effects are included in the large motion, but are not included in the small magnitude part of the flow.

The plan of this paper is: (1) derive appropriate partial differential equations and boundary conditions governing the plate deflection and the fluid pressure, and relate them to previously derived equations; (2) solve the governing partial differential equations so that numerical values of specific deflections and pressures can be obtained using a digital computer; and (3) present results displaying the effects of boundary layer thickness on panel deflection and aerodynamic pressure.

Chapter II

Derivation of the Governing Equations

In this chapter the equations governing the response of a coupled system consisting of a flat plate and a flowing fluid are derived. In addition the boundary conditions on the fluid, on the plate, and at the plate-fluid interface are obtained. A general assumption used is that the response is small, so that the equations to be obtained are linear in the dependent variables of plate displacement and fluid pressure. The system under consideration is shown in figure 1. A flat rectangular elastic plate occupies a region of the x-y plane; the remainder of the x-y plane is occupied by a baffle, or rigid plate, that serves to separate the upper half space from the lower and provide boundary conditions at the edges of the plate and at the lower surface of the fluid. A Newtonian flowing fluid fills the upper half space, $z > 0$; the lower half space, $z < 0$, is empty. A known force $q(x,y,t)$ is applied to the plate surface. This system can be thought of as an idealization of, for example, a small panel in the surface of an aircraft wing or fuselage. In the development of the equations particular attention is given to the effects of velocity and temperature gradients that form the boundary layer in the fluid near the plate, and other aspects of the system are treated in simplifying ways.

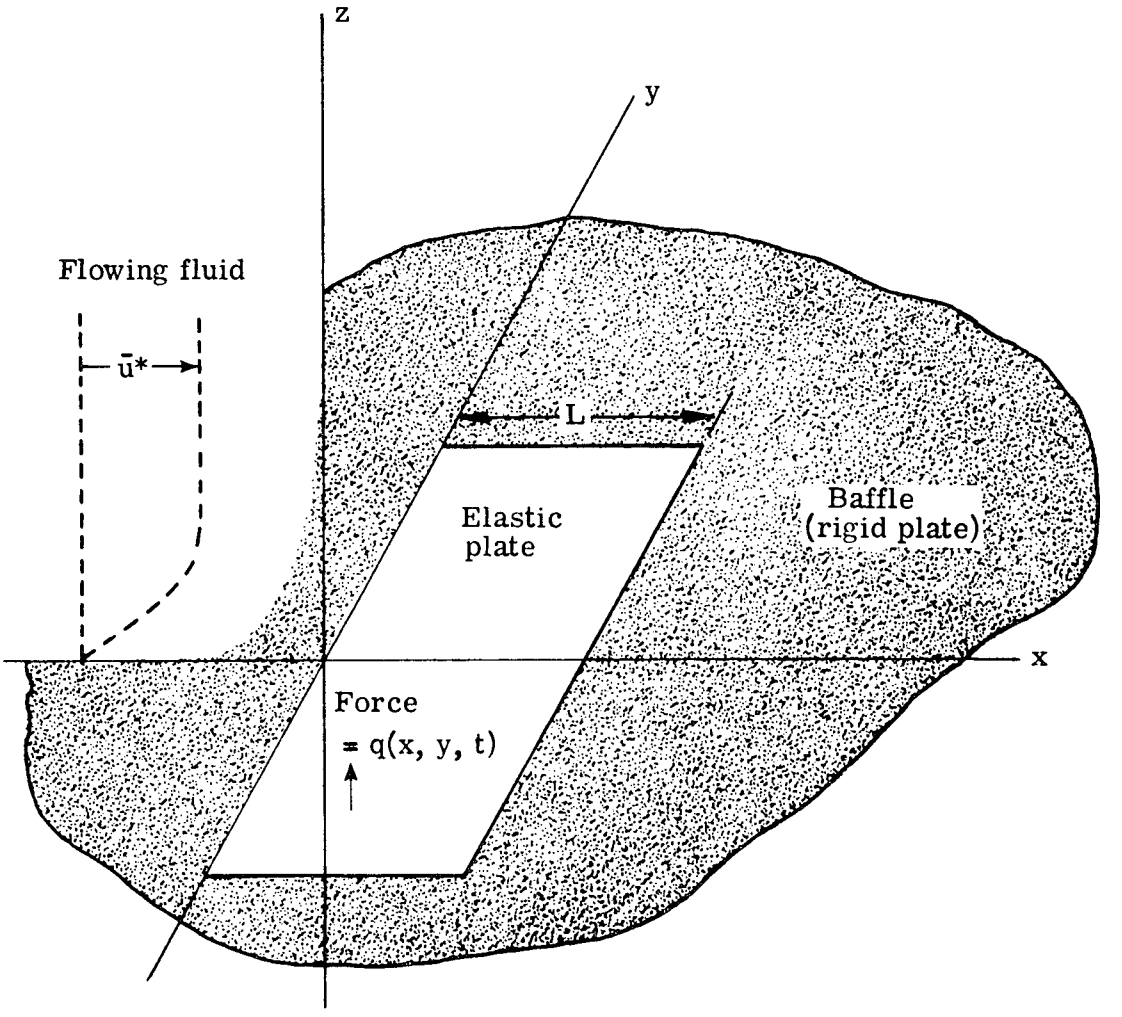

Figure 1.- Sketch of the plate-fluid system.

The Plate Equation

A sketch of a small element of the plate showing the forces acting is presented in figure 2. The equilibrium of an element of the plate is governed by the equation[23]:

$$D\nabla^4 w = \text{load intensity} \qquad 1.$$

The load intensity acting includes:

the inertia reaction force, $-\rho_p \frac{\partial^2 w}{\partial t^2}$

the fluid pressure, $-p$

and the given external force, q.

Inserting these forces on the right hand side of equation 1, and rearranging terms leads to the equation governing plate motion:

$$D\nabla^4 w + \rho_p \frac{\partial^2 w}{\partial t^2} + p\ (x,y,0,t) = q\ (x,y,t) \qquad 2.$$

For the present work the pressure $p(x,y,0,t)$ is the pressure in the fluid that results from the plate motion w, thus to solve equation 2 the relation between p and w must be obtained from the governing fluid equation and must be used in the solution. The pressure is a function of position in space and time; the form $p\ (x,y,0,t)$ indicates that the pressure at $z = 0$ is considered to be applied to the plate surface. When there is no fluid present the pressure is zero and equation 2 can be solved using known techniques.

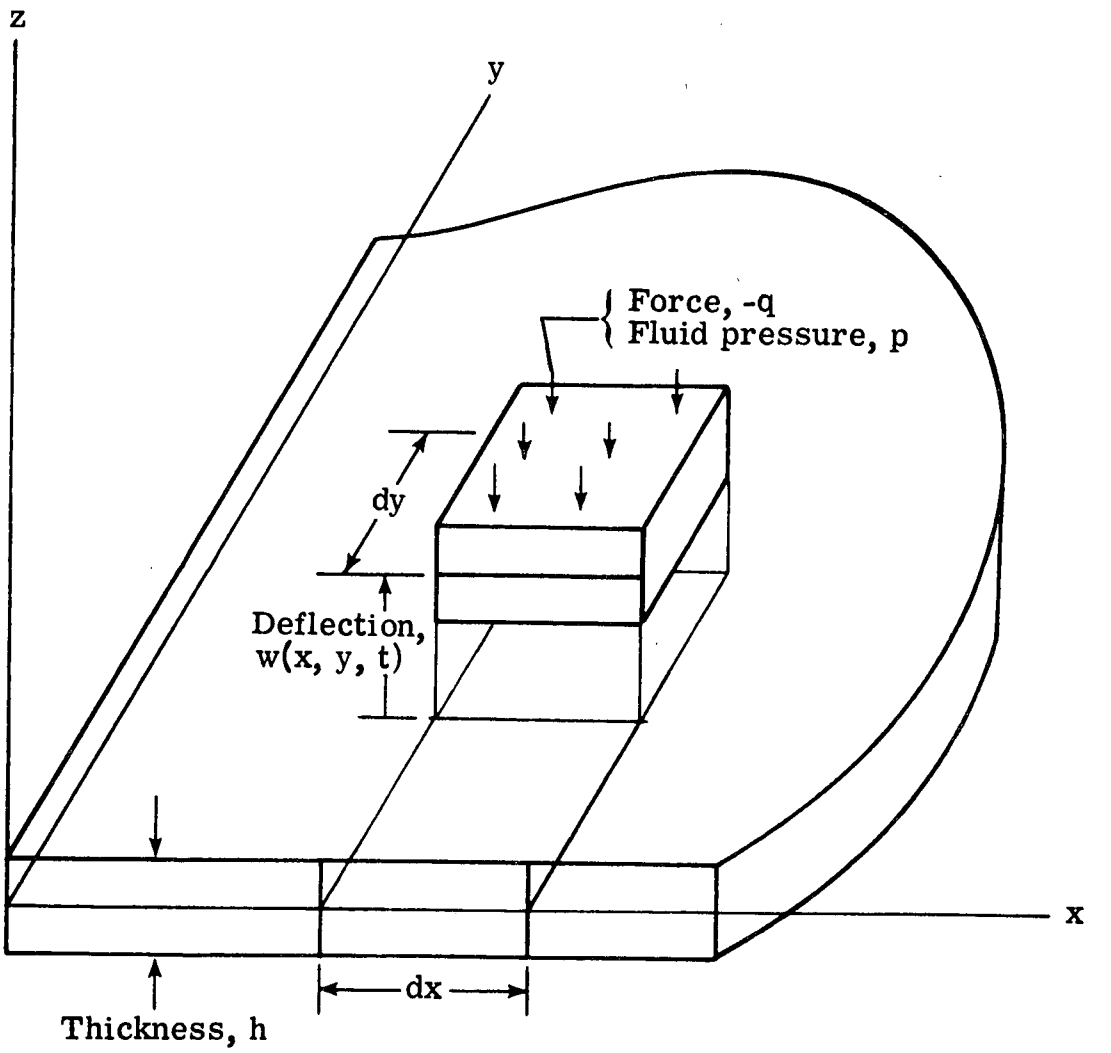

Figure 2.- Plate element and forces.

In order to focus attention on the fluid boundary layer effects a very simple type of plate has been assumed in obtaining equation 2. The plate is flat, has uniform thickness, mass and stiffness distributions, and the plate material is isotropic and elastic. There is no initial pre-stress and the response is assumed to be in the linear, small amplitude, deflection range. This simple plate is felt, however, to represent some realistic systems.

The Aerodynamic Equation

The equation governing the pressure in the fluid is obtained from the basic equations:

$$\rho^* D(\bar{u}^*) = \rho^* \bar{f}_b - \nabla p^* + \mu \nabla^2 \bar{u}^* + \mu \nabla (\nabla \cdot \bar{u}^*)/3 \qquad 3.$$

$$D(\rho^*) + \rho^* \nabla \cdot \bar{u}^* = 0 \qquad 4.$$

$$p^* = R \rho^* T^* \qquad 5.$$

$$\rho^* C_v D(T^*) = \frac{\partial}{\partial x_i} (K \frac{\partial T^*}{\partial x_i}) - p^* \frac{\partial u_i^*}{\partial x_i} + \mu \left(\frac{\partial u_i^*}{\partial x_j} + \frac{\partial u_j^*}{\partial x_i} \right) \frac{\partial u_i^*}{\partial x_j} - \frac{2}{3} \mu \left(\frac{\partial u_i^*}{\partial x_i} \right)^2 \qquad 6.$$

These equations are, respectively, the Navier-Stokes equation governing a Newtonian fluid, the continuity equation, the equation of state for an ideal perfect gas, and the energy equation for a Newtonian fluid obeying the Fourier

law of heat conduction. These six equations (equation 3 is a vector equation) are sufficient to determine the six unknowns; pressure p^*, density ρ^*, temperature T^*, and velocity (vector) $\bar{u}^*$. All six are necessary to describe the behavior of a compressible fluid.

The unknowns described by equation 3 to 6 are total quantities. For example $p^*(x,y,0,t)$ is the total pressure acting on the plate, whereas the pressure $p(x,y,0,t)$ appearing in equation 2 is only that part of the pressure caused by the motion of the plate. The unknown "starred" quantities are therefore divided into two parts, as follows:

$$\left.\begin{aligned} \bar{u}^* &= \bar{U} + \bar{u} && \text{a} \\ \rho^* &= \rho_0 + \rho && \text{b} \\ p^* &= p_0 + p && \text{c} \\ T^* &= T_0 + T && \text{d} \end{aligned}\right\} \qquad 7.$$

where the quantities $\bar{u}$, ρ, p, and T are related to the motion of the plate, and vanish when there is zero plate motion. The quantities $\bar{U}$, ρ_0, p_0, and T_0 are the values that remain when the plate motion disappears; for convenience this flow condition is referred to herein as the basic flow. Linear equations governing the "plate motion" quantities are obtained as follows. Equations 7 are substituted into equations 3 to 6 and the terms of each resulting equation are

divided into three groups. One group of terms contains only basic flow quantities, $\bar{U}$, ρ_0, p_0, T_0, and disappears under the assumption that the basic flow satisfies equations 3 to 6. Another group of terms contains squares and/or products of the "plate motion" quantities, $\bar{u}$, ρ, p, T, and disappears under the assumption that $\bar{u}$, ρ, p and T are small enough that squares and products are negligible compared to the linear terms. The group of terms remaining are the governing equations, however two additional simplifications are made. First, it is assumed that viscous effects and body forces are negligible under conditions of interest, so the terms containing viscosity and body forces are deleted. (Recall however that viscous effects were retained in the equations describing the basic flow.) Second, it is assumed that there is insufficient time for any heat flow to take place due to plate motion, so terms involving heat flow are dropped. The equations resulting from the above steps are:

$$\rho_0 \frac{\partial \bar{u}}{\partial t} + \rho_0(\bar{U} \cdot \nabla\bar{u} + \bar{u} \cdot \nabla\bar{U}) + \rho\, d(\bar{U}) = -\nabla p \qquad 8.$$

$$\frac{\partial \rho}{\partial t} + \nabla \cdot (\rho\bar{U} + \rho_0 \bar{u}) = 0 \qquad 9.$$

$$p = R(\rho_0 T + \rho T_0) \qquad 10.$$

$$\rho\, C_v\, d(T_0) + \rho_0 C_v \left(\frac{\partial T}{\partial t} + \bar{U}\cdot\nabla T + \bar{u}\cdot\nabla T_0\right) = -p_0 \nabla\cdot\bar{u} - p\nabla\cdot\bar{U} \qquad 11.$$

where $d(\,) = \frac{\partial(\,)}{\partial t} + U\frac{\partial(\,)}{\partial x}$.

Equations 8 to 11 form a set of six equations that are linear

in the six "plate motion" quantities $\bar{u}$, ρ, p, and T; therefore these equations together with given distributions of the basic flow quantities $\bar{U}$, p_0, ρ_0, T_0 and appropriate boundary conditions should be sufficient for obtaining a solution.

It should be noted that equation 10 was obtained from the equation of state for an ideal gas, and that there is no comparably simple equation for liquids.[24] In acoustical studies use is made of a sound speed relation, instead of an equation of state, but sound speed relations for liquids are not simple. For example, one empirically determined polynomial equation for sound speed in water contains terms up to fourth power in temperature and up to third power in pressure.[25] It appears that extension of the present research to flowing liquids, such as water, would require that special consideration be given to an appropriate equation of state. The present work is thus limited to an ideal gas as the flowing fluid.

In order to solve equations 8 to 11 particular distributions in space and time must be obtained for the basic flow quantities $\bar{U}$, ρ_0, p_0, and T_0. The distributions of interest for the present work are those associated with a boundary layer on a flat plate.

In addition the basic flow is assumed to be parallel flow; that is, the boundary layer thickness is taken to be constant in the direction of flow rather than increasing along the flow direction, as actually occurs. This assumption appears reasonable because parallel flow has been found adequate for hydrodynamic stability studies.[26] In addition the parallel flow assumption allows significant simplification of the equations, while still retaining important features of the boundary layer flow field, namely the gradients of velocity and temperature in the direction normal to the plate.

Instead of using equations 10 and 11 in further developments, the alternate equation

$$d(p)+\bar{u}\cdot\nabla p_0+\rho d(p_0)/\rho_0 = \gamma R T_0\left[d(\rho)+\bar{u}\cdot\nabla\rho_0+p d(\rho_0)/p_0\right] \qquad 12.$$

will be used. The derivation of equation 12 is given in Appendix A. The derivation makes use of the continuity, state, and energy equations (equations 4, 5, and 6) to obtain a pressure-density relation for the total quantities. Equations 7 and the procedure described following equations 7 are then used to obtain equation 12 from this pressure-density relation. Equation 12 is used in place of equations 10 and 11, and clearly displays the presence of gradient terms in the pressure-density-sound-speed relation.

Equations 8, 9, and 12 form a set of five equations in the five unknowns pressure p, density ρ, and velocity $\bar{u}$, and will be used in subsequent developments.

Written out in full, equations 8, 9, and 12 are:

$$\rho_0 \frac{\partial u}{\partial t} + \rho_0 \underbrace{\left[U \frac{\partial u}{\partial x} + V \frac{\partial u}{\partial y} + W \frac{\partial u}{\partial z} \right]}_{(2)} + \rho_0 \underbrace{\left[u \frac{\partial U}{\partial x} + v \frac{\partial U}{\partial y} + w \frac{\partial U}{\partial z} \right]}_{(2)} +$$

$$\underbrace{\rho \frac{\partial U}{\partial t}}_{(1)} + \rho \underbrace{\left[U \frac{\partial U}{\partial x} + V \frac{\partial U}{\partial y} + W \frac{\partial U}{\partial z} \right]}_{(2)} = - \frac{\partial p}{\partial x} \qquad 13.$$

$$\rho_0 \frac{\partial v}{\partial t} + \rho_0 \underbrace{\left[U \frac{\partial v}{\partial x} + V \frac{\partial v}{\partial y} + W \frac{\partial v}{\partial z} \right]}_{(2)} + \rho_0 \underbrace{\left[u \frac{\partial V}{\partial x} + v \frac{\partial V}{\partial y} + w \frac{\partial V}{\partial z} \right]}_{(2)} +$$

$$\underbrace{\rho \frac{\partial V}{\partial t}}_{(1)} + \rho \underbrace{\left[U \frac{\partial V}{\partial x} + V \frac{\partial V}{\partial y} + W \frac{\partial V}{\partial z} \right]}_{(2)} = - \frac{\partial p}{\partial y} \qquad 14.$$

$$\rho_0 \frac{\partial w}{\partial t} + \rho_0 \underbrace{\left[U \frac{\partial w}{\partial x} + V \frac{\partial w}{\partial y} + W \frac{\partial w}{\partial z} \right]}_{(2)} + \rho_0 \underbrace{\left[u \frac{\partial W}{\partial x} + v \frac{\partial W}{\partial y} + w \frac{\partial W}{\partial z} \right]}_{(2)} +$$

$$\underbrace{\rho \frac{\partial W}{\partial t}}_{(1)} + \rho \underbrace{\left[U \frac{\partial W}{\partial x} + V \frac{\partial W}{\partial y} + W \frac{\partial W}{\partial z} \right]}_{(2)} = - \frac{\partial p}{\partial z} \qquad 15.$$

$$\frac{\partial \rho}{\partial t} + U \frac{\partial \rho}{\partial x} + V \frac{\partial \rho}{\partial y} + W \frac{\partial \rho}{\partial z} + u \frac{\partial \rho_0}{\partial x} + v \frac{\partial \rho_0}{\partial y} + w \frac{\partial \rho_0}{\partial z} +$$

$$\rho_0 \left[\frac{\partial u}{\partial x} + \frac{\partial v}{\partial y} + \frac{\partial w}{\partial z} \right] + \rho \underbrace{\left[\frac{\partial U}{\partial x} + \frac{\partial V}{\partial y} + \frac{\partial W}{\partial z} \right]}_{(2)} = 0 \qquad 16.$$

$$\frac{\partial p}{\partial t} + U \frac{\partial p}{\partial x} + V \frac{\partial p}{\partial y} + W \frac{\partial p}{\partial z} + u \frac{\partial p_0}{\partial x} + v \frac{\partial p_0}{\partial y} + w \frac{\partial p_0}{\partial z} + \frac{\rho}{\rho_0} \frac{\partial p_0}{\partial t}$$

$$+ \frac{\rho}{\rho_0} \underbrace{\left[U \frac{\partial p_0}{\partial x} + V \frac{\partial p_0}{\partial y} + W \frac{\partial p_0}{\partial z} \right]}_{(3)} = \gamma R T_0 \left\{ \frac{\partial \rho}{\partial t} + U \frac{\partial \rho}{\partial x} + V \frac{\partial \rho}{\partial y} + W \frac{\partial \rho}{\partial z} + \right.$$

$$+ \underline{u \frac{\partial \rho_0}{\partial x}}_{③} + \underline{v \frac{\partial \rho_0}{\partial y}}_{③} + \underline{w \frac{\partial \rho_0}{\partial z}}_{③} + \underline{\frac{p}{p_0} \frac{\partial \rho_0}{\partial t}}_{①} + \frac{p}{p_0} \left\{ \underline{\left[U \frac{\partial \rho_0}{\partial x} \right]}_{③} + \underline{\left[V \frac{\partial \rho_0}{\partial y} \right]}_{②} + \underline{\left[W \frac{\partial \rho_0}{\partial z} \right]}_{②} \right\}$$

17.

The assumption that the basic flow is steady deletes the underlined terms numbered ① . The assumption that the basic flow is parallel implies that V and W are zero and that U depends only on z,[26] therefore the underlined terms numbered ② are deleted. The assumption of parallel flow also implies that the mean density ρ_0, pressure p_0 and temperature T_0 depend only on z, therefore the underlined terms numbered ③ are deleted. Finally, the usual boundary layer assumption that variation of the basic pressure p_0 over the boundary layer thickness may be neglected leads to the deletion of the underlined terms numbered ④ . Using the short hand notation

$$d(\ ) = \frac{\partial(\ )}{\partial t} + U \frac{\partial(\ )}{\partial x}$$

the equations resulting from these assumptions are:

$$d(u) + w \frac{\partial U}{\partial z} = - \frac{1}{\rho_0} \frac{\partial p}{\partial x} \qquad 18.$$

$$d(v) = - \frac{1}{\rho_0} \frac{\partial p}{\partial y} \qquad 19.$$

$$d(w) = - \frac{1}{\rho_0} \frac{\partial p}{\partial z} \qquad 20.$$

$$d(\rho) + w \frac{\partial \rho_0}{\partial z} + \rho_0 \left[\frac{\partial u}{\partial x} + \frac{\partial v}{\partial y} + \frac{\partial w}{\partial z} \right] = 0 \qquad 21.$$

$$d(p) - \gamma RT_0 \left[d(\rho) + w \frac{\partial \rho_0}{\partial z} \right] = 0 \qquad 22.$$

Equations 18-22 can be reduced by simple substitutions, differentiations and application of the operation d( ), to the single equation for the plate motion pressure p:

$$\frac{1}{c^2} d^3(p) - d(\nabla^2 p) + 2 \frac{\partial U}{\partial z} \frac{\partial^2 p}{\partial x \partial z} + \frac{1}{\rho_0} \frac{\partial \rho_0}{\partial z} d \left(\frac{\partial p}{\partial z} \right) = 0 \qquad 23.$$

Equation 23 written out in full is:

$$\frac{1}{c^2} \left[\frac{\partial^3 p}{\partial t^3} + 3U \frac{\partial^3 p}{\partial t^2 \partial x} + 3U^2 \frac{\partial^3 p}{\partial t \partial x^2} + U^3 \frac{\partial^3 p}{\partial x^3} \right] -$$

$$\left[\frac{\partial^3 p}{\partial t \partial x^2} + \frac{\partial^3 p}{\partial t \partial y^2} + \frac{\partial^3 p}{\partial t \partial z^2} \right] - U \left[\frac{\partial^3 p}{\partial x^3} + \frac{\partial^3 p}{\partial x \partial y^2} + \frac{\partial^3 p}{\partial x \partial z^2} \right]$$

$$+ 2 \frac{\partial U}{\partial z} \frac{\partial^2 p}{\partial x \partial z} + \frac{1}{\rho_0} \frac{\partial \rho_0}{\partial z} \left[\frac{\partial^2 p}{\partial t \partial z} + U \frac{\partial^2 p}{\partial x \partial z} \right] = 0 \qquad 24.$$

Equation 24 is the equation governing the plate motion pressure p, and is the equation to be used throughout the remainder of this paper. The basic flow quantities required for solution of equation 24 are the sound speed c, velocity U, and density ρ_0, all of which are functions of the space coordinate z as is appropriate for a compressible mean flow.

Equation 23 has been obtained previously by Dowell,[21] and for an incompressible basicflow equation 24 reduces to the equation obtained by Graham and Graham.[27] For classical

inviscid aerodynamic basic flow the gradients of U, ρ_0 and T_0 vanish and equation 18 to 22 can be shown to reduce to the classical convected wave equation:

$$\frac{\partial^2 p}{\partial t^2} + 2U \frac{\partial^2 p}{\partial x \partial t} + U^2 \frac{\partial^2 p}{\partial x^2} = c^2 \left(\frac{\partial^2 p}{\partial x^2} + \frac{\partial^2 p}{\partial y^2} + \frac{\partial^2 p}{\partial z^2} \right) \qquad 25.$$

Boundary and Initial Conditions

The solutions sought are for "steady" acoustic behavior in a steady basic flow. The steady state is considered to have been established by starting from complete rest throughout the system and continuing until transients have all died out. The boundary of the fluid is taken to be so far away from the plate that disturbances originating at the plate never reach the boundary: consequently one of the space boundary conditions is that for fluid locations far from the plate the acoustic disturbances must have only outgoing wave parts, or must be decreasing with increasing distance. The boundary condition at the surface where the fluid contacts the plate is basically that the fluid particles don't penetrate the plate. For the solution of the basic flow problem where viscosity has been retained this implies the "zero slip" boundary condition ordinarily used to derive boundary layer flow solutions. For the acoustic motion the boundary condition used allows particle velocities that are

tangent to the deflected plate surface. This is done to avoid the complications associated with boundary layer solutions for the acoustic flow. The fluid velocity at any point is given by

$$\bar{u}^* = \bar{U} + \bar{u},$$

$$= (U + u)\,\underline{i} + v\underline{j} + w\underline{k}.$$

Resolving velocities at the plate surfaces in figure 3 and requiring the velocity of the fluid normal to the plate to

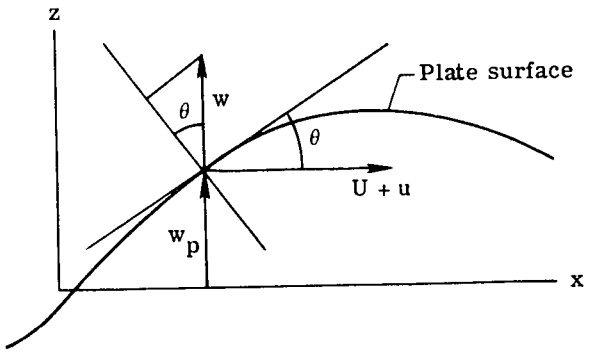

Figure 3.- Sketch of the velocity components at the plate surface.

be equal to the component of plate motion normal to plate, leads to

$$w \cos\theta - [U(z) + u] \sin\theta = \frac{\partial w_p}{\partial t} \cos\theta \qquad 26.$$

where w_p = plate displacement. But, linearizing implies θ, w_p, u, w << 1 and

$$\cos\theta = 1, \quad \sin\theta = \tan\theta = \frac{\partial w_p}{\partial x} \qquad 27.$$

This condition reduces equation 26 to

$$w\Big|_{z=0} - [U(z) + u]\Big|_{z=0} \frac{\partial w_p}{\partial x} = \frac{\partial w_p}{\partial t} \qquad 28.$$

But $u \frac{\partial w_p}{\partial x}$ is a product of small quantities, and $U(z)\big|_{z=0} = 0$.

Finally the boundary condition is

$$w(x,y,z,t)\big|_{z=0} = \frac{\partial w_p}{\partial t}(x,y,t) \qquad 29.$$

To introduce pressure in place of w, introduce the momentum equation:

$$\frac{\partial w}{\partial t} + U \frac{\partial w}{\partial x} = -\frac{1}{\rho_0} \frac{\partial p}{\partial z} \qquad 30.$$

On the plate surface U = 0, so equation 30 becomes

$$\frac{\partial w}{\partial t} = -\frac{1}{\rho_0} \frac{\partial p}{\partial z} \qquad 31.$$

Combining equations 29 and 31 yields

$$\frac{\partial w}{\partial t}\Big|_{z=0} = \frac{\partial^2 w_p}{\partial t^2} = -\frac{1}{\rho_0(0)} \frac{\partial p}{\partial z}\Big|_{z=0} \qquad 32.$$

This equation supplies the connection between the homogeneous equation governing fluid behavior (pressure) and the non-homogeneous plate equation.

For the case of constant basic flow, equation 28 becomes

$$w(x,y,z,t)\big|_{z=0} = \frac{\partial w_p}{\partial t} + U \frac{\partial w_p}{\partial x} = \left(\frac{\partial}{\partial t} + U \frac{\partial}{\partial x}\right) w_p. \qquad 33.$$

Combining equations 30 and 33 leads to

$$-\frac{1}{\rho_0}\frac{\partial p}{\partial z} = \left(\frac{\partial}{\partial t} + U\frac{\partial}{\partial x}\right) w = \left(\frac{\partial}{\partial t} + U\frac{\partial}{\partial x}\right)\left(\frac{\partial}{\partial t} + U\frac{\partial}{\partial x}\right) w_p.$$

So the boundary condition for the constant basic velocity case is

$$\frac{\partial p}{\partial z}\Big|_{z=0} = -\rho_0(0)\left(\frac{\partial}{\partial t} + U\frac{\partial}{\partial x}\right)\left(\frac{\partial}{\partial t} + U\frac{\partial}{\partial x}\right) w_p. \qquad 34.$$

Chapter III

Solutions for Plate Response and Acoustic Pressure

In this chapter solutions are obtained for the system of equations and boundary conditions obtained in Chapter II. The solutions obtained are also shown to reduce to known special cases. Attention is focused on the effects of the boundary layer; other aspects of the solution are simplified. For continuity of presentation the plate equation solution and the acoustic equation solution are each given as a separate unit, however, it will be observed that the solutions of the two equations are interdependent. Thus the effect of the fluid pressure due to plate motion is included in the solution for plate motion. Therefore, these solutions could be used to study panel flutter or stability of a boundary layer as well as panel response.

The Governing Non-Dimensional Equations

The equations to be solved are given in Chapter II, equation 2 governs plate motion, equation 24 governs the fluid pressure, and equation 32 governs the boundary condition that couples the plate motion to the acoustic pressure. Additional boundary conditions require that waves be outgoing at large distance above the plate, and that plate displacement be zero in the region of the x-y plane occupied by the baffle (see fig. 1). For simplicity only harmonic

forces, and therefore harmonic responses, will be considered. Only the steady state part of the solution, not the transient part, will be determined. In addition, the plate will be taken to be infinitely wide and the response will be taken to be independent of the y coordinate. These assumptions are expressed mathematically by putting the force in the form:

$$q(x,y,t) = \bar{q}(x)\ \exp(i\omega t), \tag{35.}$$

and by putting the responses in the form

$$\left.\begin{aligned} w_p(x,y,t) &= \bar{w}(x)\ \exp(i\omega t) && \text{a} \\ p(x,y,z,t) &= \bar{p}(x,z)\ \exp(i\omega t) && \text{b} \end{aligned}\right\} \tag{36.}$$

Greater efficiency in the solution will be obtained by using the following non-dimensional quantities:

$$\left.\begin{aligned} x &= \hat{x}L \\ z &= \hat{z}L \\ \bar{w} &= \hat{w}L \\ \bar{p} &= \rho_0(0)\ \omega^2 L^2 \hat{p} \\ \Omega^2 &= \rho_p \omega^2 L^4/D \\ \mu &= \rho_0(0)L/\rho_p \\ \hat{q} &= \bar{q}L^3/D \end{aligned}\right\} \tag{37.}$$

Note that in these equations D is the plate stiffness parameter (not the differential operator) and μ is the mass

ratio (not viscosity). Substitution of equations 35, 36, and 37 into the dimensional governing equations leads to the non-dimensional governing equations:

$$\frac{\partial^4 \hat{w}}{\partial \hat{x}^4} - \Omega^2 \hat{w} + \mu\Omega^2 \hat{p}(\hat{x},0) = \hat{q} \qquad 38.$$

$$\frac{\partial \hat{p}}{\partial \hat{z}}\Big|_{\hat{z}=0} = \hat{w} \quad \text{(on the plate)} \qquad 39.$$

and $$\left[-i\hat{p} - (3U/L\omega)\frac{\partial \hat{p}}{\partial \hat{x}} + 3i\,(U/L\omega)^2 \frac{\partial^2 \hat{p}}{\partial \hat{x}^2} + (U/L\omega)^3 \frac{\partial^3 \hat{p}}{\partial \hat{x}^3}\right]$$

$$-i\,(c/L\omega)^2\left[\frac{\partial^2 \hat{p}}{\partial \hat{x}^2} + \frac{\partial^2 \hat{p}}{\partial \hat{z}^2}\right] - (U/L\omega)(c/L\omega)^2\left[\frac{\partial^3 \hat{p}}{\partial \hat{x}^3} + \frac{\partial^3 \hat{p}}{\partial \hat{x}\partial \hat{z}^2}\right]$$

$$+2\,(c/L\omega)^2\left[\partial(U/L\omega)/\partial \hat{z}\right]\frac{\partial^2 \hat{p}}{\partial \hat{x}\partial \hat{z}} + (c/L\omega)^2 \frac{1}{\rho_0}\frac{\partial \rho_0}{\partial \hat{z}}\left[i\frac{\partial \hat{p}}{\partial \hat{z}} + (U/L\omega)\frac{\partial^2 \hat{p}}{\partial \hat{x}\partial \hat{z}}\right] = 0 \qquad 40.$$

In the following sections of this Chapter solutions are developed, first for the plate equation 38, then for the fluid acoustic equation 40 using boundary condition 39.

Solution of the Plate Equation

Reduction to Matrix Equation.- The plate differential equation 38 can be reduced to a matrix equation by means of an eigenfunction expansion as follows. First orthogonal eigenfunctions are obtained for the differential operator

by solution of:

$$\frac{\partial^4 \hat{w}_m}{\partial \hat{x}^4} = \lambda_m \hat{w}_m \qquad 41.$$

Simple support boundary conditions are used herein.

The orthogonality condition requires that

$$\int_0^1 \hat{w}_n(\hat{x})\, \hat{w}_m(\hat{x}) = 1 \quad \text{when } m = n$$
$$= 0 \quad \text{when } m \neq n. \qquad 42.$$

Then the plate displacement $\hat{w}(\hat{x})$ is expressed in the series of eigenfunctions $\hat{w}_m(\hat{x})$ as

$$\hat{w}(\hat{x}) = \sum_{n=1}^{N} a_n \hat{w}_n(\hat{x}) \qquad 43.$$

where the unknown coefficients a_n become the dependent variables to be found instead of $\hat{w}(\hat{x})$. Substitution of equation 43 into equation 38, followed by the standard use of the orthogonality condition 42 leads to the equation:

$$a_m(\lambda_m - \Omega^2) + \mu\Omega^2 \int_0^1 \hat{p}(\hat{x},0)\, \hat{w}_m(\hat{x})\, d\hat{x} = Q_m \qquad 44.$$

where the generalized force Q_m is given by

$$Q_m = \int_0^1 \hat{q}(\hat{x})\, \hat{w}_m(\hat{x})\, d\hat{x}. \qquad 45.$$

Further reduction of equation 44 can be made using knowledge of the form of the solution of pressure $\hat{p}(\hat{x},0)$. As shown

in the next section of this Chapter, solution of the acoustic equation for $\hat{p}(\hat{x},0)$ can be carried out using the Fourier transform pair

$$\left.\begin{aligned} \overset{\circ}{p}(\hat{k},\hat{z}) &= \int_{-\infty}^{\infty} \hat{p}(\hat{x},\hat{z}) \exp[-i\hat{k}\hat{x}]\, d\hat{x} \qquad \text{a} \\ \text{and}\quad \hat{p}(\hat{x},\hat{z}) &= \frac{1}{2\pi} \int_{-\infty}^{\infty} \overset{\circ}{p}(\hat{k},\hat{z}) \exp[i\hat{k}\hat{x}]\, d\hat{k} \qquad \text{b} \end{aligned}\right\} \quad 46.$$

and the series expression for transformed pressure $\overset{\circ}{p}$

$$\overset{\circ}{p}(\hat{k},\hat{z}) = \sum_{n=1}^{N} a_n \overset{\circ}{p}_n(\hat{k},\hat{z}) \qquad 47.$$

The a_n in equation 47 are the same as the a_n in equation 43. Substitution of expressions 46b and 47 into equation 44, interchange of the order of integration and summation, and use of the definitions

$$Z_m(\hat{k}) = \int_0^1 \hat{w}_m(\hat{x}) \exp(i\hat{k}\hat{x})\, d\hat{x} \qquad 48.$$

and

$$B_{mn} = \frac{1}{2\pi} \int_{-\infty}^{\infty} Z_m(\hat{k})\, \overset{\circ}{p}_n(\hat{k},0)\, d\hat{k} \qquad 49.$$

reduces equation 44 to the form

$$a_m(\lambda_m - \Omega^2) + \mu\Omega^2 \sum_{n=1}^{N} B_{mn}\, a_n = Q_m \qquad 50.$$

Equation 50 is the basic equation to be solved for the unknown coefficients a_m. The a_m determine the plate

displacement and the fluid pressures through the relations

$$w(\hat{x},y,t) = L\, e^{i\omega t} \sum_{n=1}^{N} a_n \hat{w}_n(\hat{x}) \qquad 51.$$

$$p(\hat{x},y,\hat{z},t) = \left[(\rho_0(0)\omega^2 L^2/2\pi)\, e^{i\omega t} \sum_{n=1}^{N} a_n \int_{-\infty}^{\infty} \overset{\circ}{p}_n(\hat{k},\hat{z}) e^{ik\hat{x}\hat{x}}\, d\hat{k}\right] \qquad 52.$$

Equation 51 has been obtained by combination of equations 36, 37, and 43; the $\hat{w}_n(\hat{x})$ must be found from the eigenvalue problem equation 41 together with boundary conditions at the edges of the plate. Equation 52 has been obtained by combination of equations 36, 37, 46, and 47; the functions $\overset{\circ}{p}_n(\hat{k},\hat{z})$ must of course be obtained by solution of the acoustic equation.

When the parameters entering the dimensionless equations 38 and 40 are given, the only unknowns in equation 50 are the a_m. Then equation 50 can be used to form a matrix equation that can be solved for the vector $\{a_1\ a_2 \ldots a_N\}$ using a procedure such as Gauss elimination. Equation 50 contains the coupling between the plate motion and the acoustic (aerodynamic) pressure in the term B_{mn}, therefore the stability properties (flutter, hydrodynamic instability) of the plate-fluid system can be obtained by appropriate solution procedures. In the present study, however, the system is assumed to be stable and the solution sought is the magnitude

of the plate displacement and the acoustic pressure when a given force Q_m is applied. In addition, the present study is concerned with the effects of boundary layer profiles on response, rather than with the complexities of solution of equation 50, therefore approximate response solutions of 50 are developed in the following sections.

Solution for small mass ratio μ.- Equation 50 holds for each value of m from 1 to N. When all N equations are written out they can be arranged in the following matrix form:

$$[\sim\alpha\sim]\{a\} + \mu\,[B]\,\{a\} = \{Q\}, \tag{53.}$$

where

$$\{a\} = \begin{Bmatrix} a_1 \\ a_2 \\ \vdots \\ a_N \end{Bmatrix} ; \; [\sim\alpha\sim] = \begin{bmatrix} \alpha_1 & 0 & & \\ 0 & \alpha_2 & & \\ & & \ddots & \\ & & & \alpha_N \end{bmatrix} \quad ,\alpha_j = (\lambda_j - \Omega^2)/\Omega^2 \tag{54.}$$

$$[B] = \begin{bmatrix} B_{11} & B_{12} & \cdots & B_{1N} \\ B_{21} & B_{22} & \cdots & B_{2N} \\ \vdots & \vdots & \cdots & \vdots \\ B_{N1} & B_{N2} & \cdots & B_{NN} \end{bmatrix} \quad ; \text{ and } \{Q\} = \frac{1}{\Omega^2} \begin{Bmatrix} Q_1 \\ Q_2 \\ \vdots \\ Q_N \end{Bmatrix}$$

To solve equation 53 it is assumed that $\mu << 1$, so the solution can be expressed as

$$\{a\} = \{a\}_0 + \mu\{a\}_1 + \mu^2\{a\}_2 + \cdots \tag{55.}$$

Substituting 55 into 53 and equating coefficients of each power of μ leads to the solution

$$\{a\} = [\alpha]^{-1} \left([I] - \mu[B][\alpha]^{-1}\right) \{Q\} + O(\mu^2) \qquad 56.$$

When higher order terms are dropped, equation 56 yields the following expression for each a_m.

$$a_m = \left[1 - \mu \sum_{n=1}^{N} B_{mn} \Omega^2 Q_n / [Q_m(\lambda_n - \Omega^2)] \right] Q_m/(\lambda_m - \Omega^2) \qquad 57.$$

Using the B_{mn} found from solution of the acoustic equation, the a_m from equation 57 are used in equations 51 and 52 to obtain the plate displacement and the acoustic pressure.

Solution of the Acoustic (Aerodynamic) Equation

The acoustic pressure is governed by equation 40, subject to the boundary condition equation 39 and a radiation condition. The procedure for solution of equation 40 uses a Fourier transform in the $\hat{x}$ variable to reduce the partial differential equation to an ordinary differential equation whose solutions are expressed in transfer matrix form.

Reduction to an Ordinary Differential Equation.- The transform pair for pressure, equation 46, reduces the partial differential equation 40 as follows. Equation 40 is multiplied by $\exp(-i\hat{k}\hat{x})\, d\hat{x}$, integrated from $-\infty$ to ∞, and the integrals reduced by integration by parts. The resulting

equation governing the transformed pressure $\overset{\circ}{p}$ is

$$\frac{\partial^2 \overset{\circ}{p}}{\partial \hat{z}^2} - \left[\frac{2M\hat{c}}{1+cM\bar{U}} \frac{\partial \bar{U}}{\partial \hat{z}} + \frac{1}{\rho_0} \frac{\partial \rho_0}{\partial \hat{z}} \right] \frac{\partial \overset{\circ}{p}}{\partial \hat{z}} + \left[\left(\frac{1+M\hat{c}\bar{U}}{\bar{c}\,\hat{c}} \right)^2 - 1 \right] \hat{k}^2 \overset{\circ}{p} = 0 \qquad 58.$$

Similar transformation of the boundary condition equation 39, and use of the series expression for $\hat{w}(\hat{x})$ yields

$$\frac{\partial \overset{\circ}{p}}{\partial \hat{z}} \Big|_{\hat{z}=0} = \sum_{n=1}^{N} Z_n^* (\hat{k})\, a_n \qquad 59.$$

Equation 58 is linear and homogeneous, therefore the solution will depend linearly on the boundary conditions, equation 59. As a result a solution can be obtained for each term of the boundary condition series and the complete solution is then the sum of these separate solutions. For convenience the a_n are included in the series expression as follows:

$$\overset{\circ}{p}(\hat{k},\hat{z}) = \sum_{n=1}^{N} a_n \overset{\circ}{p}_n (\hat{k},\hat{z}) \qquad (47.)$$

It is now clear that each $\overset{\circ}{p}_n$ must satisfy equation 58 and the boundary condition

$$\frac{\partial \overset{\circ}{p}_n}{\partial \hat{z}} \Big|_{\hat{z}=0} = Z_n^* (\hat{k}) \qquad 60.$$

Additional radiation boundary conditions must also be included. We now observe that when $\overset{\circ}{p}_n$ is obtained from equations

58 and 60, the result is to be inserted into equation 49 to obtain the B_{mn} which are then used to obtain the a_m coefficients from equation 57. Finally the a_m determine the plate displacement and pressure by equations 51 and 52.

General Solution by Transfer Matrix.- Equation 58 is an ordinary differential equation with variable coefficients. The coefficients are variable as a result of variations, through the boundary layer, of velocity $\bar{U} = U(\hat{z})/U_\infty$, density $\rho_0(z)$, and sound speed $\bar{c} = c(\hat{z})/c_\infty$. In general the solutions will not be obtainable as known functions, so numerical procedures must be used. In addition the boundary conditions are in two parts, that is, to obtain $\overset{o}{p}$ at $\hat{z}=0$ one boundary condition on $\partial\overset{o}{p}/\partial\hat{z}$ is given at $\hat{z}=0$ and the radiation condition is applied at some large value of $\hat{z}$. A convenient means of expressing the solution for these conditions is transfer matrices.[28] Before carrying out the solution the radiation condition will be developed.

For the profiles of interest in this study the coefficients of equation 58 are constant for very large values of $\hat{z}$ because of the boundary layer nature of the basic flow velocity, density and sound speed. In order to apply the radiation condition it is assumed that $\bar{U}$, $\bar{c}$ and ρ_0 are exactly constant for all values of $\hat{z} > \delta$. Then δ is the dimensionless boundary layer thickness. It is now convenient to change the independent variable to $\overset{o}{z}$ where: $\hat{z} = \delta\,\overset{o}{z}$.

The governing equation and boundary conditions are now:

$$\frac{\partial^2 \overset{\circ}{p}_n}{\partial \overset{\circ}{z}^2} - \left[\frac{2\hat{M}\hat{c}}{1+\hat{M}\hat{c}\bar{U}} \frac{\partial \bar{U}}{\partial \overset{\circ}{z}} + \frac{1}{\rho_0} \frac{\partial \rho_0}{\partial \overset{\circ}{z}}\right] \frac{\partial \overset{\circ}{p}_n}{\partial \overset{\circ}{z}} + \left[\left(\frac{1+\hat{M}\hat{c}\bar{U}}{\hat{c}\,\bar{c}}\right)^2 - 1\right] \delta^2 \hat{k}^2 \overset{\circ}{p}_n = 0, \tag{61.}$$

and

$$\left.\frac{\partial \overset{\circ}{p}_n}{\partial \overset{\circ}{z}}\right|_{\overset{\circ}{z}=0} = \delta\, Z_n^*(\hat{k}) \tag{62.}$$

Now, outside the boundary layer ($\overset{\circ}{z} > 1$) equation 61 reduces to

$$\frac{\partial^2 \overset{\circ}{p}_n}{\partial \overset{\circ}{z}^2} + \left[\left(\frac{1}{\hat{c}} + M\right)^2 - 1\right] \delta^2 \hat{k}^2 \overset{\circ}{p}_n = 0 \tag{63.}$$

Equation 63 has constant coefficients and solutions

$$\overset{\circ}{p}_n = A_n \exp(ia\overset{\circ}{z}) + B_n \exp(-ia\overset{\circ}{z}), \tag{64.}$$

If

$$a^2 = \left[\left(\frac{1}{\hat{c}} + M\right)^2 - 1\right] \delta^2 \hat{k}^2 > 0; \tag{65.}$$

and

$$\overset{\circ}{p}_n = c_n \exp(b\overset{\circ}{z}) + D_n \exp(-b\overset{\circ}{z}), \tag{66.}$$

If

$$a^2 = -b^2 < 0. \tag{67.}$$

Substitution of solution equation 64 into the pressure expression equation 52 shows that only outgoing waves will be

present if $A_n = 0$. Outgoing waves have the form $\exp(i\omega t - ia\overset{\circ}{z})$. Substitution of equation 66 into the pressure equation 52 shows that only decreasing pressures will be present if $C_n = 0$. Now the procedure for solution of equation 61 subject to the "radiation" condition and boundary condition equation 62 can be summarized as follows. Equation 61 will be solved for $0 < \overset{\circ}{z} < 1$, the resulting $\overset{\circ}{p}_n$ will be forced to satisfy boundary condition equation 62 at $\overset{\circ}{z}=0$, and be matched at $\overset{\circ}{z} = 1$ to the solution

$$\overset{\circ}{p}_n(\hat{k},\overset{\circ}{z}) = B_n \exp(-ia\overset{\circ}{z}), \qquad 68.$$

if $a^2 > 0$;

or to the solution

$$\overset{\circ}{p}_n(\hat{k},\overset{\circ}{z}) = D_n \exp(-b\overset{\circ}{z}), \qquad 69.$$

if $a^2 < 0$.

This procedure can be carried out efficiently using the transfer matrix technique. The transfer matrix idea is to relate the pressure $\overset{\circ}{p}_n$ and the derivative of pressure $\overset{\circ}{p}'_n$ at any two values of $\overset{\circ}{z}$ by the relation

$$\begin{Bmatrix} \overset{\circ}{p}_n \\ \overset{\circ}{p}'_n \end{Bmatrix}_{\overset{\circ}{z}=\overset{\circ}{z}_1} = \begin{bmatrix} \bar{T}_{11} & \bar{T}_{12} \\ \bar{T}_{21} & \bar{T}_{22} \end{bmatrix} \begin{Bmatrix} \overset{\circ}{p}_n \\ \overset{\circ}{p}'_n \end{Bmatrix}_{\overset{\circ}{z}=\overset{\circ}{z}_2} \qquad 70.$$

The values of the $\bar{T}_{ij}$ depend of course on the two values of

z. To apply the boundary conditions at $\overset{\circ}{z}_1 = 1$ and $\overset{\circ}{z}_2 = 0$ we use equations 68, 69 and 62 in 70 to obtain

$$B_n e^{-ia} \begin{Bmatrix} 1 \\ -ia \end{Bmatrix} = \begin{bmatrix} T_{11} & T_{12} \\ T_{21} & T_{22} \end{bmatrix} \begin{Bmatrix} \overset{\circ}{p}_n(\hat{k},0) \\ \delta\ Z_n^* \end{Bmatrix} \qquad 71.$$

when $a^2 > 0$;

and

$$D_n e^{-b} \begin{Bmatrix} 1 \\ -b \end{Bmatrix} = \begin{bmatrix} T_{11} & T_{12} \\ T_{21} & T_{22} \end{bmatrix} \begin{Bmatrix} \overset{\circ}{p}_n(\hat{k},0) \\ \delta\ Z_n^* \end{Bmatrix} \qquad 72.$$

when $a^2 < 0$.

Equations 71 and 72 each form a set of two linear algebraic equations in the two unknowns $\overset{\circ}{p}_n$ and B_n, and $\overset{\circ}{p}_n$ and D_n, respectively, and can be solved for $\overset{\circ}{p}_n$ to obtain:

$$\overset{\circ}{p}_n(\hat{k},0) = -\delta Z_n^* (ia\ T_{12} + T_{22})/(ia\ T_{11} + T_{21}), \qquad 73.$$

when $a^2 > 0$;

and

$$\overset{\circ}{p}_n(\hat{k},0) = -\delta Z_n^* (b\ T_{12} + T_{22})/(b\ T_{11} + T_{21}) \qquad 74.$$

when $a^2 < 0$.

Derivation of the T_{ij} for given coefficients of equation 61 can be carried out using standard numerical techniques; examples are presented in later sections of this paper. The expressions 73 and 74 for $\overset{\circ}{p}_n$ are now the final results required

for the computation of plate displacement and pressure using equations 51 and 52.

The solution procedure is as follows. Values for $\overset{\circ}{p}_n(\hat{k},0)$ from equations 73 and 74 are inserted into equation 49 together with the mode transform $Z_m(\hat{k})$ to obtain values of B_{mn}. These values are used in equation 57, along with the generalized forces Q_m and values of the parameters, to obtain the series coefficients a_m. The a_m are then used in equations 51 and 52 to obtain the plate displacement and acoustic pressure. In order to obtain pressure at a non-zero value of $\hat{z}$ from equation 52, values of $\overset{\circ}{p}_n(\hat{k},\hat{z})$ are obtained from the transfer matrix equation 70 using the particular values $\overset{\circ}{z}_1 = \hat{z}/\delta$ to obtain $\overset{\circ}{p}_n(\hat{k},\hat{z})$, and $\overset{\circ}{z}_2 = 0$ where $\overset{\circ}{p}_n(\hat{k},0)$ is known.

Solution for $\bar{T}_{ij}$ by Numerical Integration.- In general the coefficients of equation 61 will be sufficiently complicated that analytical or series solutions will be impractical, therefore numerical integration must be considered. Two regions of numerical solution must be considered; one region near the singular point of equation 61, and the other region covering the rest of the interval $0 \leq \overset{\circ}{z} \leq 1$.

The singularity of equation 61 is associated with the zero of the denominator of the coefficient of the first derivative term. The location of this singularity on the $\hat{k}$ axis is of interest because of the integrations on $\hat{k}$ that must be carried out to obtain B_{mn} and pressure. The

coefficient of $\partial p_n/\partial z$ is singular where

$$1 + M\lambda \hat{k}\, U\,(z) = 0 \qquad 75.$$

In this expression $\hat{c} = \hat{k}\lambda$ has been used. Equation 75 shows that when $\hat{k} > 0$ there is no singularity; when $\hat{k} < 0$ but $|\hat{k}| < 1/(\lambda M)$ there is no singularity because the velocity $\bar{U}(z)$ has values in the interval $0 < \bar{U}(z) < 1$; and when $\hat{k} < 0$ and $|\hat{k}| > 1/(\lambda M)$ the singularity is located at values of z obtained from the equation

$$\bar{U}(z) = 1/(M\lambda/|\hat{k}|) \qquad 76.$$

A sketch of these results is shown in figure 4.

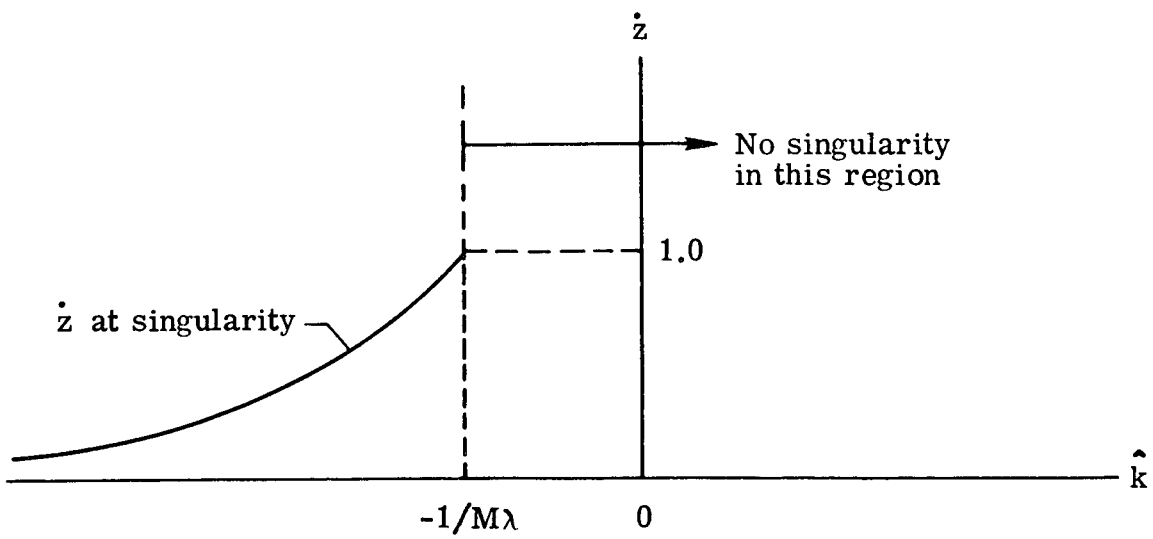

Figure 4.- Location of singularity in equation 61.

The particular shape of the curve locating the singularity will depend on the particular variation of $\bar{U}(\overset{\circ}{z})$. Solution of equation 61 in the region near the singularity could be carried out using a Taylor series expansion of the coefficients and a power series solution of the equation.

Solution of equation 61 in the region away from the singularity can be carried out using the procedure of reference 28. To begin, change notation so that equation 61 appears as

$$\frac{\partial^2 p}{\partial \overset{\circ}{z}^2} - a(\overset{\circ}{z}) \frac{\partial p}{\partial \overset{\circ}{z}} + b(\overset{\circ}{z})\, p = 0. \qquad 77.$$

The definition of $a(\overset{\circ}{z})$, $b(\overset{\circ}{z})$ and p can be seen by comparison of equation 77 with equation 61. Next define

$$z_1 = p \ , \ z_2 = \frac{\partial p}{\partial \overset{\circ}{z}} \ , \text{ and } \overset{\circ}{z} = s \qquad 78.$$

so that now equations 77 and the second of these relations can be written

$$\frac{\partial}{\partial s} \begin{Bmatrix} z_1 \\ z_2 \end{Bmatrix} = \begin{bmatrix} 0 & 1 \\ -b(s) & a(s) \end{bmatrix} \begin{Bmatrix} z_1 \\ z_2 \end{Bmatrix} \qquad 79.$$

Equation 79 is the same form as equation 5-45 of reference 28, therefore 79 has the solution presented in the reference.

Writing

$$\{Z\} = \begin{Bmatrix} Z_1 \\ Z_2 \end{Bmatrix} \quad \text{and} \quad \left[A(s)\right] = \begin{bmatrix} 0 & 1 \\ -b(s) & a(s) \end{bmatrix} \qquad 80.$$

the solution obtained from reference 28 is

$$z_{n+1} = z_n + \frac{1}{6}\,(k_0 + 2k_1 + 2k_2 + k_3)$$

where $k_0 = hA(s_n)Z_n \qquad k_1 = hA\left(s_n + \frac{h}{2}\right)\left(Z_n + \frac{k_0}{2}\right)$

$$k_2 = hA\left(s_n + \frac{h}{2}\right)\left(Z_n + \frac{k_1}{2}\right)$$

$$k_3 = hA\left(s_n + h\right)\left(Z_n + k_2\right)$$

$A(s_n)$, $A(s_n + h)$, and $A(s_n + h/2)$ are, respectively, the values of the matrix A(s) at the sections n and n + 1 and at the section midway between n and n + 1.

Combining the above unnumbered equations gives the relation between z_{n+1} and z_n :

$$Z_{n+1} = \Bigg\{ I + \frac{h}{6}\left[A(s_n) + 4A\left(s_n + \frac{h}{2}\right) + A(s_n + h)\right] + \frac{h^2}{6}\left[A\left(s_n + \frac{h}{2}\right)A(s_n) + A(s_n + h)A\left(s_n + \frac{h}{2}\right) + A^2\left(s_n + \frac{h}{2}\right)\right] + \frac{h^3}{12}\left[A^2\left(s_n + \frac{h}{2}\right)A(s_n) +\right.$$

$$+ A(s_n + h)\ A^2\left(s_n + \frac{h}{2}\right)\Big] + \frac{h^4}{24}\ A(s_n + h)\ \times$$

$$A^2\left(s_n + \frac{h}{2}\right) A(s_n)\Big\}\ Z_n \qquad 81.$$

where the contents of the braces represents the transfer matrix linking the state vectors Z_n and Z_{n+1}. Equation 81 relates Z at two closely spaced points. To relate Z at two arbitrarily spaced points in $\overset{\circ}{z}$, write 81 as

$$\{Z\}_{n+1} = [t_n]\{Z\}_n$$

and then combine by substitution for several values of n to obtain

$$\{Z\}_N = [t_{N-1}][t_{N-2}] \ \ldots\ [t_2][t_1][t_0]\{Z\}_0, \qquad 82.$$

where N is the number of the station corresponding to the desired value of $\overset{\circ}{z}$ and 0 denotes the station where the vector {Z} is known. Reverting to the notation 78 and combining the product of the $[t_i]$ matrices into a single matrix, equation 82 appears as

$$\left\{\begin{matrix} p \\ \frac{\partial p}{\partial z} \end{matrix}\right\}_{\substack{\circ \\ z=z_1}}^{\circ} = \begin{bmatrix} \bar{T}_{11} & \bar{T}_{12} \\ \bar{T}_{21} & \bar{T}_{22} \end{bmatrix} \left\{\begin{matrix} p \\ \frac{\partial p}{\partial z} \end{matrix}\right\}_{\substack{\circ \\ z=z_0}}^{\circ} \qquad 83.$$

The $\bar{T}_{ij}$ appearing in equation 83 are the required transfer matrix elements for use in equation 70.

Solution for $\bar{T}_{ij}$ by Series for Mach No. < 1.- Temperature profiles presented in reference 29 indicate that the rise of temperature in a compressible boundary layer is not large when Mach number is less than 1. For these Mach numbers a reasonable approximation is that sound speed ratio, $\bar{c} = c(z)/c_\infty$, is unity and that density ρ_0 is constant. In addition, the velocity profiles presented in reference 29 suggest that the simplest representation having the character of a boundary layer profile is:

$$\text{velocity ratio } \bar{U} = U(\overset{\circ}{z})/U_\infty = \overset{\circ}{z} \qquad 84.$$

While this representation is not a closely accurate description, it does have two advantageous uses. First, equation 84 does represent the general character of the boundary layer profile, therefore results obtained using it are expected to be at least a first approximation to the correct results. This linear description has been used previously in acoustic studies.[27] Second, use of the description 84 leads to a reasonably simple equation governing pressure, such that solutions can be obtained in series form. These series results can be compared with results from the numerical integration procedure to help gain confidence in the results of both procedures by providing two independent solutions. Having this confidence the numerical integration procedure can then be used to obtain more precise results using more realistic representation of the boundary layer

profile. No essential increase of difficulty appears to be associated with the inclusion of temperature variations in the numerical integration technique.

Using the representation $\bar{c} = 1$, ρ_0 = constant and $\bar{U} = \overset{\circ}{z}$ equation 61 becomes

$$\frac{\partial^2 \overset{\circ}{p}_n}{\partial \overset{\circ}{z}^2} - \frac{2M\hat{c}}{1+M\hat{c}\overset{\circ}{z}} \frac{\partial \overset{\circ}{p}_n}{\partial \overset{\circ}{z}} + \left[\left(\frac{1+M\hat{c}\overset{\circ}{z}}{\hat{c}} \right)^2 - 1 \right] \hat{c}^2 \hat{\delta}^2 \overset{\circ}{p}_n = 0 \qquad 85.$$

Introducing the notation

$$\begin{aligned} x &= 1 + M\hat{c}\overset{\circ}{z} & p &= \overset{\circ}{p}_n \\ \alpha &= \hat{\delta}^2/M^2\hat{c}^2 & \beta &= \hat{\delta}^2/M^2 \end{aligned} \qquad 86.$$

reduces 85 to

$$x^2 p'' - 2xp' - (\beta x^2 - \alpha x^4)\, p = 0 \qquad 87.$$

Equation 87 has a regular singular point at $x = 0$, and can be solved in series form in the neighborhood of the singularity by the method described in reference 30, Theorem 4.4, p. 188 (Frobenius method). The solution obtained is:

$$p(x) = A\, p_1(x) + B\, p_2(x) \qquad 88.$$

where

$$p_1(x) = |x|^3 \left\{ 1 + a_2 x^2 + \sum_{\substack{n=4 \\ n \text{ even}}}^{\infty} a_n x^n/[n(n+3)] \right\} \qquad 89.$$

with $a_0 = 1$, $a_2 = .1\beta$, $a_n = \beta\, a_{n-2} - \alpha\, a_{n-4}$

and

$$p_2(x) = 1 + a_2\, x^2 + \sum_{\substack{n=4 \\ n \text{ even}}}^{\infty} a_n\, x^n/[n(n-3)] \qquad 90.$$

with $a_0 = 1$,

$a_2 = -.5\beta$,

$a_n = \beta\, a_{n-2} - \alpha\, a_{n-4}$

From the theorem of reference 30, the series appearing in equations 89 and 90 are convergent. Equations 89 and 90 show that $p_1(x)$ and $p_2(x)$ are defined for both positive and negative values of x, and are finite and continuous at x = 0. Because Mach number M appears in the denominator of α and β, the solution 89 and 90 may converge slowly for small M. The reduction of this solution to the limits M = 0 or $\delta = 0$, $M \neq 0$ to demonstrate reduction to known solution does not appear to be straightforward. For these reasons a second series solution is developed.

In the neighborhood of an ordinary point of equation 85 a series solution can be obtained by the method of reference 30, theorem 4.1. The solution obtained by that method is:

$$\overset{\circ}{p}_n\ (\overset{\circ}{z}) = c\ f_1\ (\overset{\circ}{z}) + D\ f_2\ (\overset{\circ}{z}) \qquad 91.$$

where

$$f_1(\overset{\circ}{z}) = 1 + a_2\,\overset{\circ}{z}^2 + a_3\,\overset{\circ}{z}^3 + a_4\,\overset{\circ}{z}^4 + \sum_{n=5}^{\infty} a_n\,\overset{\circ}{z}^n \qquad 92.$$

with

$$a_0 = 1 \qquad a_1 = 0$$

$$a_2 = -\frac{1}{2}\,\hat{\delta}^2[1 - \hat{c}^2]$$

$$a_3 = -\frac{1}{3}\,M\hat{c}\hat{\delta}^2\,[2 - \hat{c}^2]$$

$$a_4 = \frac{1}{4}\,\hat{\delta}^2\left[\frac{1}{6}\,\hat{\delta}^2[1 - \hat{c}^2]^2 - M^2\,\hat{c}^2\right]$$

and

$$f_2(\overset{\circ}{z}) = \overset{\circ}{z} + a_2\,\overset{\circ}{z}^2 + a_3\,\overset{\circ}{z}^3 + a_4\,\overset{\circ}{z}^4 + \sum_{n=5}^{\infty} a_n\,\overset{\circ}{z}^n \qquad 93.$$

with

$$a_0 = 0, \qquad a_1 = 1$$

$$a_2 = M\hat{c}$$

$$a_3 = \frac{1}{3}\left[M^2\,\hat{c}^2 - \frac{1}{2}\,\hat{\delta}^2\,[1 - \hat{c}^2]\right]$$

$$a_4 = -\frac{1}{6}\,M\hat{c}\hat{\delta}^2\,[2 - \hat{c}^2]$$

and, for both $f_1(\overset{\circ}{z})$ and $f_2(\overset{\circ}{z})$

$$a_n = \Big\{-(n-1)(n-2)M\hat{c}\,a_{n-1} + 2(n-1)M\hat{c}\,a_{n-1} - [1-\hat{c}^2]\,\hat{\delta}^2\,a_{n-2}$$
$$-[3-\hat{c}^2]\,M\hat{c}\hat{\delta}^2\,a_{n-3} - 3M^2\hat{c}^2\,\hat{\delta}^2\,a_{n-4} - M^3\,\hat{c}^3\,\hat{\delta}^2\,a_{n-5}\Big\}$$
$$/[n(n-1)].$$

The function $\hat{p}_n(\hat{z})$ defined by equations 91-93 can be used to obtain the transfer matrices for use in equation 70. The particular transfer matrix relating pressure on the plate surface $\overset{\circ}{z} = 0$ to pressure at the edge of the boundary layer

$\overset{\circ}{z} = 1$ is obtained as follows. The relation for $\overset{\circ}{p}_n$ and its derivative can be written as

$$\begin{Bmatrix} \overset{\circ}{p}_n \\ \overset{\circ}{p}'_n \end{Bmatrix}_{\overset{\circ}{z}} = \begin{bmatrix} f_1(\overset{\circ}{z}) & f_2(\overset{\circ}{z}) \\ f'_1(\overset{\circ}{z}) & f'_2(\overset{\circ}{z}) \end{bmatrix} \begin{Bmatrix} a_0 \\ a_1 \end{Bmatrix} \tag{94.}$$

Evaluation of the f matrix for $\overset{\circ}{z} = 0$ using equations 92 and 93 shows that

$$\begin{Bmatrix} \overset{\circ}{p}_n \\ \overset{\circ}{p}'_n \end{Bmatrix}_{\overset{\circ}{z}=0} = \begin{Bmatrix} a_0 \\ a_1 \end{Bmatrix} \tag{95.}$$

Combining equations 94 and 95 and evaluating at $\overset{\circ}{z} = 1$ shows that the transfer matrix elements required for solution of equations 73 and 74 are given by

$$\begin{bmatrix} T_{11} & T_{12} \\ T_{21} & T_{22} \end{bmatrix} = \begin{bmatrix} f_1(1) & f_2(1) \\ f'_1(1) & f'_2(1) \end{bmatrix} \tag{96.}$$

Solution for Zero Boundary Layer Thickness

The solution procedures developed in this Chapter can be checked by comparing a pressure distribution for zero boundary layer thickness with the pressure distribution presented in reference 31 based on inviscid aerodynamic flow. The pressures given in reference 31 are based on an elastic

plate of infinite extent undergoing displacements in the form of a traveling harmonic wave. The pressures for this situation are obtained using the method of this thesis starting with equations 39 and 40. Equations 39 and 40, and the "radiation" boundary condition, are sufficient to determine the pressures for a given plate displacement $\hat{w}$. A traveling wave in the plate can be represented as

$$w\ (x,y,\ t) = a_0\ \exp\ i\ (\omega t + kx), \qquad 97.$$

and the pressure solution corresponding to this plate motion can be written as

$$p\ (x,y,z,t) = \sigma(z)\ \exp\ i\ (\omega t + kx) \qquad 98.$$

Converting to non-dimensional quantities and substituting equations 97 and 98 into equations 39 and 40 leads to the results that $\sigma(z)$ must satisfy the ordinary differential equation 58, (and therefore 85), subject to the boundary conditions of "radiation" at $\hat{z} \to \infty$ and

$$\left.\frac{\partial \hat{\sigma}}{\partial \hat{z}}\right|_{\hat{z}=0} = a_0 \qquad 99.$$

This boundary value problem is the same as that satisfied by $\overset{\circ}{p}_n$ when $Z_n^*(\hat{k})$ is replaced by "a_0", as can be seen from equations 58-60. (This result suggests the following interpretation of the $\overset{\circ}{p}_n(\hat{k},\hat{z})$: $\overset{\circ}{p}_n(\hat{k},\hat{z})$ represents the

pressure in the fluid due to an infinitely long harmonic wave on the plate surface traveling with wave speed ω/k and wavelength $1/k$. The function $Z_n^*(\hat{k})$ determines the amplitude of each wave component so that the sum of all the traveling waves on the plate will form the model function $\hat{w}_n(\hat{x})$.) Therefore the solution derived for $\overset{\circ}{p}_n(\hat{k},0)$ can be used for σ, with Z_n^* replaced by "a_0". From equation 74, the solution for $\hat{\sigma}$ is

$$\hat{\sigma}(\hat{k},0) = -\delta a_0 \ (b\ T_{12} + T_{22})/(b\ T_{11} + T_{21}) \qquad 100.$$

Note that this solution, derived for $a^2 < 0$, reduces to the solution (equation 73) derived previously for $a^2 > 0$. The T_{ij} are related to the series solutions of the governing equation 58, $f_1(\overset{\circ}{z})$ and $f_2(\overset{\circ}{z})$ by

$$\begin{bmatrix} T_{11} & T_{12} \\ T_{21} & T_{22} \end{bmatrix} = \begin{bmatrix} f_1(1) & f_2(1) \\ f_1'(1) & f_2'(1) \end{bmatrix} \qquad (96)$$

The function f_1 and f_2 and their derivatives can be evaluated for zero boundary layer thickness $\hat{\delta} = 0$ from equations 92 and 93 to obtain

$$\begin{bmatrix} T_{11} & T_{12} \\ T_{21} & T_{22} \end{bmatrix} = \begin{bmatrix} 1 & 1 + M\hat{c} + \frac{1}{3} M^2 \hat{c}^2 \\ 0 & 1 + 2M\hat{c} + M^2 \hat{c}^2 \end{bmatrix} \qquad 101.$$

Substitution of the T_{ij} from equation 101 into equation 100 yields

$$\hat{\sigma}(\hat{k},0) = -\lambda\ a_0\ (1+M\hat{c})^2 / \sqrt{\hat{c}^2-(1+M\hat{c})^2} \qquad 102.$$

Substitution of 102 into the dimensional pressure expression, equation 98, yields

$$p(x,0,t) = -\rho_0\ \omega^2 L^2 \lambda\ a_0 (1+M\hat{c})^2 / \sqrt{\hat{c}^2-(1+M\hat{c})^2}\ \exp i(\omega t+kx) \qquad 103.$$

Comparison of this result with the pressure expression given in reference 31 must take account of the use by reference 31 of a coordinate system moving at the free stream velocity U; and the use of a wave moving in the positive x direction, whereas the wave described by equation 97 is moving in the negative x direction. The coordinate relative to the moving axis x' is related to the fixed axis x by

$$x' = x - Ut$$

and the speed of the wave relative to x' is

$$c' = \frac{\omega}{k} - U \qquad 104.$$

Using the definition of $\hat{c}$ leads to

$$(1+M\hat{c}) = 1 + \left(\frac{U}{c_\infty}\right)(kL)\left(\frac{c_\infty}{L\omega}\right) = \frac{k}{\omega}\left(\frac{\omega}{k} + U\right) \qquad 105.$$

so the pressure expression equation 103 reduces to

$$p(x,0,t) = -\rho_0 c'^2\ a_0\ k \left[1-\left(\frac{c'}{c_\infty}\right)^2\right]^{-\frac{1}{2}} \exp i(-k)\left[c't-x'\right] \qquad 106.$$

When the names of the variables in equation 106 are changed to agree with the notation used in reference 31, the pressure expression, equation 106, is the same as the expression for surface pressure obtained by combining equations (2.4a) and (3.5) of reference 31. This result lends confidence in the correctness of the analysis methods used in this paper.

Computations

The computation procedures used to obtain numerical values of plate displacement and acoustic pressure are described in this section. The primary quantities required to obtain displacement from equation 51 and pressure from equation 52 are the coefficients a_n and the pressure quantities $\overset{\circ}{p}_n(\hat{k},\hat{z})$.

The coefficients a_m are determined from equation 57, the approximation for small μ :

$$a_m = \left[1 - \mu \sum_{n=1}^{N} B_{mn}\, \Omega^2 Q_n / [Q_m(\lambda_n - \Omega^2)] \right] Q_m / (\lambda_m - \Omega^2). \qquad (57)$$

To determine a_m the quantities B_{mn} and Q_m are needed:

$$B_{mn} = \frac{1}{2\pi} \int_{-\infty}^{\infty} \overset{\circ}{p}_n(\hat{k},0)\; Z_m(\hat{k})\, d\hat{k}, \qquad (49)$$

where $$Z_m(\hat{k}) = \int_0^1 \hat{w}_m(\hat{x})\; e^{i\hat{k}\hat{x}} d\hat{x}; \qquad (48)$$

and $$Q_m = \int_0^1 \hat{q}(\hat{x})\; \hat{w}_m(\hat{x})\; d\hat{x}. \qquad (45)$$

The eigenfunctions $\hat{w}_m(\hat{x})$ and eigenvalues λ_m are obtained by solution of

$$\frac{\partial^4 \hat{w}_m(\hat{x})}{\partial \hat{x}^4} = \lambda_m \hat{w}_m(\hat{x}) \tag{41}$$

subject to boundary conditions at $\hat{x} = 0$ and $\hat{x} = 1$. For the conventional simply supported boundary conditions where plate deflection and moment are zero at both ends of the plate the solutions of 41 are

$$\hat{w}_m(\hat{x}) = \sqrt{2} \sin m\pi \hat{x}, \quad \lambda_m = (m\pi)^4 \tag{107.}$$

From these eigenfunctions equation 48 yields

$$Z_m(\hat{k}) = m\pi \sqrt{2} \left\{ \frac{1-(-1)^m \cos \hat{k}}{m^2\pi^2-\hat{k}^2} - i \frac{(-1)^m \sin \hat{k}}{m^2\pi^2-\hat{k}^2} \right\} \tag{108.}$$

The real and imaginary parts of $Z_1(\hat{k})$ are illustrated in figure 5. Figure 5 shows that the Z_m functions decrease in magnitude quickly as $\hat{k}$ increases, indicating that integrals such as equation 49 need not necessarily cover a large range of $\hat{k}$.

The force distribution used in these computations is

$$\hat{q}(\hat{x}) = \sqrt{2} \sin \pi \hat{x} \tag{109.}$$

so the generalized force Q_m, equation 45, is

$$\left.\begin{aligned} Q_m &= 1 \quad \text{for} \quad m = 1 \\ Q_m &= 0 \qquad\quad m \neq 1 \end{aligned}\right\} \tag{110.}$$

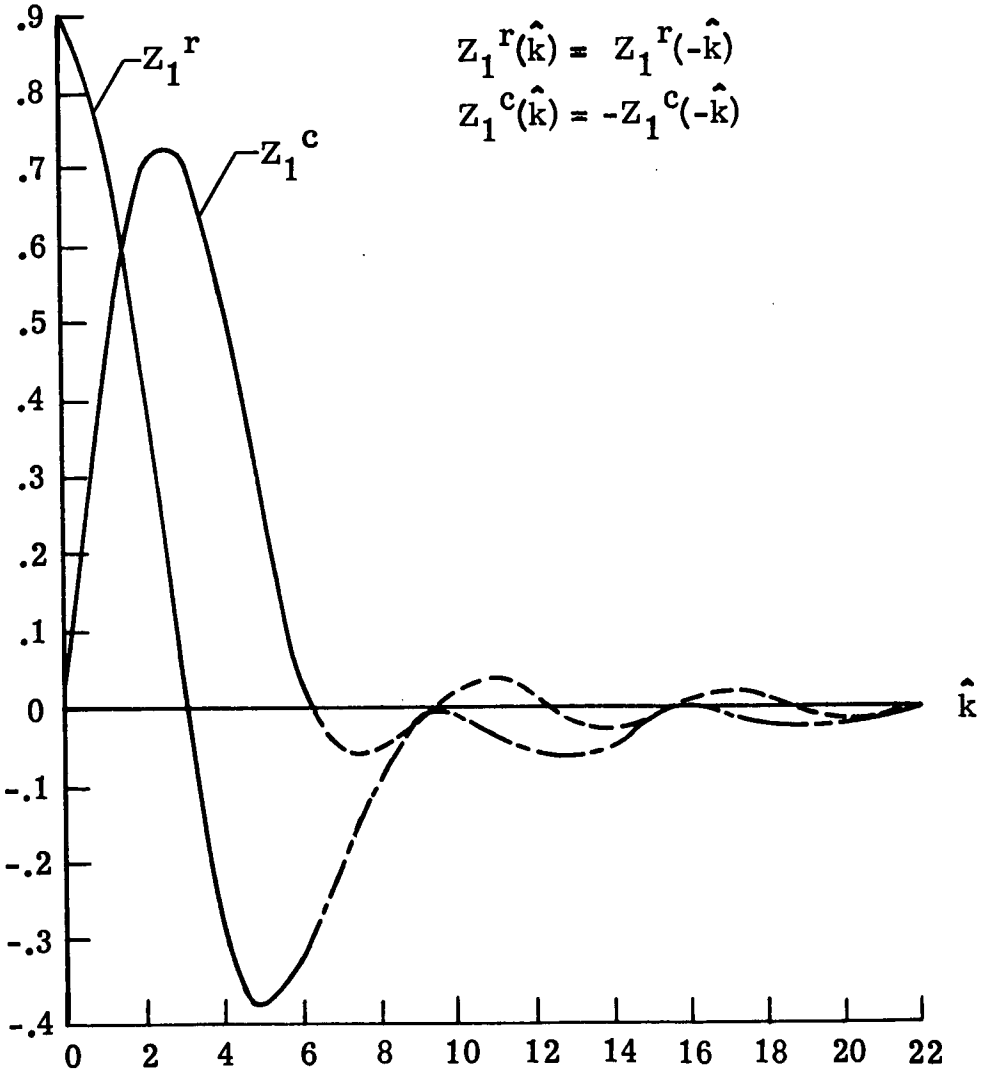

Figure 5.- Transform of the mode function.

Using this result, and the eigenvalues from equation 107, in equation 57 leads to the expressions for the first few coefficients a_m

$$\left.\begin{aligned} a_1 &= \left[1 - \mu B_{11} \Omega^2/(\pi^4 - \Omega^2)\right] /(\pi^4 - \Omega^2) && \text{a} \\ a_2 &= -\mu B_{21} \Omega^2/\left[(\pi^4 - \Omega^2)(2^4\pi^4 - \Omega^2)\right] && \text{b} \\ a_3 &= -\mu B_{31} \Omega^2/\left[(\pi^4 - \Omega^2)(3^4\pi^4 - \Omega^2)\right] && \text{c} \end{aligned}\right\} \quad 111.$$

For Ω^2 very nearly equal to π^4 the first coefficient a_1 is large compared to the other a_m, therefore for this study it is assumed that $a_m = 0$ for $m \neq 1$ and equations 111a is used for a_1. Using this result the plate displacement and pressure are written:

$$\left.\begin{aligned} \hat{w}(x,t) &= a_1\sqrt{2} \sin \pi\hat{x}\, e^{i\omega t} \\ p(x,z,t) &= \left(\rho_0(0)\omega^2 L^2/2\pi\right)\, a_1\, e^{i\omega t} \int_{-\infty}^{\infty} \overset{\circ}{p}_1(\hat{k},\overset{\circ}{z}) e^{i\hat{k}\hat{x}}\, d\hat{k} \end{aligned}\right\} \quad 112.$$

The next quantities required are the $\overset{\circ}{p}_n(\hat{k},\hat{z})$ so the integrals in equations 112 and 49 (the B_{mn} integral required for calculation of a_1) can be evaluated. The expressions for the $\overset{\circ}{p}_n(\hat{k},0)$ are (only $\overset{\circ}{p}_1$ is needed):

$$\overset{\circ}{p}_1(\hat{k},0) = -\delta\, Z_1^*\, (ia\, T_{12} + T_{22})/(ia\, T_{11} + T_{21}) \qquad (73)$$

when $a^2 > 0$;

and

$$\overset{\circ}{p}_1(\hat{k},0) = -\delta\ Z_1^*\ (b\ T_{12} + T_{22})/(b\ T_{11} + T_{21}) \tag{74}$$

when $a^2 < 0$.

The transfer elements are given by

$$\begin{bmatrix} T_{11} & T_{12} \\ T_{21} & T_{22} \end{bmatrix} = \begin{bmatrix} f_1(1) & f_2(1) \\ f_1'(1) & f_2'(1) \end{bmatrix} \tag{96}$$

and the functions f_1 and f_2 used here are the series expressions derived for small Mach number, equations 92 and 93. To evaluate $\overset{\circ}{p}_n(\hat{k},\hat{z})$ the general form of the transfer matrix, equation 70, is used, to obtain

$$\overset{\circ}{p}_n(\hat{k},\hat{z}) = \bar{T}_{11}\ \overset{\circ}{p}_n(\hat{k},0) + \bar{T}_{12}\ \overset{\circ}{p}_n'(\hat{k},0) \tag{113.}$$

For these calculations pressures were calculated only on the plate $\overset{\circ}{z}=0$ and at the edge of the boundary layer $\overset{\circ}{z}=1$. On the plate surface

$$\bar{T}_{11} = 1 \quad \bar{T}_{12} = 0 \tag{114.}$$

and at the edge of the boundary layer

$$\bar{T}_{11} = T_{11},\ \bar{T}_{12} = T_{12} \tag{115.}$$

The real and imaginary parts of $\overset{\circ}{p}_1(\hat{k},0)$ are defined by

$$\overset{\circ}{p}_1(\hat{k},0) = -\lambda\ Z_1^* \left[\frac{\delta p_r}{\lambda} + i\ \frac{\delta p_c}{\lambda}\right] \tag{116.}$$

The quantities $\frac{\delta p_r}{\lambda}$ and $\frac{\delta p_c}{\lambda}$ are shown in figures 6 and 7

plotted as a function of $\hat{c}$ for Mach number of 0.5 and several values of δ/λ. Figure 6 shows that for moderate values of δ/λ the curves for $\frac{\delta p_c}{\lambda}$ are smooth, so no numerical difficulties were anticipated in numerical integration of this function (and none were encountered). Figure 6 also shows that, as the value of δ/λ becomes smaller, the curves approach the curve for $\delta/\lambda = 0$. This result provides numerical support for the result obtained previously by analytical methods.

Figure 7 shows that the real part $\frac{\delta p_r}{\lambda}$ is a smooth function except in the region $\hat{c} \simeq -.65$. Further examination shows that $\frac{\delta p_r}{\lambda}$, and therefore $\overset{\circ}{p}_1(\hat{k},0)$, has a singularity in this region of $\hat{c}$; the exact value of $\hat{c}$ depends on the Mach number and on δ/λ. Examination of the equation for $\overset{\circ}{p}_1(\hat{k},0)$, equation 74, shows that the singularity is associated with a zero of the denominator, i.e.

$$b\, T_{11} + T_{21} = 0, \qquad 117.$$

and is of the form $|\hat{c} - \hat{c}_0|^{-1}$. Numerical values of the integrands of B_{11} and I_1 (an integral involving $\overset{\circ}{p}_1(\hat{k},0)$ to be discussed in a later section of this paper) are shown in figure 8. Figure 8 indicates also that the singularity has the form $|\hat{c} - \hat{c}_0|^{-1}$. The appearance of this singularity for a real value of $\hat{c}$ indicates that the function being transformed - $\hat{p}(\hat{x},0)$ - has some sort of non-regular behavior, such

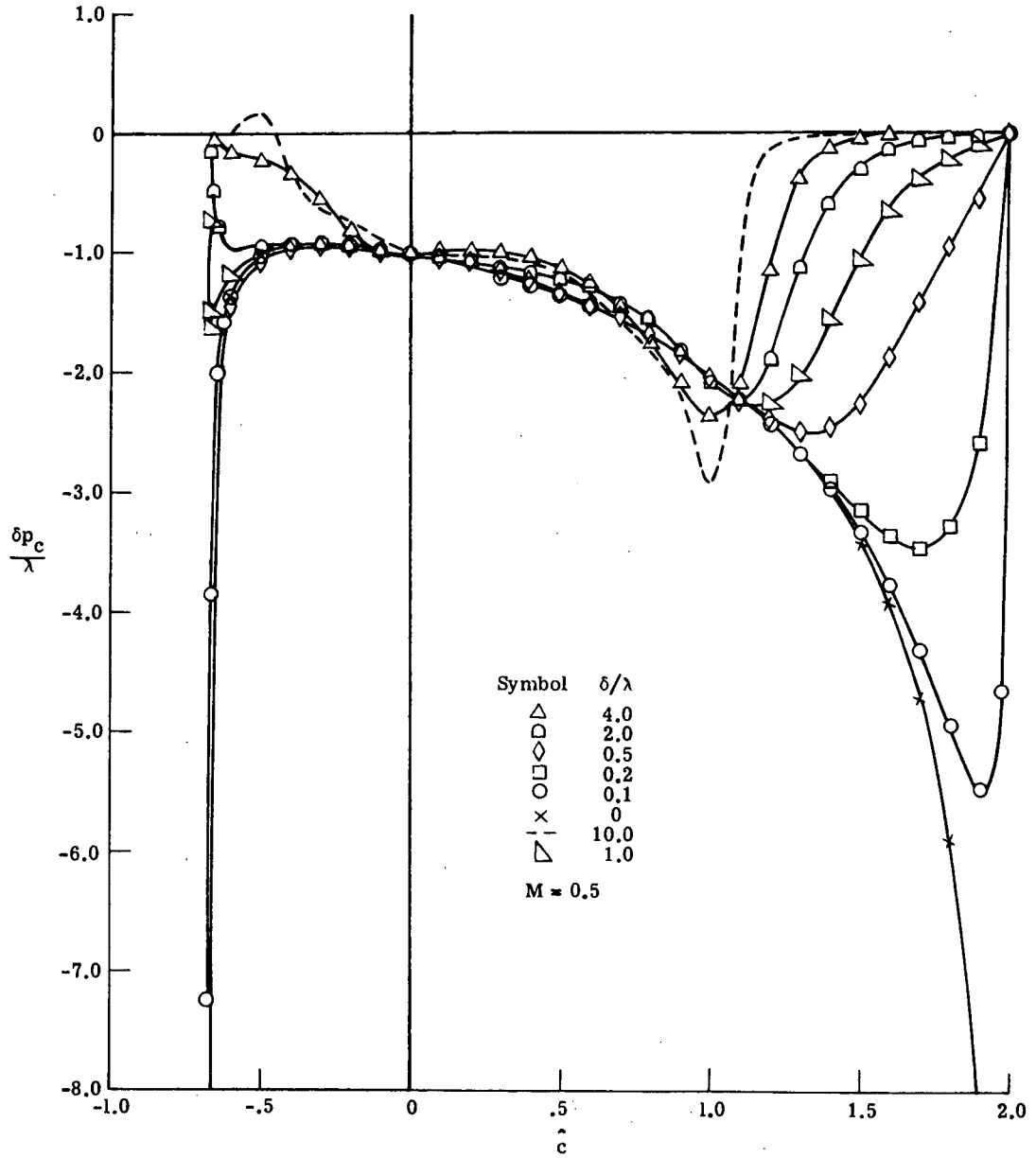

Figure 6.- Complex part of the pressure coefficient, $\delta p_c/\lambda$.

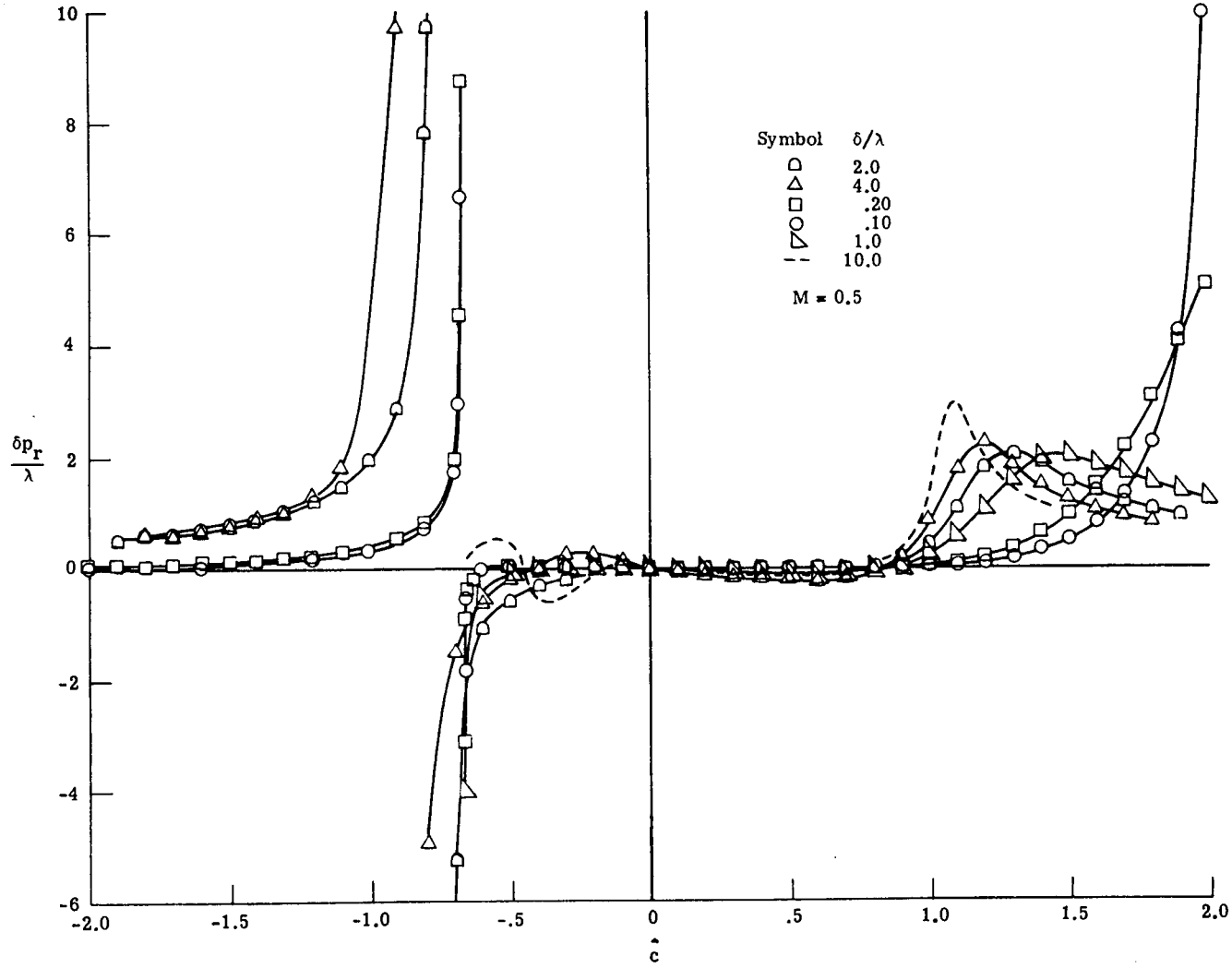

Figure 7.- Real part of the pressure coefficient, $\delta p_r/\lambda$.

as not becoming zero for large $\hat{x}$, for the value of $\hat{c}$ at the singularity. Consequently the transforms, equation 46, must be regarded in a generalized sense and their existence established by an extension of the Fourier integral theorem as discussed in reference 33. The result of this generalization is that the variable $\hat{c}$ or $\hat{k}$ must be regarded as a complex variable, the integral involving $\overset{\circ}{p}_1(\hat{k},0)$ must be regarded as a contour integral, and the path of integration must be carefully chosen so that appropriate boundary (radiation) conditions are satisfied.

Referring to equation 112, p. 53, shows that an inverse transform of the function $\overset{\circ}{p}_1(\hat{k},0)$ must be performed to obtain the pressure on the plate surface $p(x,0,t)$. Comparison of equation 73 with 74 shows that $\overset{\circ}{p}_1(\hat{k},0)$ can be written

$$\overset{\circ}{p}_1(\hat{k},0) = -\delta Z_1^* \frac{\frac{T_{12}\delta}{\lambda}\sqrt{\hat{c}^2 - (1+M\hat{c})^2} + T_{22}}{\frac{T_{11}\delta}{\lambda}\sqrt{\hat{c}^2 - (1+M\hat{c})^2} + T_{21}} \qquad 118.$$

provided that the square root is handled properly to yield the form in equation 73 when the radical changes sign. Equation 118 shows that $\overset{\circ}{p}_1(\hat{k},0)$ has two branch points in addition to the simple pole resulting from the vanishing of the denominator. Writing the radical in the form

$$\sqrt{\hat{c}^2 - (1+M\hat{c})^2} = \sqrt{1-M^2}\sqrt{\hat{c} + (M+1)^{-1}}\sqrt{\hat{c} + (M-1)^{-1}} \qquad 119.$$

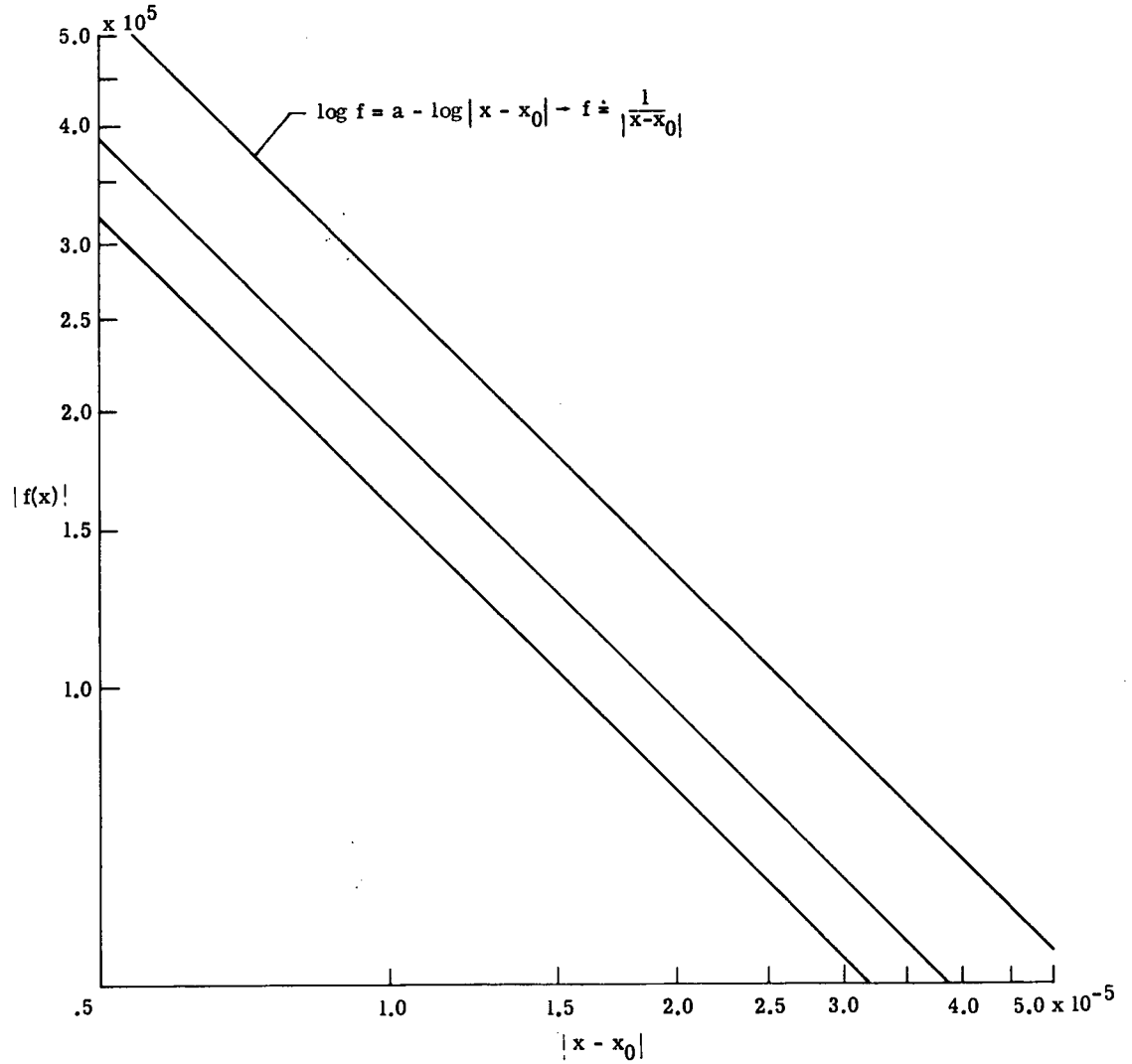

Figure 8.- Integrands of B_{11} and I_1 near the singular point.

shows the branch points to be at $\hat{c} = -\frac{2}{3}$ and $\hat{c} = 2$ when Mach number M is 0.5. These branch points and their corresponding branch cuts are shown in figure 9 along with the pole and the chosen path of integration. The location of the branch cuts was chosen so that the radical would assume the correct form for real values of $\hat{c}$ as demanded by equations 73 and 74. The path of integration was indented below the pole for the following reason. Assume the integration for p(x,0,t), equation 112 was to be performed by contour integration for positive $\hat{x}$. With the path closed in the upper half $\hat{c}$ plane the integral around $\hat{c}$ = infinity would vanish by Jordan's Lemma and the residue of the pole would be included with a contribution from integration along the branch cut and any other singularities present. It can be shown that the residue from this pole contributes a wave that propagates in the positive $\hat{x}$ direction; this wave satisfies the outgoing wave radiation condition and is appropriately included only for positive $\hat{x}$.

In view of the path of integration shown in figure 9, the integration of equation 112 must be broken up into Cauchy principle parts along the real axis and integration along the semi-circles around the poles and branch points. The Cauchy principle part of the integration along the real axis was carried out numerically using a 10-point Runge-Kutta for region away from the singularity (pole) and a rectangular rule using the value of the function

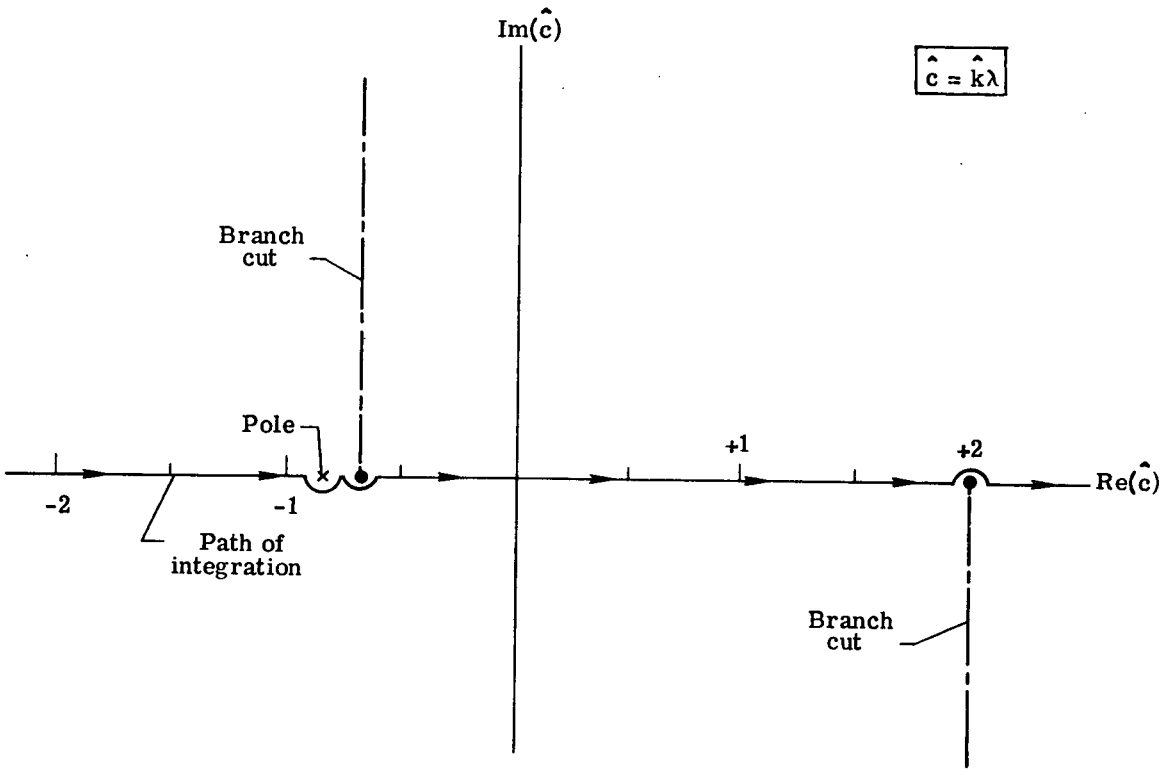

Figure 9.- Complex transform variable $\hat{c}$ plane.

at the mid-point of the interval in the region including the pole. The limit was taken by increasing the number of integration steps with a fixed $\hat{c}$ interval until the value of the integral was unchanged by doubling the number of steps. As the number of steps was increased the values of the function for symmetrically placed steps (with respect to the pole) became closer and closer together in absolute value near the singularity (as the function $\frac{1}{x}$ would be for $x = +1$ and $x = -1$) but having opposite signs and thus canceling out each others contribution to the integral. The integral on the semi-circle around the pole was evaluated using the half-residue in accordance with theorem IV, p. 530 of reference 34. The integrals on the semi-circles around the branch points are always zero according to theorem III, p. 530 of reference 34.

The numerical values presented in this paper were calculated using the equations presented in Tables I to V. A sample of the functions integrated as indicated in Table II is shown in figures 10-13. These figures show that the values of the integrands are small near the ends of the $\hat{c}$ interval shown, indicating that integration over this interval will give correct values of the integrals.

TABLE I: Complete Pressure Coefficient - Including Integral and Singularity Contributions

A. Complete Pressure Coefficient C_p^c is given by:

$$C_p^c = \left\{1+i\mu\frac{\lambda \text{Res}2}{2a_1}\frac{\Omega^2}{(\pi^4-\Omega^2)^2}\right\} C_p(\hat{x})+i\pi a_1 \text{Res}1-\mu\lambda\frac{\pi}{2}\frac{\Omega^2}{(\pi^4-\Omega^2)^2}\text{Res}1\text{Res}2 \qquad \text{I-1}$$

where

$$\text{Res } 1 = \left\{-\frac{\delta}{\lambda} Z_1^* e^{i\hat{k}\hat{x}}(b\ T_{12}+T_{22})/\left[\frac{d}{d\hat{k}}(b\ T_{11}+T_{21})\right]\right\}_{\hat{k}=\hat{k}_0} \qquad \text{I-2}$$

$$\text{Res } 2 = \left\{\frac{\delta}{\lambda}\left[(Z_1^r)^2+(Z_1^c)^2\right](b\ T_{12}+T_{22})/\left[\frac{d}{d\hat{k}}(b\ T_{11}+T_{21})\right]\right\}_{\hat{k}=\hat{k}_0} \qquad \text{I-3}$$

$$a_1 = \frac{1}{\pi^4-\Omega^2}\left[\left(1-\mu B_{11}^r\frac{\Omega^2}{\pi^4-\Omega^2}\right)-i\left(\mu B_{11}^c\frac{\Omega^2}{\pi^2-\Omega^2}\right)\right] \qquad \text{I-4}$$

B.

To obtain:	See Table:
$C_p(x)$	II
b, T_{ij}	III or IV
$\frac{d}{d\hat{k}}\left[b\ T_{11} + T_{21}\right]$	V
B_{11}^r, B_{11}^c	II

C. The quantitiy $\hat{k}_0$ is the value of $\hat{k}$ satisfying $b\ T_{11} + T_{21} = 0$.

TABLE II: The Integral Part of Pressure Coefficient $C_p(\hat{x})$

A. The magnitude $R(\hat{x})$ and phase $\phi(\hat{x})$ of the pressure coefficient (integral part) are given by

$$R(\hat{x}) = \sqrt{\left[C_p^r(\hat{x})\right]^2 + \left[C_p^c(\hat{x})\right]^2} \qquad \text{II-1}$$

$$\phi(\hat{x}) = \tan^{-1} \frac{C_p^c(\hat{x})}{C_p^r(\hat{x})} \qquad \text{II-2}$$

$$C_p(\hat{x}) = C_p^r(\hat{x}) + i\, C_p^c(\hat{x}) \qquad \text{II-3}$$

and

$$C_p(x) = \frac{I_1^r + i\, I_1^c}{\pi^4 - \Omega^2} \left[\left(1 - \mu B_{11}^r \frac{\Omega^2}{\pi^4 - \Omega^2} \right) - i \left(\mu B_{11}^c \frac{\Omega^2}{\pi^4 - \Omega^2} \right) \right] =$$

$$\frac{a_1}{\lambda} (I_1^r + i\, I_1^c) \qquad \text{II-4}$$

where

$$B_{11}^r = \frac{-\lambda}{2\pi} \int_{-20}^{20} \left[(Z_1^r)^2 + (Z_1^c)^2 \right] \frac{\delta p_r}{\lambda} \, d\hat{k}, \qquad \text{II-5}$$

$$B_{11}^c = \frac{-\lambda}{2\pi} \int_{-20}^{20} \left[(Z_1^r)^2 + (Z_1^c)^2 \right] \frac{\delta p_c}{\lambda} \, d\hat{k}, \qquad \text{II-6}$$

$$Z_1^r = \pi \sqrt{2} \, \frac{1 + \cos \hat{k}}{\pi^2 - \hat{k}^2}, \qquad \text{II-7}$$

$$Z_1^c = \pi \sqrt{2} \, \frac{\sin \hat{k}}{\pi^2 - \hat{k}^2} \qquad \text{II-8}$$

TABLE II (concl.)

$$I_1^r = \int_{-20}^{20} \left(\frac{\delta \bar{T}_{12}}{\lambda} - \frac{\delta p_r}{\lambda} \bar{T}_{11} \right) \left(z_1^r \cos \hat{k}\hat{x} + z_1^c \sin \hat{k}\hat{x} \right) d\hat{k}$$

$$+ \int_{-20}^{20} \frac{\delta p_c}{\lambda} \bar{T}_{11} \left(z_1^r \sin \hat{k}\hat{x} - z_1^c \cos \hat{k}\hat{x} \right) d\hat{k} \qquad \text{II-9}$$

$$I_1^c = -\int_{-20}^{20} \frac{\delta p_c}{\lambda} \bar{T}_{11} \left(z_1^r \cos \hat{k}\hat{x} + z_1^c \sin \hat{k}\hat{x} \right) d\hat{k}$$

$$+ \int_{-20}^{20} \left(\frac{\delta \bar{T}_{12}}{\lambda} - \frac{\delta p_r}{\lambda} T_{11} \right) \left(z_1^r \sin \hat{k}\hat{x} - z_1^c \cos \hat{k}\hat{x} \right) d\hat{k} \qquad \text{II-10}$$

B. To obtain: See Table

$\frac{\delta p_r}{\lambda}$, $\frac{\delta p_c}{\lambda}$, T_{ij} III or IV

C. The values of $\bar{T}_{11}$ and $\bar{T}_{12}$ are,

i) $\hat{z} = 0$ $\bar{T}_{11} = 1$, $\bar{T}_{12} = 0$ II-11

ii) $\hat{z} = 1$ $\bar{T}_{11} = T_{11}$ $\bar{T}_{12} = T_{12}$ II-12

TABLE III: Pressure Coefficients $\frac{\delta p_r}{\lambda}$, $\frac{\delta p_c}{\lambda}$ by Series Solution

A. Pressure Coefficients are determined by:

i) when $a^2 > 0$

$$\frac{\delta p_r}{\lambda} + i\,\frac{\delta p_c}{\lambda} = \frac{\delta}{\lambda}\,\frac{i\,a\,T_{12} + T_{22}}{i\,a\,T_{11} + T_{21}} \qquad \text{III-1}$$

ii) when $a^2 < 0$

$$\frac{\delta p_r}{\lambda} + i\,\frac{\delta p_c}{\lambda} = \frac{\delta}{\lambda}\,\frac{b\,T_{12} + T_{22}}{b\,T_{11} + T_{21}} \qquad \text{III-2}$$

B. To calculate T_{11}, T_{21}:

$$T_{11} = 1 + a_2 + a_3 + a_4 + \sum_{n=5}^{N} a_n \qquad \text{III-3}$$

$$T_{21} = 2a_2 + 3a_3 + 4a_4 + \sum_{n=5}^{N} n\,a_n \qquad \text{III-4}$$

where $a_0 = 1 \quad a_1 = 0$

$$a_2 = -\frac{\delta^2}{2\lambda^2}\,(1 - \hat{c}^2) \qquad a_3 = -\frac{\hat{Mc}\,\delta^2}{3\lambda^2}\,(2 - \hat{c}^2)$$

$$a_4 = \frac{\delta^4}{24\lambda^4}\,(1 - \hat{c}^2)^2 - \frac{\delta^2 M^2 \hat{c}^2}{4\lambda^2} \qquad \text{III-5}$$

$$a_n = \frac{1}{n(n-1)}\left\{-(n-1)(n-4)\hat{Mc}\,a_{n-1} - \frac{\delta^2}{\lambda^2}\,(1 - \hat{c}^2)\,a_{n-2}\right.$$

$$\left. - \frac{\hat{Mc}\delta^2}{\lambda^2}\,(3 - \hat{c}^2)\,a_{n-3} - \frac{3\delta^2}{\lambda^2}\,M^2\hat{c}\,a_{n-4} - \frac{\delta^2}{\lambda^2}\,M^3\hat{c}^3 a_{n-5}\right\}$$

TABLE III (concl.)

C. To calculate T_{12}, T_{22}:

$$T_{12} = 1 + a_2 + a_3 + a_4 + \sum_{n=5}^{N} a_n \qquad \text{III-6}$$

$$T_{22} = 1 + 2a_2 + 3a_3 + 4a_4 + \sum_{n=5}^{N} n\, a_n \qquad \text{III-7}$$

where $a_0 = 0$ $a_1 = 1$ $a_2 = M\hat{c}$

III-8

$$a_3 = \frac{M^2\hat{c}^2}{3} - \frac{\delta^2}{6\lambda^2}(1 - \hat{c}^2) \qquad a_4 = \frac{M\hat{c}\delta^2}{6\lambda^2}(2 - \hat{c}^2)$$

a_n = (same as for T_{11}, T_{21})

D. To determine whether $a^2 > 0$ or $a^2 < 0$ either

i) Test a^2 for each value of $\hat{c}$, given M, δ, λ

ii) Use (for M < 1)

$a^2 > 0$ when $(-1/M+1) < \hat{c} < (1/1-M)$

$a^2 < 0$ otherwise

iii) $a^2 = \delta^2 [(1 + M\hat{c})^2 - \hat{c}^2]/\lambda^2$ III-9

$a^2 = -b^2$ III-10

E. For series convergence terms are added until the new sum divided by the old sum is less than ε. A typical ε value is 0.001.

TABLE IV: Pressure Coefficients $\frac{\delta p_r}{\lambda}$, $\frac{\delta p_c}{\lambda}$, by Runge-Kutta Numerical Integration

A. The quantities $\frac{\delta p_r}{\lambda}$, $\frac{\delta p_c}{\lambda}$, a^2, b^2 and the sign of a^2 are as given in Table III.

B. The Formulae to calculate T_{ij} are

i) $$\begin{Bmatrix} p \\ \frac{\partial p}{\partial z} \end{Bmatrix}^{\circ}_{z=1} = \begin{bmatrix} T_{11} & T_{12} \\ T_{21} & T_{22} \end{bmatrix} \begin{Bmatrix} p \\ \frac{\partial p}{\partial z} \end{Bmatrix}^{\circ}_{z=0} \qquad \text{IV-1}$$

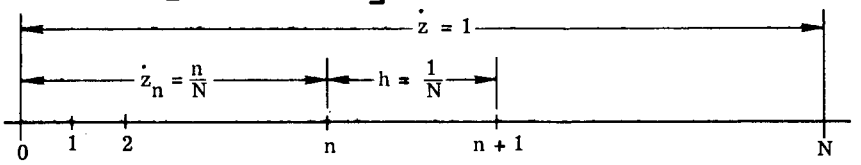

Sketch of numerical integration range.

ii) $$\begin{bmatrix} T_{11} & T_{12} \\ T_{21} & T_{22} \end{bmatrix} = [t_{N-1}][t_{N-2}]\cdots[t_2][t_1][t_0] \qquad \text{IV-2}$$

iii) $$[t_n] = \left\{ I + \frac{h}{6}\left[A(\overset{\circ}{z}_n) + 4A(\overset{\circ}{z}_n + \frac{h}{2}) + A(\overset{\circ}{z}_n + h)\right] \right.$$

$$+ \frac{h^2}{6}\left[A(\overset{\circ}{z}_n + \frac{h}{2})\, A(\overset{\circ}{z}_n) + A(\overset{\circ}{z}_n + h)\, A(\overset{\circ}{z}_n + \frac{h}{2}) + A^2(\overset{\circ}{z}_n + \frac{h}{2})\right]$$

$$+ \frac{h^3}{12}\left[A^2(\overset{\circ}{z}_n + \frac{h}{2})\, A(\overset{\circ}{z}_n) + A(\overset{\circ}{z}_n + h)\, A^2(\overset{\circ}{z}_n + \frac{h}{2})\right]$$

$$\left. + \frac{h^4}{24}\left[A(\overset{\circ}{z}_n + h)\, A^2(\overset{\circ}{z}_n + \frac{h}{2})\, A(\overset{\circ}{z}_n)\right] \right\} \qquad \text{IV-3}$$

iv) $$I = \begin{bmatrix} 1 & 0 \\ 0 & 1 \end{bmatrix} \qquad \text{IV-4}$$

$$A(\overset{\circ}{z}_n) = \begin{bmatrix} 0 & 1 \\ -b(\overset{\circ}{z}_n) & a(\overset{\circ}{z}_n) \end{bmatrix} \qquad \text{IV-5}$$

$$a(\overset{\circ}{z}_n) = \left[\frac{2M\hat{c}}{1 + M\hat{c}\bar{U}(\overset{\circ}{z}_n)} \frac{\partial \bar{U}}{\partial \overset{\circ}{z}} + \frac{1}{\rho_0} \frac{\partial \rho_0}{\partial \overset{\circ}{z}} \right] : \quad b(\overset{\circ}{z}_n) = \left(\frac{\delta}{\lambda}\right)^2 \hat{c}^2 \left[\left(\frac{1 + M\hat{c}\bar{U}}{\bar{c}\ \hat{c}} \right)^2 - 1 \right] \qquad \text{IV-6}$$

C. Case 1: Check of previous series results

Velocity profile $\bar{U}(\overset{\circ}{z}_n) = \overset{\circ}{z}_n$

$$\frac{\partial \bar{U}}{\partial \overset{\circ}{z}_n} = 1$$

Density profile $\rho_0(\overset{\circ}{z}_n) = \text{constant}$

$$\frac{\partial \rho_0}{\partial \overset{\circ}{z}_n} = 0$$

Sound speed profile

$$\bar{c}(\overset{\circ}{z}_n) = 1$$

D. Case 2: "Blasius" profile. See Table 7.1, Reference 29, $\eta = 8\overset{\circ}{z}$

Velocity profile $\bar{U}(\overset{\circ}{z}) = f'(\eta/8)$

$$\frac{\partial \bar{U}}{\partial \overset{\circ}{z}} = 8\, f''(\eta/8)$$

Density profile $\rho_0(\overset{\circ}{z}) = \text{constant}$

$$\frac{\partial \rho_0}{\partial z} = 0$$

Sound speed profile

$$\bar{c}(z) = 1$$

TABLE V: Derivative Entering Singularity in Complete Pressure Coefficient

A. The derivative is determined from

$$\frac{d}{dk}\,[b\,T_{11} + T_{21}] = \lambda\,\frac{d}{dc}\,[b\,T_{11} + T_{21}] = \lambda\,b\,\frac{dT_{11}}{d\hat{c}} + \lambda\,T_{11}\,\frac{db}{dc} + \lambda\,\frac{dT_{21}}{d\hat{c}} \qquad \text{V-1}$$

where

$$\frac{db}{dc} = \frac{\delta}{\lambda}\,[\hat{c}^2 - (1+M\hat{c})^2]^{-\frac{1}{2}}\,[(1-M^2)\hat{c} - M], \qquad \text{V-2}$$

$$\frac{dT_{11}}{dc} = \frac{da_2}{dc} + \frac{da_3}{dc} + \frac{da_4}{dc} + \sum_{n=5}^{N}\frac{da_n}{dc}, \qquad \text{V-3}$$

$$\frac{dT_{21}}{dc} = \frac{2da_2}{dc} + \frac{3da_3}{dc} + \frac{4da_4}{dc} + \sum_{n=5}^{N} n\,\frac{da_n}{dc}, \qquad \text{V-4}$$

and

$$\left.\begin{aligned} &\frac{da_0}{dc} = 0 \qquad \frac{da_1}{dc} = 0 \qquad \frac{da_2}{dc} = \frac{\delta^2}{\lambda^2}\,\hat{c} \\ &\frac{da_3}{dc} = -\tfrac{1}{3}M\,\frac{\delta^2}{\lambda^2}\,(2 - 3\hat{c}^2) \\ &\frac{da_4}{dc} = -\frac{1}{6}\,\frac{\delta^4}{\lambda^4}\,\hat{c}(1 - \hat{c}^2) - \frac{1}{2}\,M^2\,\hat{c}\,\frac{\delta^2}{\lambda^2} \end{aligned}\right\} \qquad \text{V-5}$$

$$\frac{da_n}{dc} = \frac{1}{n(n-1)}\left\{(n-1)(n-4)\,M\,\hat{c}\,\frac{da_{n-1}}{dc} - \frac{\delta^2}{\lambda^2}\,(1 - \hat{c}^2)\,\frac{da_{n-2}}{dc} -\right.$$

$$M\hat{c}\,\frac{\delta^2}{\lambda^2}\,(3-\hat{c}^2)\,\frac{da_{n-3}}{d\hat{c}} - 3M^2\,\hat{c}\,\frac{\delta^2}{\lambda^2}\,\frac{da_{n-4}}{d\hat{c}} - M^3\,\hat{c}^3\,\frac{\delta^2}{\lambda^2}\,\frac{da_{n-5}}{d\hat{c}}\Bigg\}$$

$$+\frac{1}{n(n-1)}\Bigg\{-(n-1)(n-4)M\,a_{n-1} + 2\hat{c}\,\frac{\delta^2}{\lambda^2}\,a_{n-2} - M\,\frac{\delta^2}{\lambda^2}\,(3-$$

$$2\hat{c})\,a_{n-3} - 3M^2\,\frac{\delta^2}{\lambda^2}\,a_{n-4} - 3M^3\,\hat{c}^2\,\frac{\delta^2}{\lambda^2}\,a_{n-5}\Bigg\} \qquad \text{V-6}$$

B. In the range of $\hat{c}$ considered Re {b} > 0, Im {b} = 0

where $b = \delta[\hat{c}^2 - (1 + M\hat{c})^2]^{\frac{1}{2}} / \lambda$ V-7

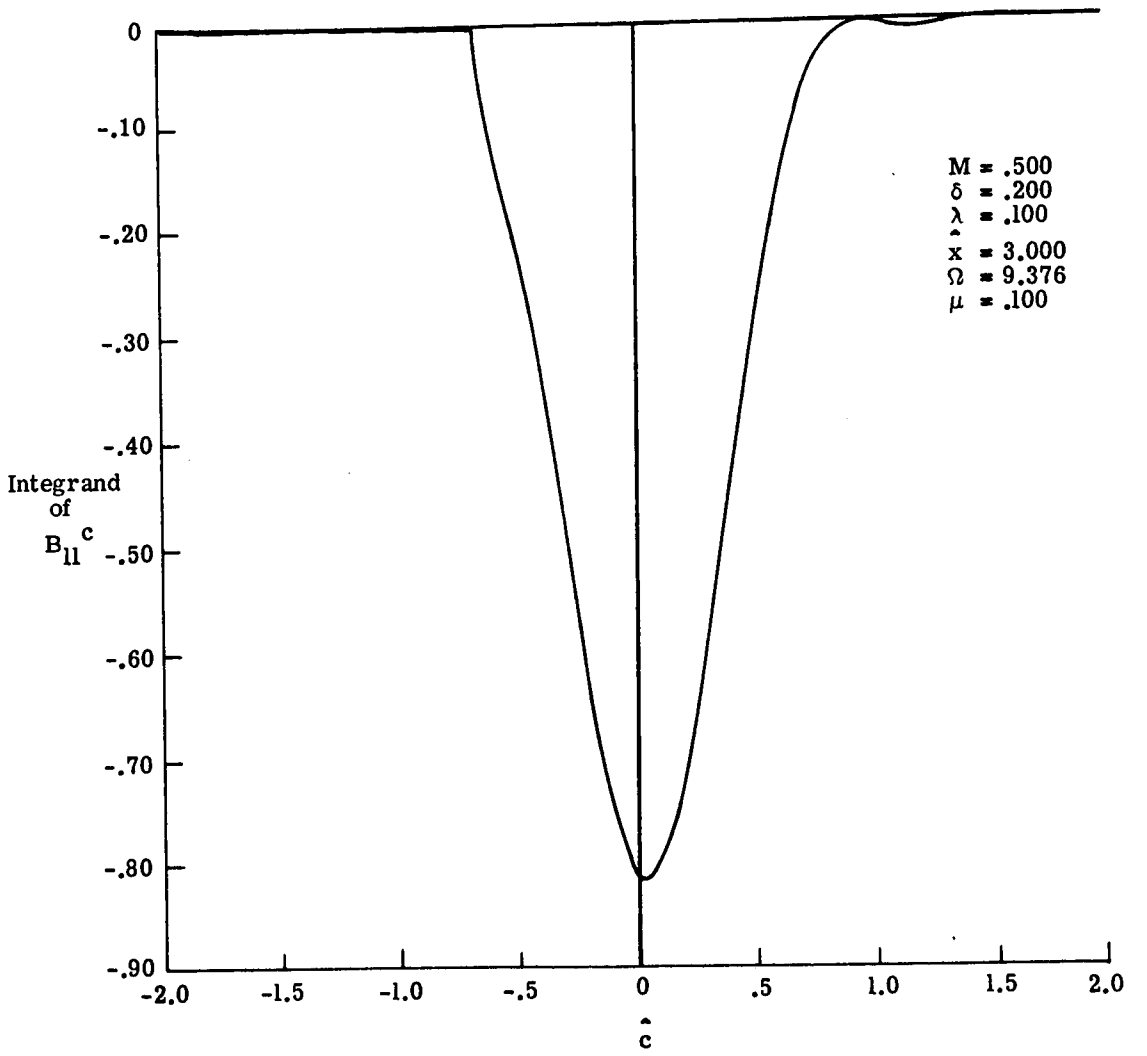

Figure 10.- Integrand of B_{11}^c.

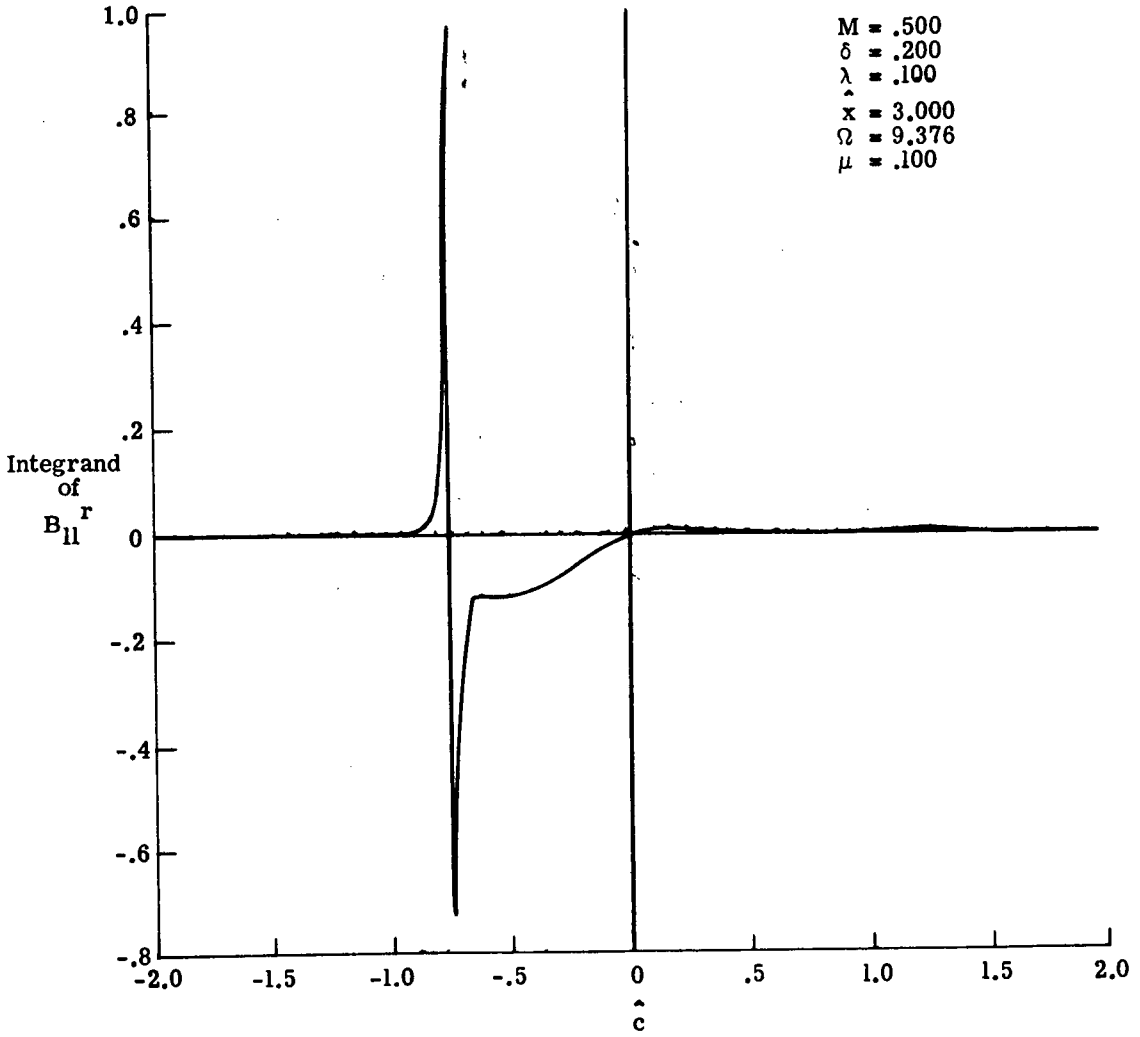

Figure 11.- Integrand of B_{ll}^r.

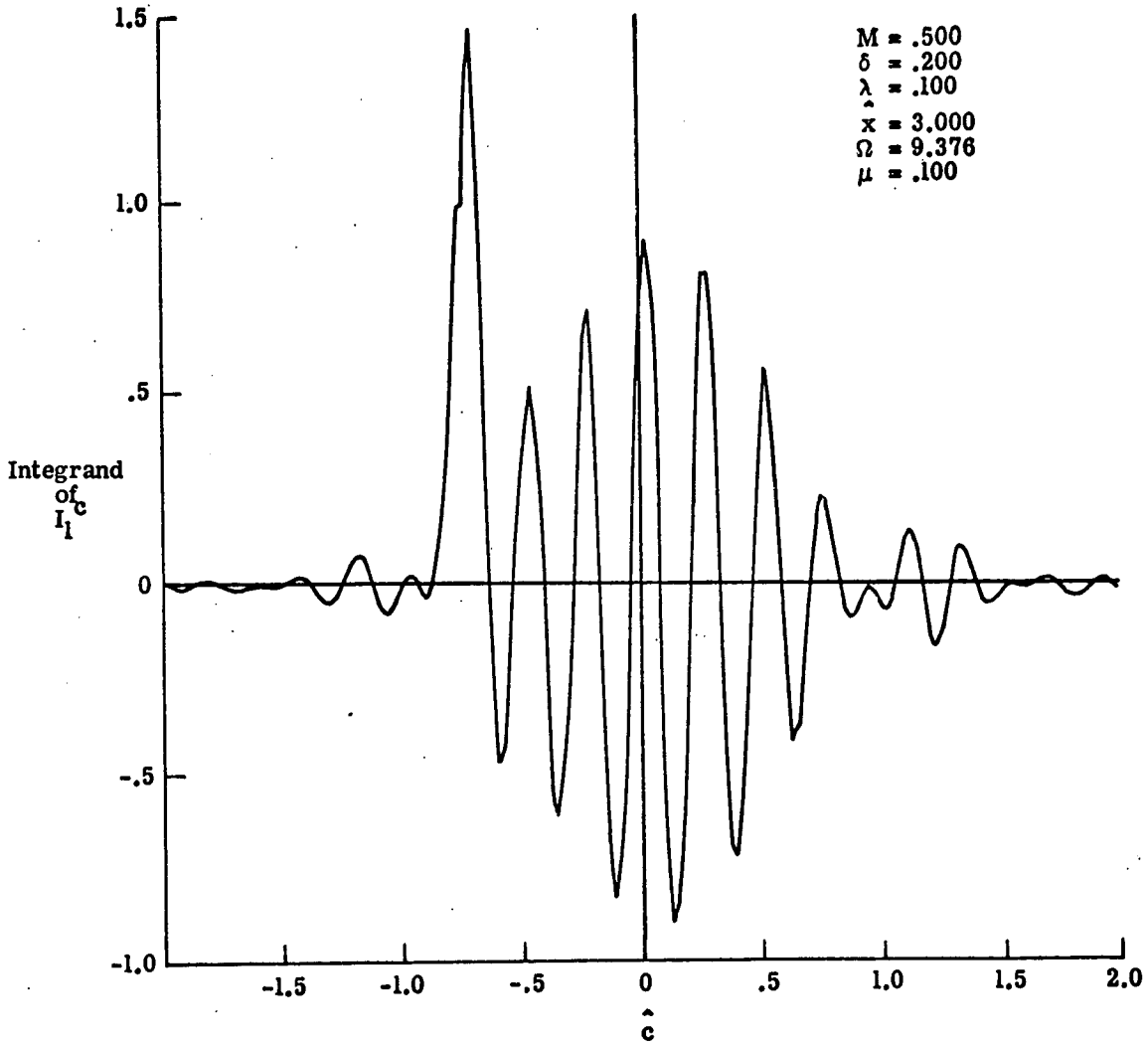

Figure 12.- Integrand of I_1^c.

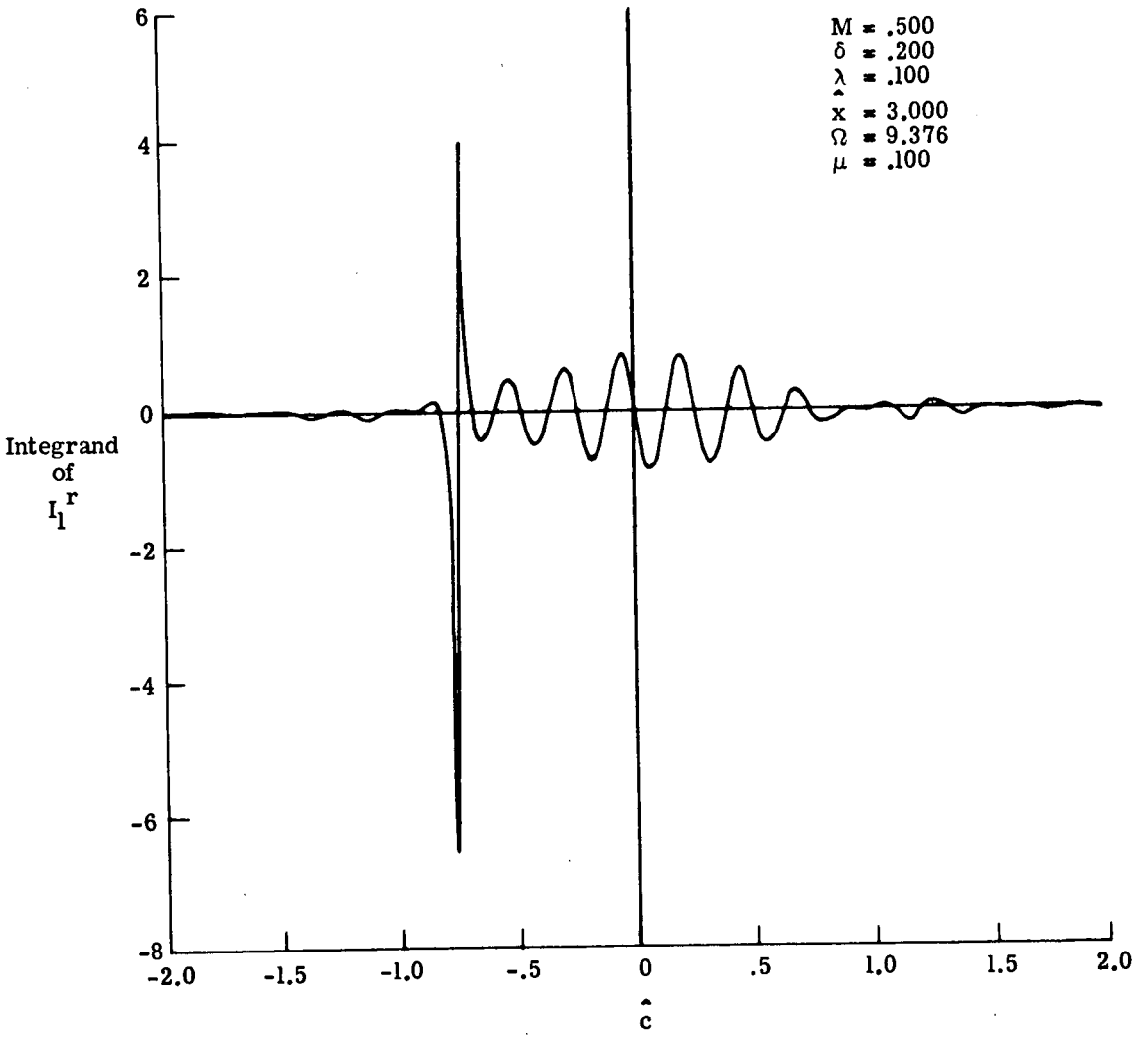

Figure 13.- Integrand of I_1^r.

Chapter IV

Results and Discussion

Numerical results are presented in this Chapter for a plate-fluid system that can be described briefly as follows. Referring to figure 1, an elastic flat thin plate lies in the x-y plane and is surrounded by an infinite rigid plate (baffle) also lying in the x-y plane. The elastic plate is infinitely wide, has length L, is simply supported by the rigid plate at x = 0 and x = L, and is forced by a force having the distribution

$$q(x,y,t) = (\sqrt{2}\,D/L^3) \sin \pi\hat{x} \exp (i\omega t) \qquad 120.$$

This force is orthogonal to all of the uncoupled plate modes but the first. The forcing frequency ω has been chosen as .95 of the natural (uncoupled) frequency of this mode and the solution has assumed that the plate responds only in this mode shape. A frequency change and damping effect due to the fluid flowing past the plate in the upper half z space are allowed for, however. (The lower half z space is not occupied.) The fluid properties are considered in two parts. The first part is a uni-directional, boundary-layer flow in the positive x direction that is independent of the motion of the plate. The second part has arbitrary direction and is dependent only on the plate motion. Linear equations governing the second part of the

fluid properties are obtained by small perturbations of the governing Navier-Stokes, gas-state, energy, and continuity equations from the first part of the flow and are solved together with the plate equation as a coupled set of equations. Gradients of velocity (and temperature), of the first part of the fluid flow are present near the plate associated with a boundary layer; these gradients enter the coupled plate-fluid equations as variable coefficients. The results presented here were developed in an effort to determine the effects of these gradients of velocity on the response of the plate-fluid system.

Pressure on plate surface

Calculated pressure distributions on the surface of the plate are presented in figure 14 for three boundary layer thicknesses. The velocity profile was linear from zero velocity at the plate surface to Mach number M = 0.5 at $z/L = \delta$, and the velocity was constant at M = 0.5 for all larger values of z. Figure 14 presents magnitude and phase of pressure coefficient C_p which is related to pressure by

$$p(x,z,t) = \rho_0 c \, fL \, |C_p| \exp(i\omega t + i\phi). \qquad 121.$$

The phase angle ϕ thus represents time lag relative to the forcing function, equation 120. Figure 14 shows that the pressure is largest on the surface of the vibrating plate, $0 < \hat{x} < 1$, where the effect of increasing boundary layer

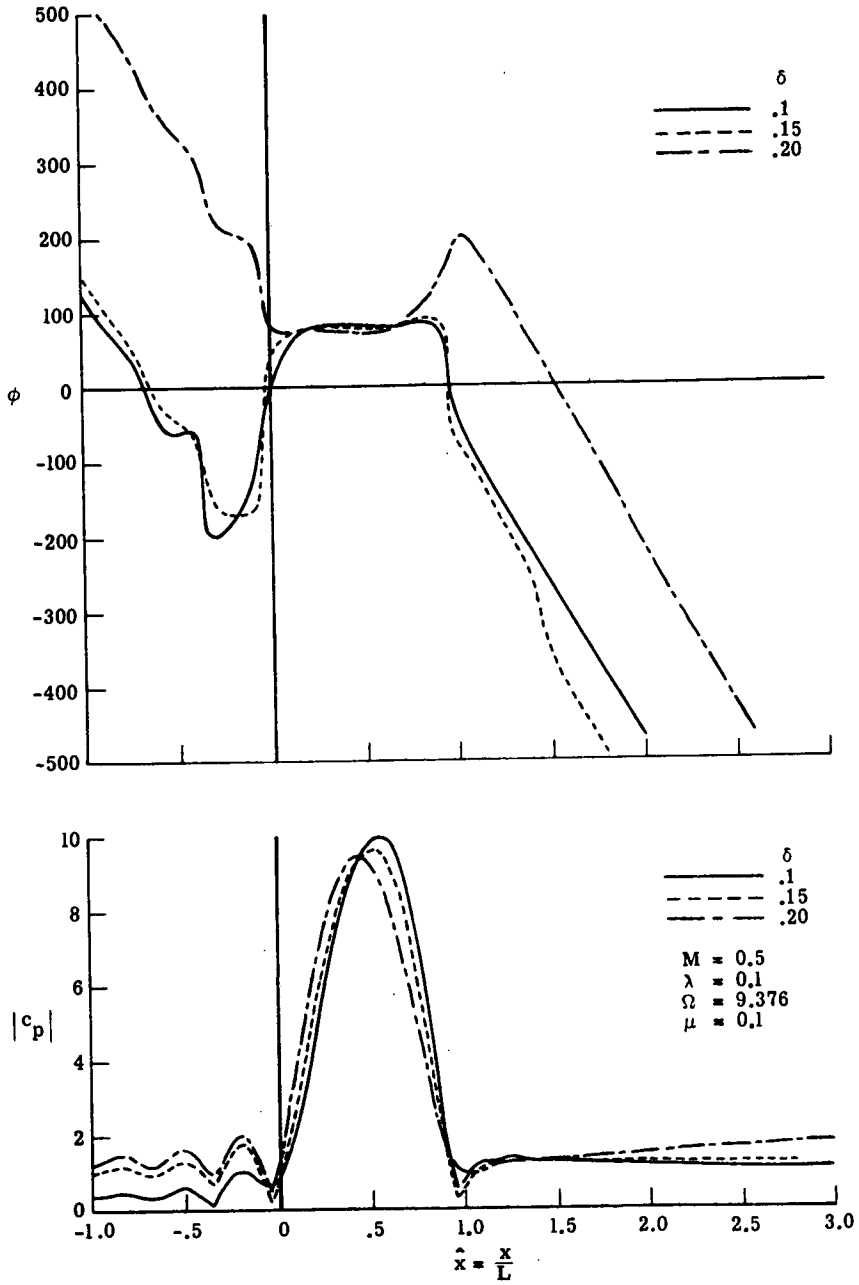

Figure 14.- Pressure distribution along plate surface, δ = .1, .15, .20.

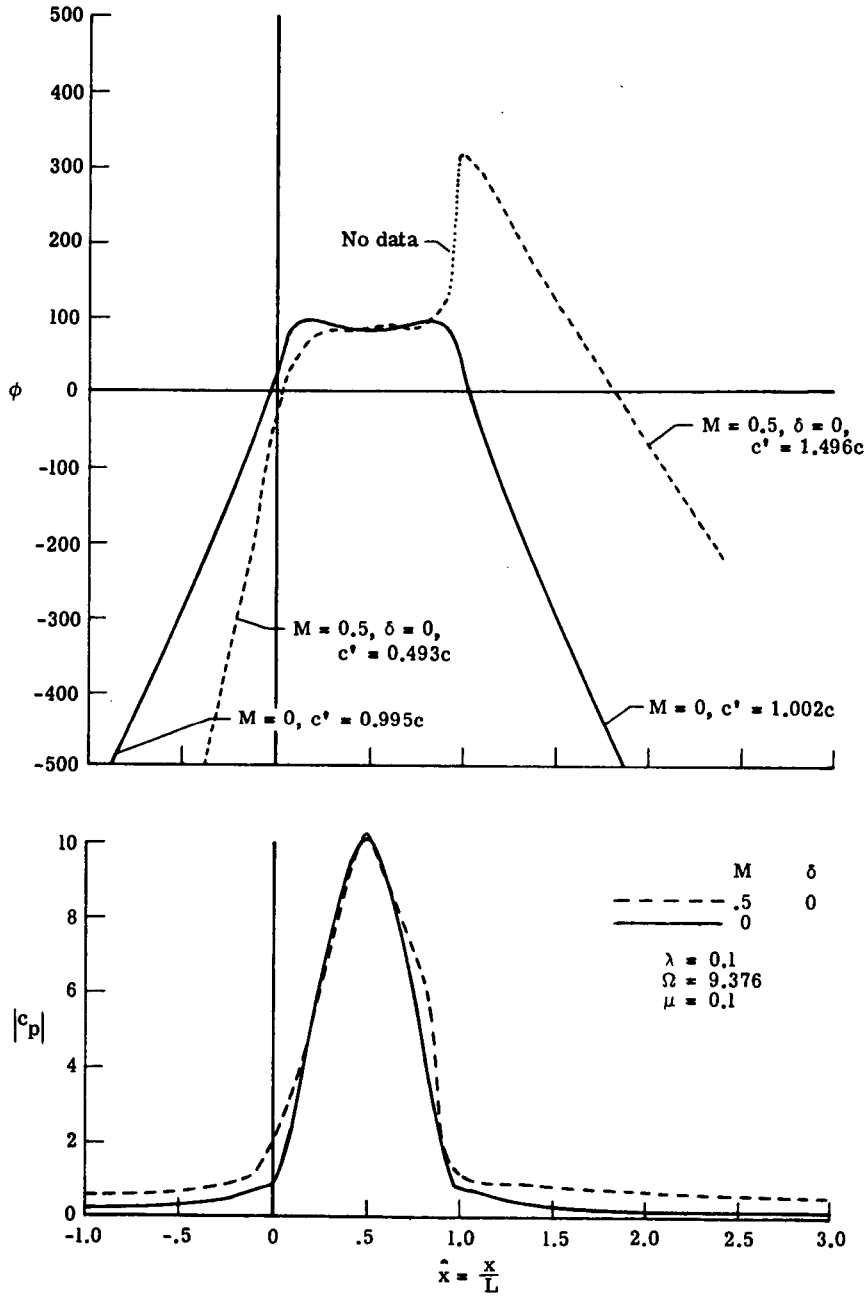

Figure 15.- Pressure distribution along plate surface, M = 0, δ = 0.

thickness δ is a slight decrease of maximum pressure and a shift of the distribution toward the upstream edge of the plate, $\hat{x} = 0$. Increasing δ also increases the pressure both upstream ($\hat{x} < 0$) and downstream ($\hat{x} > 1$) of the plate.

The phase angle ϕ is nearly constant over the middle of the plate ($\hat{x} \sim .5$) but varies off the plate. For large $\hat{x}$ the phase angle can be expressed by the linear relation

$$\phi = a + b\,\hat{x} \qquad 122.$$

where a and b are constants. Inserting equation 122 into 121 leads to

$$p(x,z,t) = \rho_0\, c\, fL\, |C_p|\, \exp(ia)\, \exp\left\{i\,\frac{b}{L}\left[\frac{c}{\lambda b}\,t + x\right]\right\} \qquad 123.$$

Equation 123 describes a pressure wave that is moving with speed c', where

$$c' = \frac{c}{\lambda b} \qquad 124.$$

Measurement of the slope b from the curves reproduced in figure 14 leads to the following values for c'.

TABLE VI: Wave speeds from pressure curves

δ =	.10	.15	.20
$\left\|\frac{c'}{c}\right\|$ =	1.43	1.35	1.35

Since b is negative these waves are moving downstream. This speed is somewhat greater than sound speed c' = c, but somewhat less than the convected wave speed for this Mach number c' = 1.5 c. This result seems natural in view of the boundary

layer nature of the mean velocity profile.

In the region upstream of the plate $\hat{x} < 0$ the phase curve can also be represented in part by the linear relation equation 122. The corresponding slope of the phase curve is negative, as it is in the region downstream, indicating that "waves" are coming toward the plate from an upstream region where no disturbances are supposed to exist. This result was not anticipated, and is not intuitively satisfying, since these waves "should" be traveling upstream, and requires further investigation. Great care was taken in the derivation, solution, and numerical analysis of the equations to avoid numerical problems, and several checks will be presented that suggest that these unexpected waves do not arise from errors in the solution technique or execution. Unusual wave behavior has been observed previously in problems of sound propagarion in ducts,[35,36] where the anomaly was resolved by observing that energy is the true quantity whose flow must be controlled by a radiation condition, and that energy and pressure waves do not always propagate in the same direction. Investigations along these lines (among others) should be undertaken with regard to the waves in the upstream region shown in figure 14.

Check cases $M = 0$ and $\delta = 0$

To gain confidence in the methods used to obtain the results shown in figure 14 the limiting cases of zero

boundary layer thickness ($\delta = 0$, $M = .5$) and zero flow speed ($M = 0$) were calculated using those methods. The results are shown in figure 15. No independent solutions have been found for comparison with these results, it has been implied[37] that the results for $M = 0$ have not been previously obtained. The results of figure 15 appear reasonable, and therefore suggest the correctness of the methods of this paper, for the following reasons. The pressure and phase angle distribution for $M = 0$ is symmetric about $\hat{x} = .5$ as would be expected in still air; the pressure magnitude drops off continuously with distance away from the plate, and in particular the phase plot indicates that the pressure waves are propagating away from the plate in both upstream and downstream directions at very near the speed of sound, $c' = c$. The curves in figure 15 for $M = .5$ and $\delta = 0$ show that the pressure magnitude has dis-symmetry that would be expected for the flow situation. The phase curve shows that pressure waves are propagating away from the plate in both directions at very near the expected speeds of .5 c in the upstream direction and 1.5 c in the downstream direction.

Free Wave Speeds

The wave speeds discussed in connection with figure 14 are the result of two parts of the solution, namely one part arising from integration over the whole $\hat{k}$ range and a second

part arising from the contribution of the residue of the pole on the path of integration. In the case of figure 15 where $M = 0$ or $M = .5$ and $\delta = 0$ there are no poles and the wave nature arises entirely from the integration over $\hat{k}$. It is of interest to determine the nature of the waves associated with the singularity and their contribution to the total solution.

The transfer matrix solution, equation 72, of the governing ordinary differential equation can be re-arranged into the form

$$\begin{bmatrix} T_{11} & -1 \\ T_{21} & b \end{bmatrix} \begin{Bmatrix} \overset{\circ}{p}_n(\hat{k},0) \\ D_n \; e^{-b} \end{Bmatrix} = \begin{Bmatrix} -T_{12} & \delta Z_n^* \\ -T_{22} & \delta Z_n^* \end{Bmatrix} \qquad 125.$$

In equation 125 the unknowns are $\overset{\circ}{p}_n$ and $\underline{D}$, and the knowns are the T_{ij}, b and the Fourier amplitudes Z_n^* of the plate displacement. When there is no plate motion $Z_n^* = 0$ and equation 125 has non-trivial solutions only where

$$b\, T_{11} + T_{21} = 0 \qquad (117)$$

This condition also is responsible for the pole on the path of the $\hat{k}$ integration; the pole therefore represents a free wave solution for waves propagating parallel to a non-moving plate. In this case the solution of the fluid equation can be written

$$p(x,z,t) = h(z) \exp i\, k'(c't + x)$$

where the wave length of the wave is, relative to the dimensional boundary layer thickness δ^*,

$$\gamma = \frac{\text{wave length}}{\delta^*} = \frac{2\pi\lambda}{\delta \hat{c}_0} \qquad 126.$$

and the wave speed is

$$c' = \frac{1}{\hat{c}_0} c \qquad 127.$$

where $\hat{c}_0$ is the value of $\hat{c}$ satisfying equation 117. Values of c' determined for various values of γ are presented in figure 16. These waves are downstream-propagating waves as indicated by the negative values of $\hat{c}$. (See figures 11 - 13.) Figure 16 shows that short wave lengths (small δ) propagate at about the sound speed c, but long waves (large γ) propagate at about the convected wave speed 1.5 c. Intermediate wave lengths ($1 < \gamma < 10$) travel at some intermediate speed. Wave speeds determined from the slope of the phase curve of the complete solution (figure 14 & 15) are shown as the square symbols in figure 16, and are seen to be near, but somewhat below, the free wave speed (phase velocity). The propagation of energy in free waves is usually associated with the group velocity, rather than phase velocity. Group velocity was determined by graphically differentiating the phase velocity curve in figure 16 and using the formula

$$\frac{c'(\text{group})}{c} = \frac{c'(\text{phase})}{c} - \gamma \frac{d}{d\gamma}\left[\frac{c'(\text{phase})}{c}\right]. \qquad 128.$$

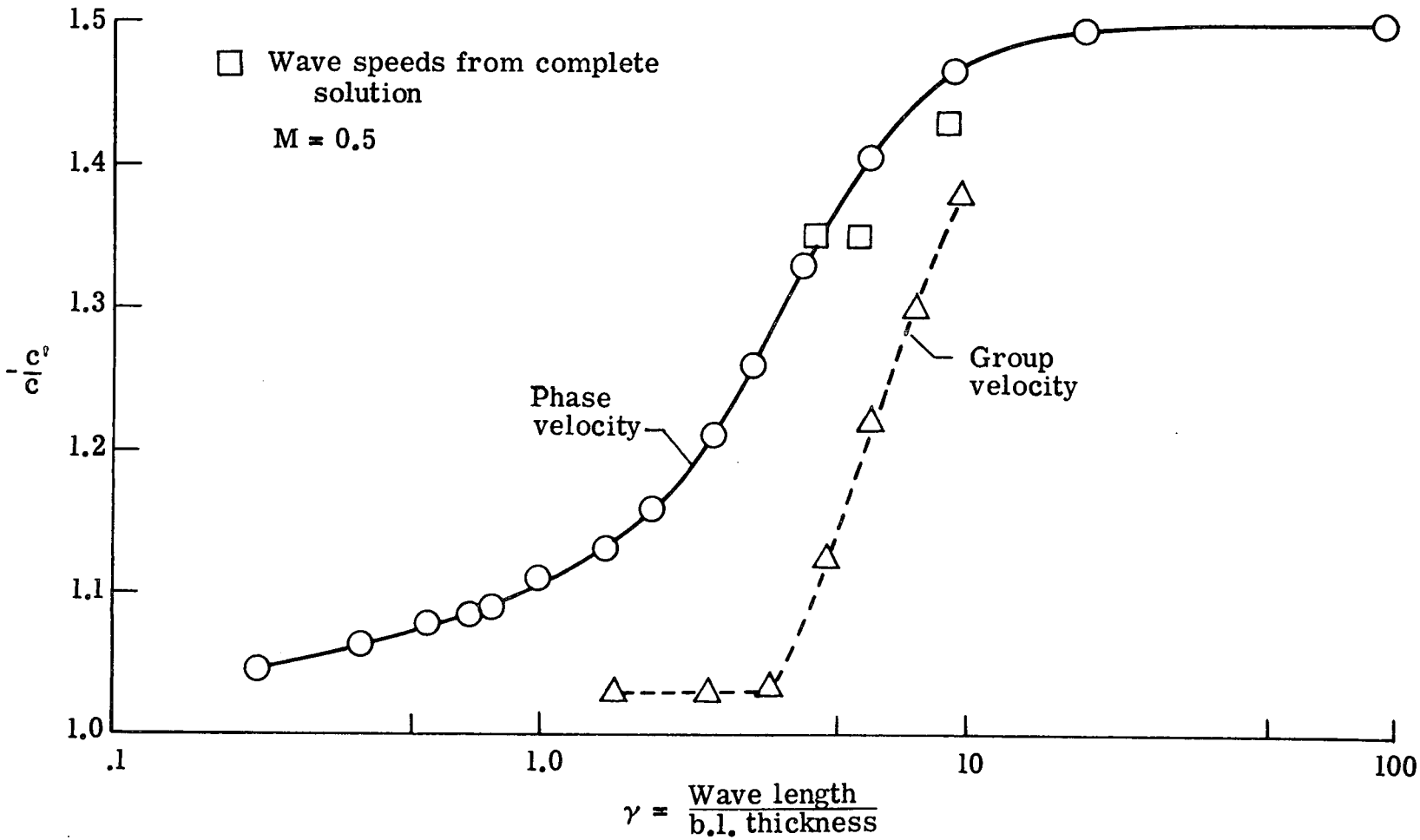

Figure 16.- Free wave speeds.

The resulting group velocities are shown in figure 16 to be less than the phase velocity but still between sound speed c and 1.5 c. The sign of the group velocity is the same as the sign of phase velocity, indicating that for these waves the energy is propagated in the same direction as the pressure wave.

The contribution of the residue (representing a free wave) to the pressure distribution is shown in figure 17, where pressure distributions calculated using only the integral over $\hat{k}$ (the dot-dash curves) are plotted along with distributions including the residue term along with the integral. Figure 17 parts a), b), and c) shows that inclusion of the residue decreases the pressure magnitude $|C_p|$ in the upstream region $\hat{x} < 0$, and increases the magnitude over the rest of the $\hat{x}$ region. The changes are not large especially on the plate, $0 < \hat{x} < 1$. The change of phase is small for $\delta = .2$ and $\delta = .1$. The difference in phase for $\delta = .15$ figure 17b appears to be caused by a phase shift of 360° occuring at a value of $\hat{x}$ where the pressure is small and the data points widely separated; additional calculations might remove the differences shown. For the smallest boundary layer value, $\delta = .01$, shown in figure 17d, the residue has a large contribution to the total solution. The residue contribution appears to be of an undesirable nature because it adds a downstream-moving wave in the upstream

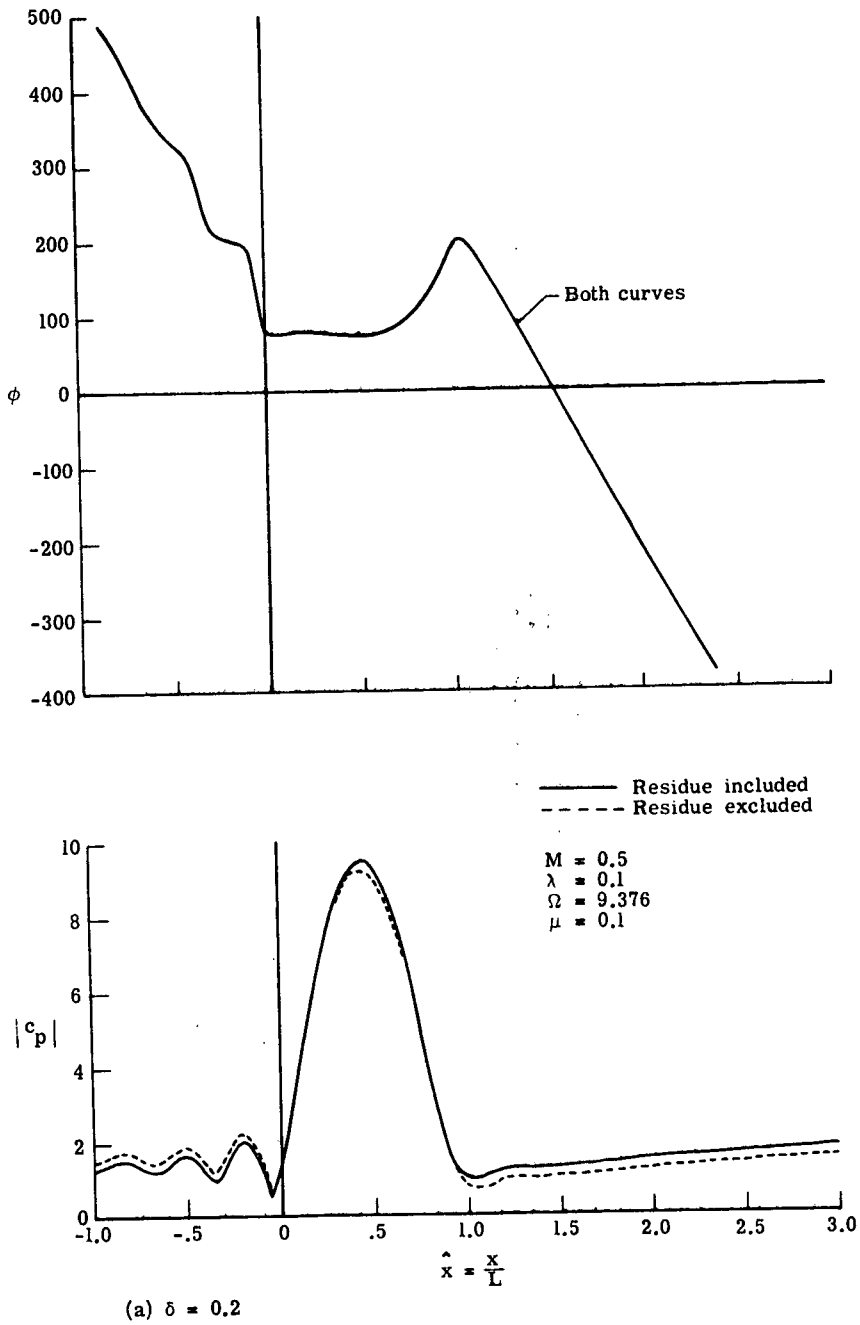

(a) $\delta = 0.2$

Figure 17.- Residue contribution to the pressure distribution.

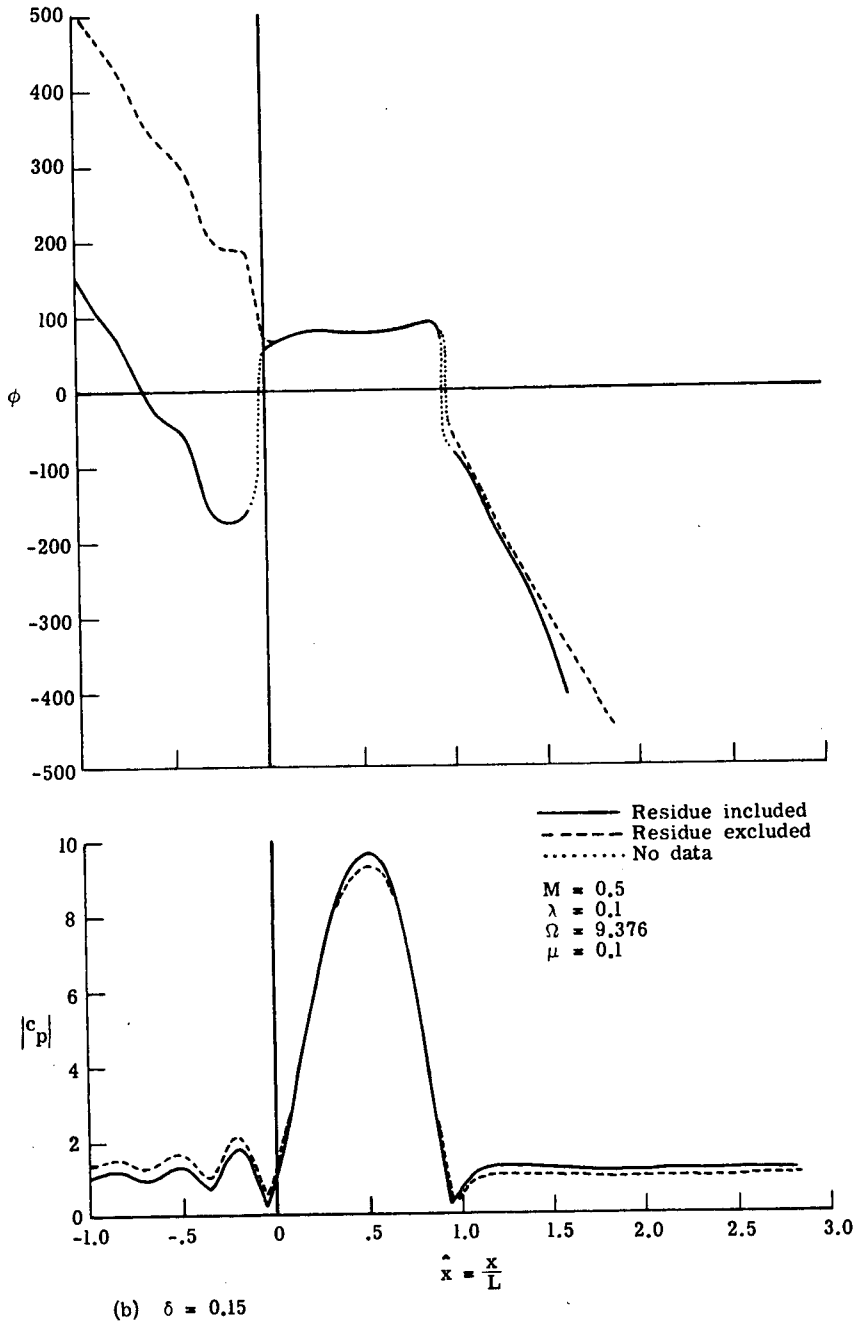

(b) $\delta = 0.15$

Figure 17.- Continued.

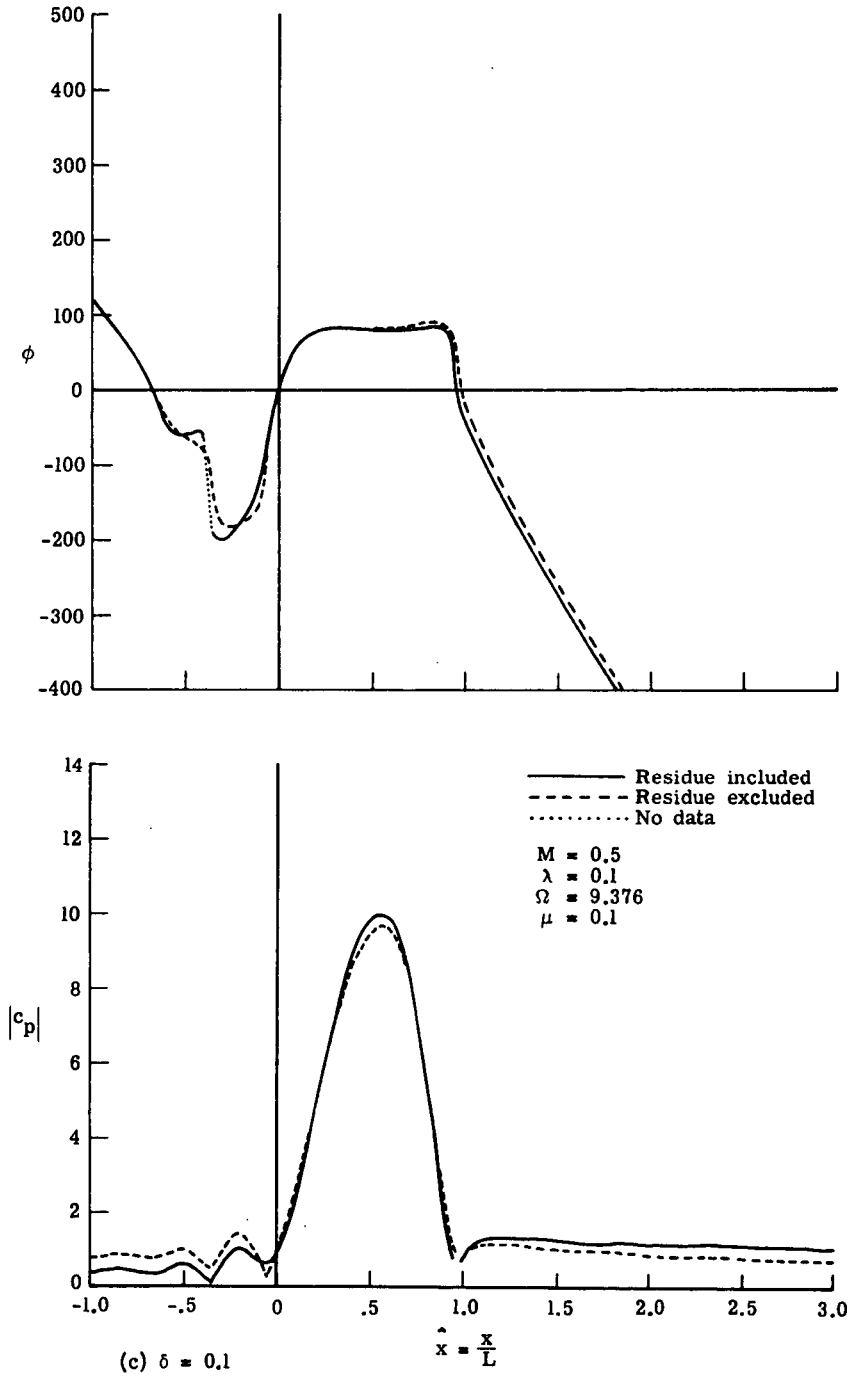

Figure 17.- Continued.

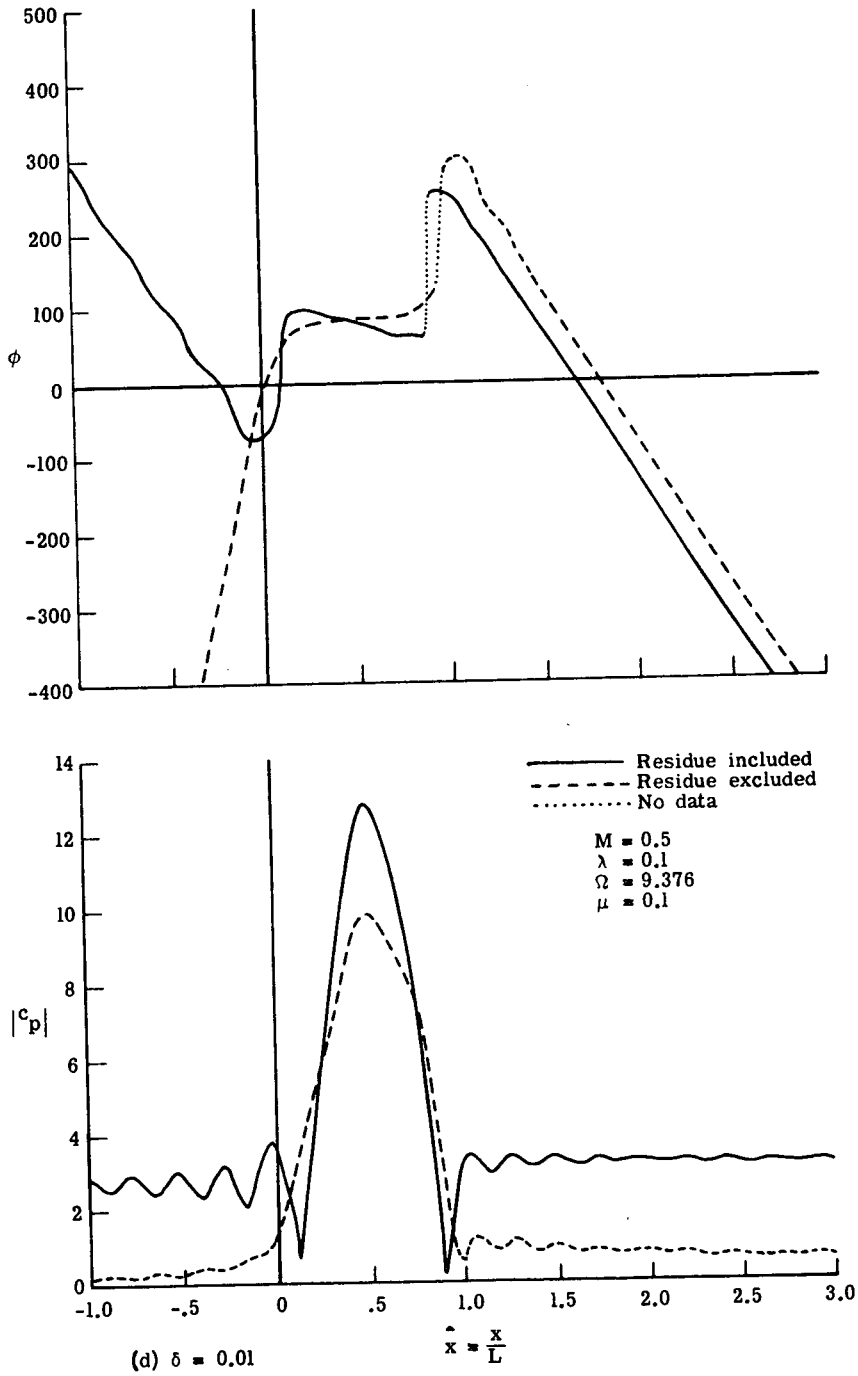

Figure 17.- Concluded.

region and because the agreement of this data (figure 17d) with the limiting case of $\delta = 0$ (figure 15) is better when the residue is not included. These results for $\delta = .01$ may be due to numerical inaccuracies in the integration over $\hat{k}'$ since it was observed that the functions integrated (equivalent to those shown in figures 12 and 13, but for $\delta=.01$) had not become negligible near the ends of the $\hat{k}$ interval. The $\hat{k}$ interval was not extended because the series solution used was divergent outside the interval used.

Plate response

The response of the plate as shown be equation 112 is harmonic in time and has a half-sine shape over the plate length. Additional information can be obtained by examination of the coefficient a_1 appearing in equation 112. The process of analysis leading to equation 111 for a_1, when applied to the complete matrix equation 53, leads to the equation

$$\left\{[(\lambda_1 - (1 - \mu B_{11}^r)\ \Omega^2] + i\ [\mu\Omega^2\ B_{11}^c]\right\} a_1 = Q_1. \qquad 129.$$

The equation for a plate vibrating with an additional mass, m, added to its own mass ρ_p and with a distributed viscous damping is derived in appendix B, and is

$$\left\{[\lambda_m - (1 + \frac{m}{\rho_p})\Omega^2] + i\Omega^2[2\zeta\ \frac{\omega_m}{\omega}\ (1 + \frac{m}{\rho_p})]\right\} a_m = Q_m. \qquad 130.$$

Comparison of equations 129 and 130 suggests the analogy

that the effects of the fluid on the plate can be interpreted as the addition of a surface mass m/ρ, where

$$\frac{m}{\rho_p} = -\mu B_{11}^r, \qquad 131.$$

and an added viscous damping ζ, where

$$\zeta = \mu B_{11}^c \sqrt{\Omega^2/\lambda_1}/2\sqrt{1+m/\rho_p} \qquad 132.$$

Added mass and damping equivalents from equations 131 and 132 are shown in figures 18 and 19. Figure 18 shows that the equivalent added mass is positive for small boundary layer thickness δ and for the limit case of $M = 0$ but has various values for intermediate values $.1 < \delta < 1$. These results imply that the resonant frequency of the plate as affected by the added mass m can be either increased or decreased by the fluid effects. Similar results have been observed experimentally.[38] Figure 19 shows that the damping is positive for the values of δ used, and is about one-half percent of critical.

Results for Blasius Velocity Profile

The results presented so far have used the linear velocity profile with the series solution of the ordinary differential equation. The formulae are given in Table III. The effect of using a different velocity profile will now be considered. Use of a different velocity profile than the simple linear profile requires use of the numerical

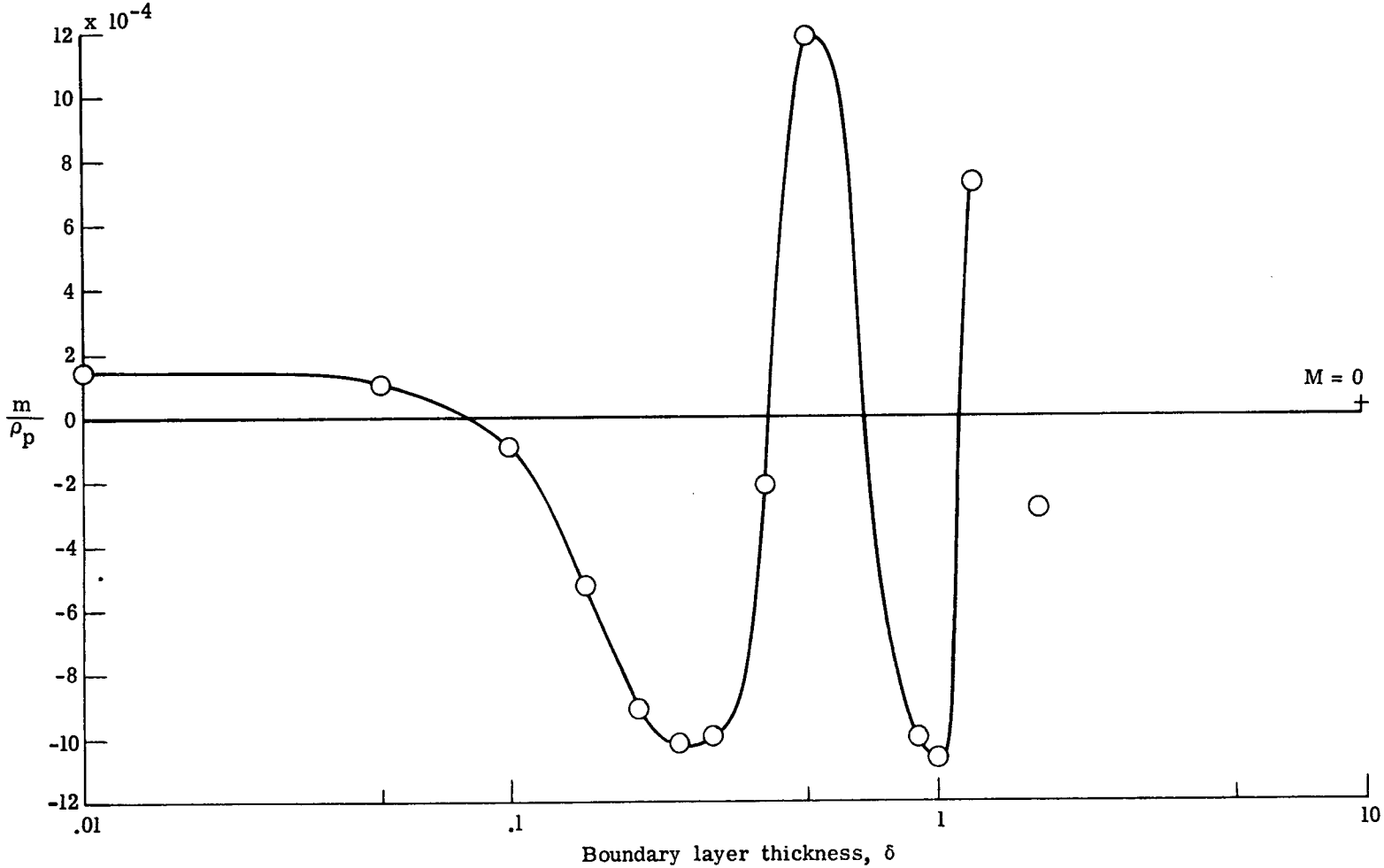

Figure 18.- Equivalent mass due to fluid loading.

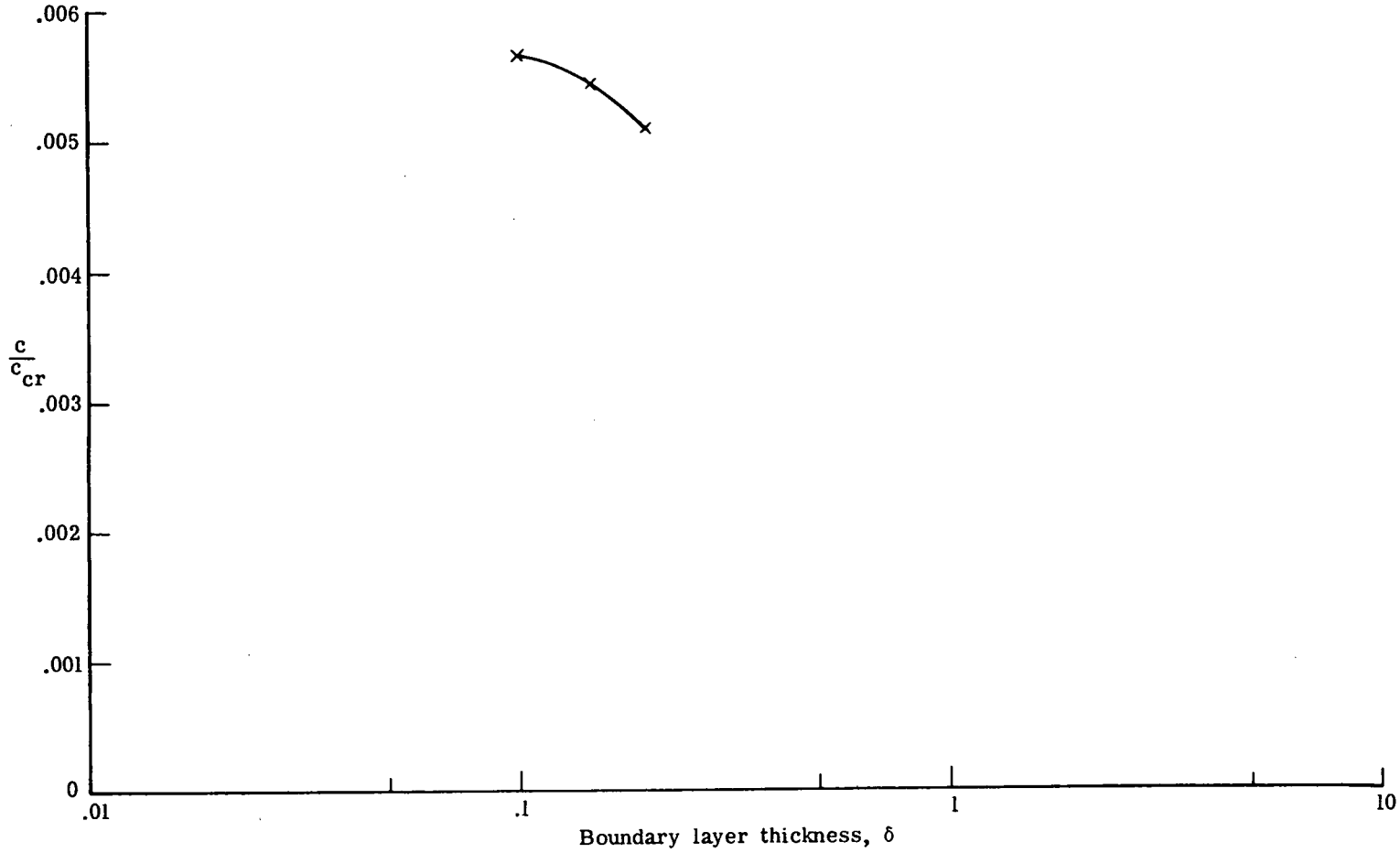

Figure 19.- Equivalent damping due to fluid loading.

integration method of Runge-Kutta. The formulae for this method are given in Table IV. In order to check the numerical processes the basic pressure integrands $\delta p_r/\lambda$ and $\frac{\delta p_c}{\lambda}$ were calculated using both series and Runge-Kutta methods for the linear velocity profile. A (non-typical) example result is shown in figure 20. In order to determine whether the differences shown in figure 20 are significant or not it would be necessary to carry through both solutions to pressure coefficient distributions; such a calculation has not yet been carried out. The differences shown in figure 20 were the largest observed between the two methods; for other values of δ the curves were close enough that they could not be distinguished from each other on the scale used in figure 20.

Results for a Blasius boundary layer velocity profile are compared with results for the linear profile in figure 21. Figure 21 shows that curves for the same value of δ/λ for both profiles, say $\delta/\lambda = 2$, do not agree. However, the curve for $\delta/\lambda = .8$ for the linear profile falls directly on the curve for $\delta/\lambda = 2$ for the Blasius profile (to the scale of figure 21). The definition of δ - boundary layer thickness - is arbitrary however and is different for each velocity profile. The actual velocity profiles for $\delta/\lambda = .8$ - linear profile - and $\delta/\lambda = 2$ - Blasius profile - are compared in figure 22. Considering the agreement of velocities shown

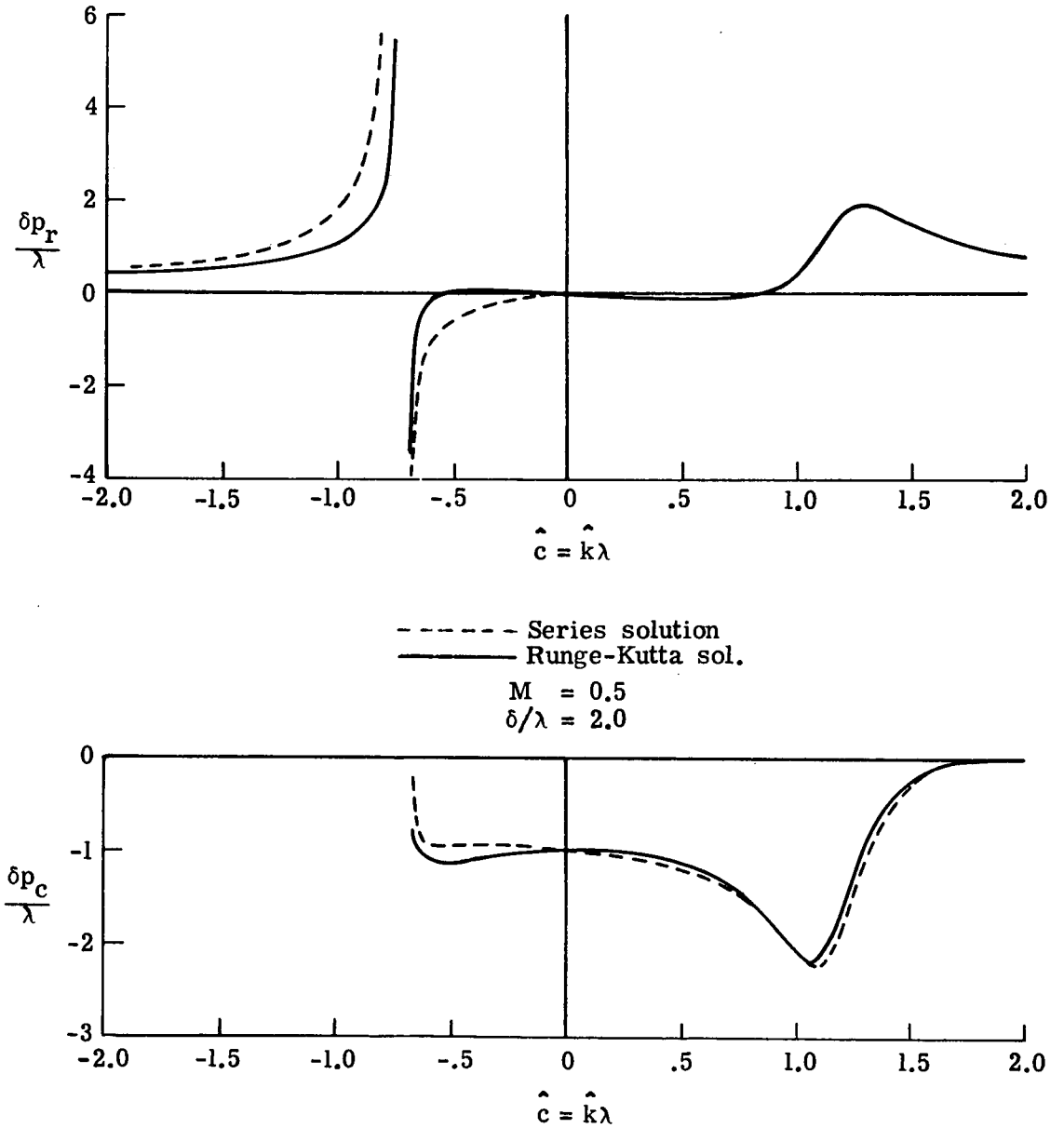

Figure 20.- Comparison of basic integrand functions obtained from series and numerical solutions.

in figure 22, the agreement of the pressure parameters for the two different values of δ shown in figure 21 is not surprising.

The effect of the velocity profile enters the solution for plate response and fluid pressure only through the parameters $\frac{\delta p_r}{\lambda}$ and $\frac{\delta p_c}{\lambda}$. The results shown in figure 21 imply that a linear velocity profile can be used with an appropriate equivalent boundary layer thickness δ to produce results that are the same as if a Blasius profile had been used. Since the Blasius profile is known to be hydrodynamically stable, it can be inferred that the results presented herein for the linear velocity profile are valid for some hydrodynamically stable velocity profile.

Constant Phase Curves

In view of the unexpected results for wave propagation shown in figure 14, namely that pressure waves appear to be originating in a region that should be free of disturbances, it is natural to seek understanding by study of the propagation of the waves. It is emphasized that the propagation of energy is the property that must be studied for correct understanding of the fluid behavior and to determine whether any radiation conditions have been violated. The calculation of energy propagation is a very complex task in a medium having velocity gradients and has not been carried out for the plate-fluid system of this paper. In particular the

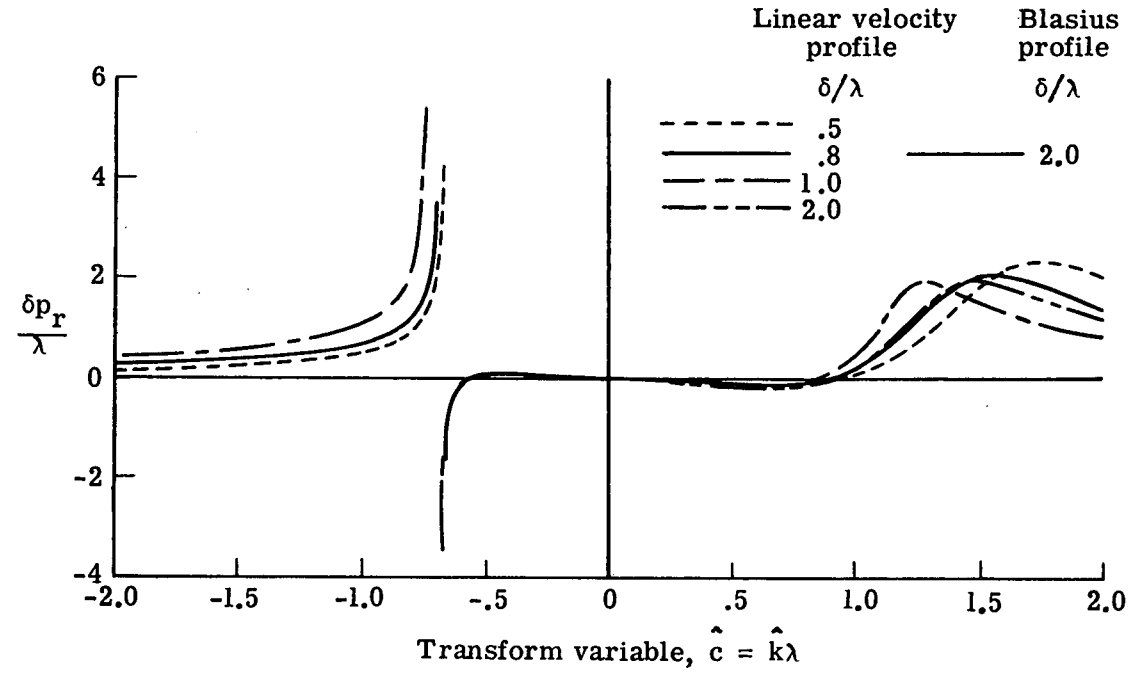

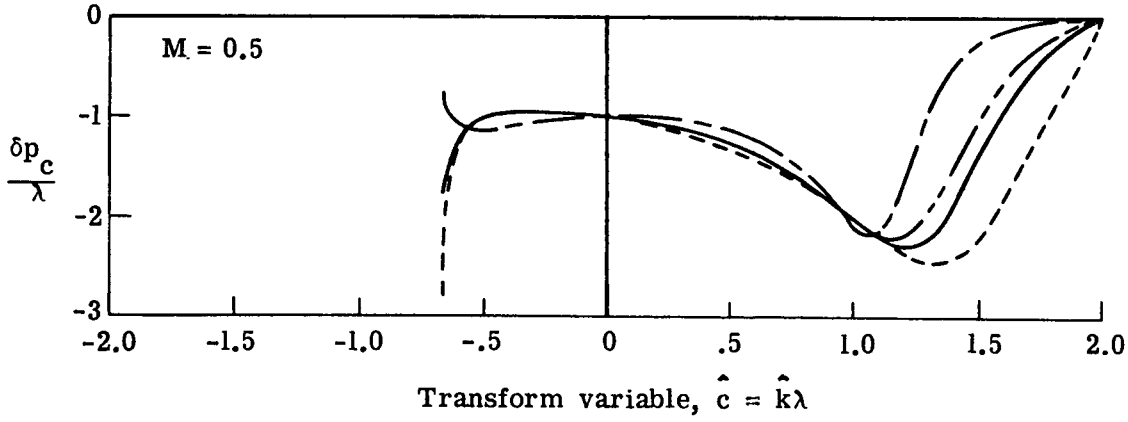

Figure 21.- Comparison of basic integrand functions for linear and Blasius velocity profiles.

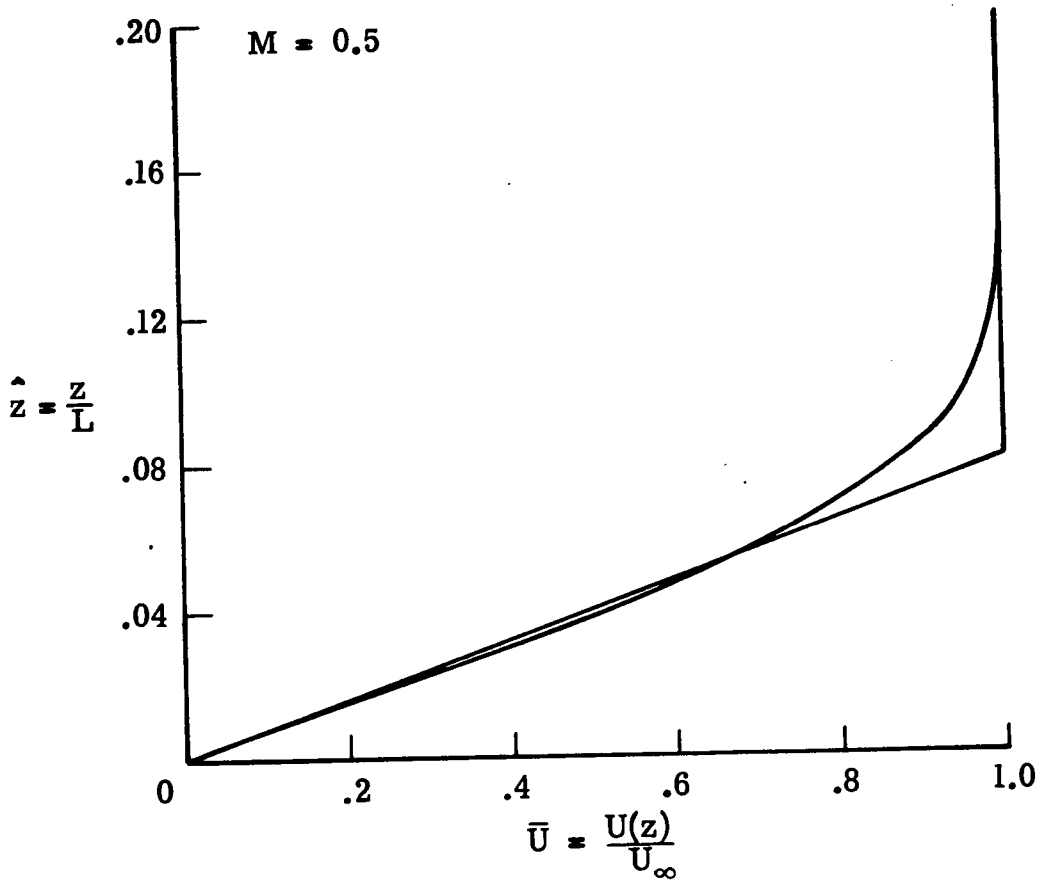

Figure 22.- Equivalent velocity profiles based on equal transform integrands.

directions of energy propagation cannot be assumed to coincide with the direction of propagation of pressure waves.

The direction of propagation of pressure waves can be determined using the phase plots in figures such as figure 14. Recalling the relation between the phase curve and the associated wave propagation direction developed in connection with equations 122-124 leads to the conclusion that the waves flow "downhill" toward smaller values of ϕ. A phase minimum such as occurs at $\delta = .1$ $\hat{x} = -.3$ in figure 14 thus takes on the character of a sink for waves, whereas a maximum of phase has the character of a source. For non-zero boundary layer values the maxima and minima of phase shown in figure 14 all occur off of the vibrating plate, whereas the maxima for the limiting cases of $M = .5$ $\delta = 0$, and $M = 0$ all occur on the plate.

Phase curves for pressure on the plate and at the edge of the boundary layer ($\delta = .2$) are shown in figure 23, together with a sketch of possible constant phase curves inferred from those phase curves. Assuming waves flow from large phase values to smaller phase values, figure 23 also shows pressure waves originating in the region upstream of the plate and near the plate surface, where no disturbances are supposed to exist. The residue contribution has not been included at the edge of the boundary layer, however the small differences shown in figure 17a on the plate surface suggest

that the residue contribution might not be large.

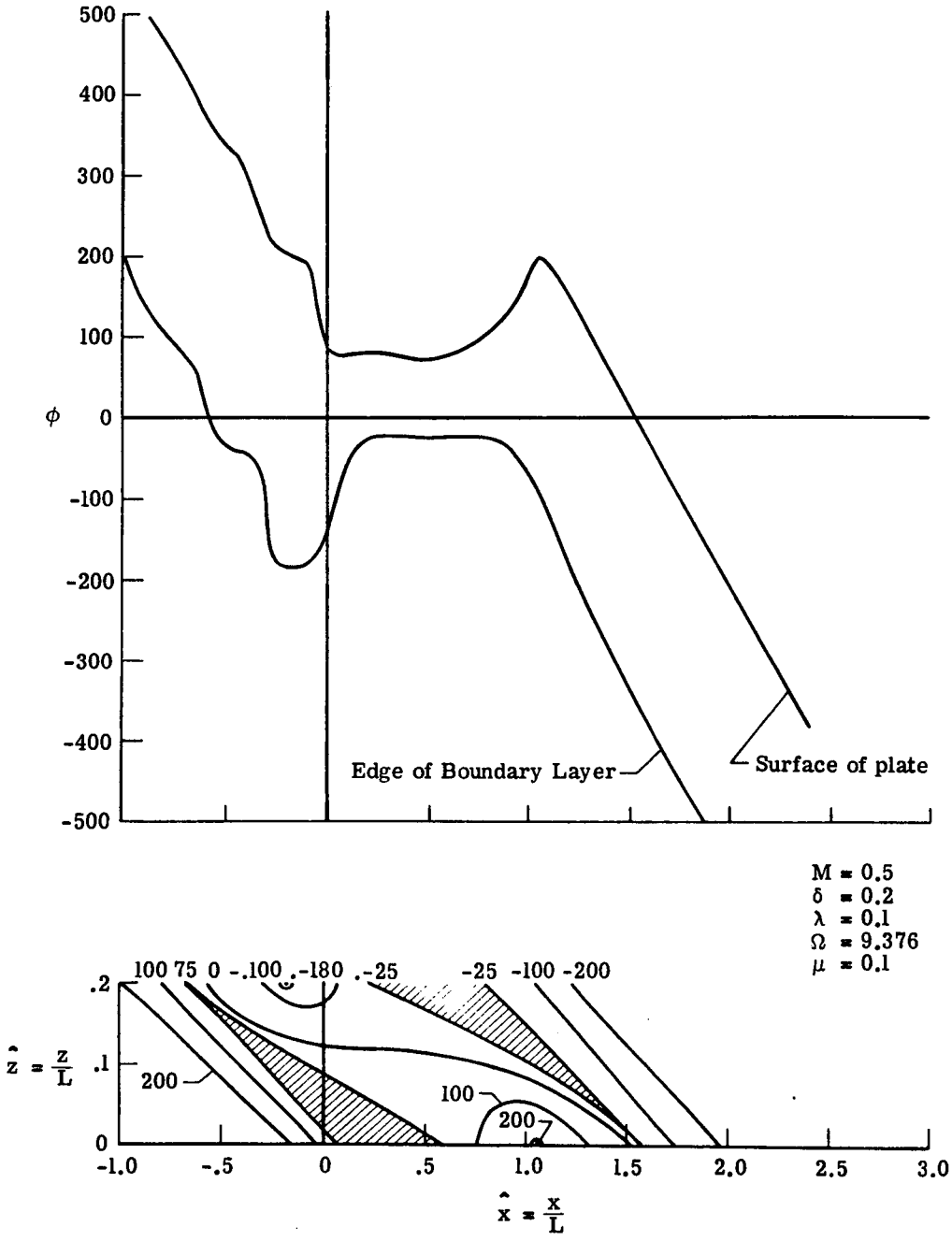

Figure 23.- Constant phase curves.

Chapter V

Concluding Remarks

Resume

This thesis has described a theoretical study of the harmonic forced response of a thin, elastic, two-dimensional flat plate that is dynamically coupled to a passing air stream having a boundary-layer type gradient of velocity. The solution used a modal series solution of the plate equation, a Fourier transform of the fluid equation in the direction parallel to the plate surface, and either Frobenius series or numerical integration solution of the resulting ordinary differential equation with variable coefficients. Numerical inversion of the Fourier transform leads to solutions for distributions of pressure over the plate surface and plate response properties. Numerical results for example values of the parameters are presented to illustrate the method of solution and the effects of the boundary layer on the fluid pressures and the plate response. Calculations for the limiting cases of zero Mach number, Mach number of 0.5 with zero boundary layer thickness, and an analytical solution with zero boundary layer on an infinite plate that was previously solved by Miles were carried out to lend confidence in the methods and techniques used herein.

Conclusions

The calculated surface pressure distributions showed that varying the boundary layer thickness changed the magnitude of the pressure, however the changes were not large for the parameter values used. The phase of the pressure distribution showed that a pressure wave associated with the boundary layer apparently originates in the region upstream of the plate where no disturbances are supposed to exist. The explanation of the origin and nature of this wave was not determined. Alternate methods of solution, together with experimental investigation if necessary, should be used to explain this wave.

Analysis of harmonic wave motion in the fluid with zero plate motion showed the existence of a pressure wave whose amplitude decreased exponentially with distances from the surface (and in this sense roughly analogous to Rayleigh waves on the surface of a solid). At short waves lengths these waves travel at the sound speed c of the medium, but at long wave lengths they travel at the convected wave speed, 1.5 c.

In an effort to display the effects of the fluid on the plate's dynamic behavior an analogy was developed that showed the fluid effects to be equivalent to adding a distributed mass and damping to the plate surface. This analogy is commonly used in fluid-structure dynamic interaction problems.

Varying the boundary layer thickness caused significant percentage changes in the added mass and damping, however, for the parameter values chosen the maximum added mass was only 0.1 percent of the plate mass and the added damping was about 0.55 percent of the critical damping.

The effect of variations in the detail of the velocity profile was studied by calculating values of the fundamental "transformed modal pressure" parameter for a linear velocity profile (velocity of zero at the plate, increasing linearly out to the edge of the boundary layer and constant from there outward) and for a Blasius profile. This calculation showed that the same result could be obtained from each velocity profile provided that an appropriate value of boundary layer thickness was chosen for each profile. The appropriate boundary layer thickness was shown to cause the velocities of each profile to be nearly equal in the region near the plate.

Recommendations for future work

Further topics of research suggested by these results include the following:

a) Theoretical and experimental studies to clarify the nature of the waves apparently originating upstream of the plate.

b) Use of these methods of solution for study of panel flutter, as an alternative to the time-domain solution methods used by Dowell.

c) Use of these methods to search for appropriate fluid-panel parameters for maximizing damping of the system with the aim of reducing turbulence in the boundary layer and thus reducing drag, or with the aim of reducing noise transmitted from a turbulent boundary layer into the interior of an aircraft.

d) Development of approximate procedures, based on the methods developed herein, that could be used in engineering studies instead of these lengthy calculations.

Bibliography

1. Lin, Y. L.: Structural Response to Boundary Layer Noise. Ph.D. Dissertation, Princeton Univ., 1969.

2. Bhat, W. V. and Wilby, J. F.: Interior Noise Radiated by an Airplane Fuselage Subjected to Turbulent Boundary Layer Excitation and Evaluation of Noise Reduction Treatments. Jour. Sound & Vib., (1971), 18(4), 449-464.

3. el Baroudi, M. Y.: Turbulence-Induced Panel Vibration. Univ. of Toronto, UTIAS Rept. No. 98, 1964.

4. Dowell, E. H.: Response of Plates to Fluid Loading. Jour. Sound & Vib., (1967), 6(1), 164-165.

5. Nelson, H. C. and Cunningham, H. J.: Theoretical Investigation of Flutter of Two-Dimensional Flat Panels with one Surface Exposed to Supersonic Potential Flow. NACA Report 1280, 1956.

6. Houbolt, J. C.: A Study of Several Aerothermoelastic Problems of Aircraft Structures. Ph.D. Thesis, ETH, Zurich, 1958.

7. Alper, S. and Magrab, E. B.: Radiation from the Forced Harmonic Vibrations of a Clamped Circular Plate in an Acoustic Field. Jour. Acoust. Soc. Amer., Vol. 48, No. 3 (Part 2), 1970, pp. 681-691.

8. Strawderman, W. A. and Christman, R. A.: Some Effects of Water Loading on Turbulence Induced Plate Vibrations. Paper B-2 presented at 82nd Mtg. Acoust. Amer. Soc., Denver, Oct. 1971.

9. Dowell, E. H.: Transmission of Noise from a Turbulent Boundary Layer Through a Flexible Plate into a Closed Cavity. Jour. Acoust. Soc. Amer. Vol. 46, No. 1 (Part 2), 1969, pp. 238-252.

10. Davies, H. G.: Low Frequency Random Excitation of Water-Loaded Rectangular Plates. J. Sound. Vib. (1971), 15(1), 107-126.

11. Morse, P. M. and Ingard, K. U.: Theoretical Acoustics. McGraw-Hill Book Co., New York, 1968, Ch. 10.

12. Rebner, H. S.: Response of a Flexible Panel to Turbulent Flow: Running-Wave versus Modal-Density Analysis. J. Acoust. Soc. Amer. Vol. 40, No. 3, pp. 721-726, 1966.

13. Maidanik, G.: Acoustic Radiation from a Driven Infinite Plate Backed by a Parallel Infinite Baffle. J. Acoust. Soc. Amer. Vol. 42, No. 1, pp. 27-31, 1967.

14. Strawderman, W. A. and Brand, R. S.: Turbulent-Flow-Excited Vibration of a Simply Supported, Rectangular Flat Plate. J. Acoust. Soc. Amer. Vol. 45, No. 1, Jan. 1969, pp. 177-192.

15. Strawderman, W. A.: Turbulence-Induced Plate Vibrations: an Evaluation of Finite- and Infinite-Plate Models. J. Acoust. Soc. Amer. Vol. 46, No. 5, (Part 2), 1969, pp. 1294-1307.

16. Maestrello. L.: Radiation from and Panel Response to a Supersonic Turbulent Boundary Layer. J. Sound. Vib. (1969), 10(2), 261-295.

17. White, P. W.: Transduction of Boundary-Layer Noise by a Rectangular Panel. J. Acoust. Soc. Amer. Vol. 40, No. 6, 1966.

18. Maestrello, L. and Linden, T. L. J.: Response of an Acoustically Loaded Panel Excited by Supersonically Convected Turbulence. J. Sound Vib. (1971), 16(3), 365-384.

19. Leibowitz, R. C.: Methods for Computing Fluid Loading and the Vibratory Response of Fluid-Loaded Finite Rectangular Plates Subject to Turbulence Excitation... Option 3. Naval Ship Research and Development Center, Report 2976 C, Sept. 1971, Washington D. C.

20. Muhlstein, L., Jr.; Gaspers, P. A., Jr. and Riddle, D. W.: An Experimental Study of the Influence of the Turbulent Boundary Layer on Panel Flutter. NASA TN D-4486, March 1968.

21. Dowell, E. H.: Generalized Aerodynamic Forces on a Flexible Plate Undergoing Transient Motion in a Shear Flow With an Application to Panel Flutter. AIAA J., Vol. 9, No. 5, May 1971.

22. Dowell, E. H.: Noise or Flutter or Both? J. Sound. Vib., (1970), 11(2), 159-180.

23. Timoshenko, S.: Theory of Plates and Shells. McGraw-Hill Book Co., New York, 1940, p. 88.

24. Stoever, Herman J.: Engineering Thermodynamics. John Wiley and Sons, New York, 1951.

25. Wilson, Wayne D.: Speed of Sound in Distilled Water as a Function of Temperature and Pressure. Jour. Acoust. Soc. Amer., Vol. 31, No. 8, Aug. 1959, pp. 1067-1072.

26. Lin, C. C.: The Theory of Hydrodynamic Stability. Cambridge Univ. Press., 1955.

27. Graham, E. W. and Graham, B. B.: Effect of a Shear Layer on Plane Waves of Sound in a Fluid. Jour. Acoust. Soc. Amer. Vol. 46, No. 1, (Part 2), July 1969.

28. Pestel, E. C. and Lickie, F. A.: Matrix Methods in Elasto-Mechanics. McGraw-Hill, 1963.

29. Schlichting, H. : Boundary Layer Theory (Trans. by J. Kestin), McGraw-Hill, 6th Ed., 1968, p. 320.

30. Boyce, W. E. and DiPrima, R. C.: Elementary Differential Equations. John Wiley & Son, New York, 2nd Edition, 1969.

31. Miles, John W.: On the Aerodynamic Instabiltiy of Thin Panels. Jour. Aero. Sci., Aug. 1956, p. 771-780.

32. Meirovitch, L.: Analytical Methods in Vibration. MacMillam Co., 1967.

33. Carrier, G. F.; Krook, M. and Pearson, C. E.: Functions of a Complex Variable. McGraw-Hill Book Co., New York, 1966, Ch. 7.

34. Hildebrand, F. B.: Advanced Calculus for Engineers. Prentice-Hall, Inc., Englewood Cliffs, N.J., 1949.

35. Eversman, W.: Energy Flow Criteria for Acoustic Propagation in Ducts with Flow. J. Acoust. Soc. Amer. Vol. 49, No. 6, (Part 1), 1971.

36. Eversman, W.: Signal Velocity in a Duct with Flow. J. Acoust. Soc. Amer. Vol. 50, No. 2, (Part 1), 1971.

37. Skudrzyk, E.: Simple and Complex Vibratory Systems. Univ. of Penn. Press, 1968.

38. Muhlstein Jr., L.: AIAA paper #66-769, 1966.

APPENDIX A.- Perturbation Pressure-Density Relation in a General Mean Flow

In this Appendix an equation is derived relating the perturbation pressure to the perturbation density in an arbitrary mean flow. The appropriate governing equations are:

$$\left(\frac{\partial}{\partial t} + \bar{u}^* \cdot \nabla\right) \rho^* + \rho^* \nabla \cdot \bar{u}^* = 0 \qquad \text{A-1}$$

$$p^* = R\rho^* T^* \qquad \text{A-2}$$

$$\rho^* C_v \left(\frac{\partial}{\partial t} + \bar{u}^* \cdot \nabla\right) T^* = -p^* \nabla \cdot \bar{u}^* + (\text{heat}) + (\text{viscosity}) \qquad \text{A-3}$$

These equations are the continuity, state, and energy equations governing the total flow quantities denoted by the "star". In the energy equation A-3 the terms involving heat flow and viscosity effects are represented simply by (heat) and (viscosity) because these terms will soon be dropped from the equations governing the perturbation quantities.

Equation A-1 and A-3 can be combined to eliminate the velocity term $\nabla \cdot \bar{u}^*$ to obtain

$$(\rho^*)^2 C_v \, D(T^*) = p^* D\rho^* + (\text{heat}) + (\text{viscosity}) \qquad \text{A-4}$$

where

$$D(\,) \equiv \left(\frac{\partial}{\partial t} + \bar{u}^* \cdot \nabla\right)(\,)$$

Next, using T^* from equation A-2 in equation A-4, carrying

out the differentiations, and simplifying leads to:

$$\rho^* D(p^*) = \gamma\, p^* D(\rho^*) + (\text{heat}) + (\text{viscosity}) \qquad \text{A-5}$$

Note that if the effects of heat flow and viscosity are neglected for the total flow then equation A-5 implies that

$$p^* = c^2 \rho^*$$
$$\text{where} \quad c^2 = \gamma R T^*.$$

This result is ordinarily used in classical inviscid aerodynamics. To obtain the relation between perturbation pressure and density, the relations

$$\rho^* = \rho_0 + \rho,$$
$$p^* = p_0 + p,$$
$$\text{and } \bar{u}^* = \bar{U} + \bar{u}$$

are substituted into equation A-5, and the resulting terms separated into three groups. One group of terms contains only basic flow quantities $\bar{U}$, ρ_0, p_0, and heat flow and viscosity terms; these terms vanish under the assumption that the basic flow satisfies equation A-5. The second group of terms contains squares and products of the perturbation quantities $\bar{u}$, p, ρ; these terms are dropped under the assumption that the perturbation motion is small enough that higher order terms are small compared to the first order terms. The third group of terms are linear in the perturbation

quantities and provide the desired equation:

$$d(p) + \bar{u} \cdot \nabla p_0 + \rho\, d(p_0)/\rho_0 = \gamma R T_0 [d(\rho) + \bar{u} \cdot \nabla \rho_0 + p\, d(\rho_0)/p_0] \qquad \text{A-6}$$

where $d(\ ) = (\frac{\partial}{\partial t} + \bar{U} \cdot \nabla)(\ )$.

APPENDIX B.- Plate Equations With Damping And Added Mass

In this Appendix the equations governing the response of a plate having a mass and a damping force added to its surface are derived. The procedures and notations used in the body of this paper are used so that the equations obtained here can be compared directly with the equations obtained in the body of the paper for the acoustically coupled plate. These equations are derived to aid in the interpretation of the acoustic-coupled equations.

When a mass m and damping c are added to the forces acting on an element of the plate, the governing equation is:

$$D\nabla^4 w + (\rho_p + m)\frac{\partial^2 w}{\partial t^2} + c\frac{\partial w}{\partial t} = q\ (x,y,t) \qquad \text{B-1}$$

Assuming that the plate motion is independent of y and nondimensionalizing changes equation B-1 to

$$\frac{\partial^4 \hat{w}}{\partial \hat{x}^4} + \frac{\rho_p L^4}{D}\left(1 + \frac{m}{\rho_p}\right)\frac{\partial^2 \hat{w}}{\partial t^2} + \frac{CL^4}{D} = \frac{q(x,t)L^4}{D} \qquad \text{B-2}$$

Next use the orthogonal eigenfunctions of

$$\frac{\partial^4 \hat{w}_m}{\partial \hat{x}^4} = \lambda_m \hat{w}_m \qquad \text{B-3}$$

and the eigenfunction expansion

$$\hat{w}\ (\hat{x},t) = \sum_{n=1}^{N} a_n(t)\ \hat{w}_n(\hat{x}) \qquad \text{B-4}$$

to reduce B-2 to

$$\frac{\partial^2 a_m}{\partial t^2} + \frac{c}{\rho_p(1+m/\rho_p)} \frac{\partial a_m}{\partial t} + \frac{\lambda_m D}{\rho_p L^4 (1+m/\rho_p)} a_m = \frac{1}{\rho_p L(1+m/\rho_p)} \int_0^1 \{ q(\hat{x},t)\hat{w}_m(\hat{x})d\hat{x} \} \qquad \text{B-5}$$

By analogy with a single degree of freedom system[32] the coefficients of equation B-5 can be identified as

$$\left.\begin{aligned} \frac{c}{\rho_p(1+m/\rho_p)} &= 2\zeta\omega_m \qquad \text{a} \\ \omega_m^2 &= \frac{\lambda_m D}{\rho_p L^4(1+m/\rho_p)} \qquad \text{b} \end{aligned}\right\} \qquad \text{B-6}$$

where ω_m is the natural (circular) frequency and ζ is the ratio of actual damping to the critical value of damping. Taking the force $q(\hat{x},t)$ and the response $a_m(t)$ to be harmonic, i.e.

$$\left.\begin{aligned} q(x,t) &= \bar{q}(\hat{x})e^{i\omega t} \\ a_m(t) &= \bar{a}_m e^{i\omega t} \end{aligned}\right\} \qquad \text{B-7}$$

and introducing equations B-6 and B-7 into equation B-5 leads to

$$\left\{\lambda_m - (1+\frac{m}{\rho_p})\,\Omega^2 + i\,\Omega^2\left[2\,\zeta\,\frac{\omega_m}{\omega}\,(1+\frac{m}{\rho_p})\right]\right\}\bar{a}_m = Q_m \qquad \text{B-8}$$

Equation B-8 is to be compared with acoustic coupled plate results.